The potential use of laser cladded functionally graded materials to mitigate degradation in boiler tube heat exchangers for power plant applications: A review

Article *in* Surface Engineering · August 2023

DOI: 10.1080/02670844.2023.2249653

CITATIONS
5

READS
124

4 authors:

Joseph Morake
Botswana International University of Science and Technology
4 PUBLICATIONS **14** CITATIONS
SEE PROFILE

James Mutuku Mutua
Jomo Kenyatta University of Agriculture and Technology
29 PUBLICATIONS **319** CITATIONS
SEE PROFILE

Martin Ruthandi Maina
Jomo Kenyatta University of Agriculture and Technology
24 PUBLICATIONS **146** CITATIONS
SEE PROFILE

Eyitayo Olatunde Olakanmi
Botswana International University of Science and Technology, Palapye, Botswana
38 PUBLICATIONS **2,460** CITATIONS
SEE PROFILE

Surface Engineering

ISSN: (Print) (Online) Journal homepage: https://www.tandfonline.com/loi/ysue20

The potential use of laser cladded functionally graded materials to mitigate degradation in boiler tube heat exchangers for power plant applications: a review

Joseph B. Morake, James M. Mutua, Martin M. Ruthandi & Eyitayo O. Olakanmi

To cite this article: Joseph B. Morake, James M. Mutua, Martin M. Ruthandi & Eyitayo O. Olakanmi (2023) The potential use of laser cladded functionally graded materials to mitigate degradation in boiler tube heat exchangers for power plant applications: a review, Surface Engineering, 39:6, 677-721, DOI: 10.1080/02670844.2023.2249653

To link to this article: https://doi.org/10.1080/02670844.2023.2249653

Published online: 31 Aug 2023.

SURFACE ENGINEERING
2023, VOL. 39, NO. 6, 677–721
https://doi.org/10.1080/02670844.2023.2249653

I·M3 Institute of Materials, Minerals & Mining
Taylor & Francis Taylor & Francis Group

The potential use of laser cladded functionally graded materials to mitigate degradation in boiler tube heat exchangers for power plant applications: a review

Joseph B. Morake[a], James M. Mutua[a], Martin M. Ruthandi[a] and Eyitayo O. Olakanmi[b,c,d]

[a]School of Mechanical Manufacturing and Materials Engineering, Jomo Kenyatta University of Agriculture and Technology (JKUAT), Nairobi, Kenya; [b]Department of Mechanical, Energy & Industrial Engineering, Botswana international University of Science & Technology, Palapye, Botswana; [c]UNESCO Chair on Sustainable Manufacturing & Innovation Technologies (UCoSMIT), Botswana International University of Science & Technology, Palapye, Botswana; [d]Advanced Manufacturing & Engineering Education (AMEE) Research Group, Botswana International University of Science & Technology, Palapye, Botswana

ABSTRACT

Surface modification is essential to safeguard heat exchangers from premature failure spurred by deterioration mechanisms such as corrosion and wear, which diminish performance. Meanwhile, modifying some substrates with dissimilar materials is challenging due to a mismatch in material properties. Moreover, individual alloy coatings on substrates are usually insufficient in the required material properties, leading to accelerated failure of equipment, especially in power plant industries. This article summarised the knowledge base on functionally graded materials (FGMs) while emphasising how this promising class of novel materials can reduce deterioration. Additionally, laser cladding is established to be a suitable technique for processing FGMs. A particular focus is laid on the laser beam interaction with the FGM and expounding on the processing and material parameters that affect the microstructural properties of FGMs. The development prospects for processing FGMs with superior clad quality characteristics to increase boiler pipes' service life and performance are also highlighted.

ARTICLE HISTORY
Received 9 May 2023
Revised 4 August 2023
Accepted 14 August 2023

KEYWORDS
Corrosion; heat exchanger; laser cladding; optimisation; process parameters; functionally graded materials; wear; failure

Introduction

Heat exchangers (HXs) are indispensable devices used to exchange thermal energy in the form of heat transfer/dissipation between fluids (liquid or gas), from one medium to another [1,2]. Pipes are one of the most heavily stressed major components of HXs used in harsh working environments, such as power plant sectors, resulting in frequent premature failures. Studies have been carried out to investigate heat exchanger pipe failure due to corrosion and wear attack aggravated by elevated temperatures, reducing gases, high pressures, and cyclic stresses [3–5]. Degradation of HX pipes can be mitigated by careful material selection and applying resilient coatings to tube surfaces because some metals are better suited to endure attack in a particular environment than others [6].

Generally, alloys are usually used as coating materials for exchanger piping because they form anti-corrosion protective oxide layers. As such, heat exchanger pipes are usually made of copper alloys (90-10 Cu-Ni), stainless steel (SS316L, SS304L), Inconel (In625, In718, IN825), and titanium alloys (Ti6Al4V). The high content of Cr in some stainless steel ranging between 10.5 and 26 wt-% improves their corrosion resistance, and the alloying elements with strengthening phases resist chemical degradation in heat exchanger parts [7]. Apart from having the highest thermal conductivity, copper also forms a natural protective oxide layer called patina on the metal surface to protect the material from degrading agents, initially taking the form of a thin cuprate layer (Cu_2O) [8]. Similarly, other ideal materials, such as aluminium also form a thin aluminium oxide layer that protects against oxidation from degrading agents such as CO_2 and H_2S [9]. However, chromate formation and other degrading reactions tend to attack protective layers. Sadeghi et al. [10] posited that despite research efforts in developing advanced alloys for corrosion resistance and high strength applications, they suffer from other degradation attacks beyond a certain threshold of operating temperatures. Hence, they recommend coating tubes with functional materials to simultaneously take advantage of two functions such as high corrosion resistance and high wear resistance. Therefore, it can be argued that individual alloys are preferred as surface modifiers of boiler pipes due to their superior material properties. However, individual alloys have limited resilience in aggressive environments [11,12]. Thus, functionally graded materials (FGMs) offer a

CONTACT James M. Mutua mutuajay@eng.jkuat.ac.ke School of Mechanical Manufacturing and Materials Engineering, Jomo Kenyatta University of Agriculture and Technology (JKUAT), PO Box 62000-00200, Nairobi, Kenya

potential solution to overcome the coating drawbacks of individual material because there are more resistant and durable against degradation in severe conditions containing different corrosion products.

The concept of material alloying has led to the development of an emerging class of novel materials termed functionally graded materials (FGMs), [13] because they offer better resistance to material degradation. FGMs are realised through a combination of two or more materials characterised by spatial composition profiles that exhibit variation to change the material properties for the required function and functionality in industrial applications [14,15]. Typical applications of FGMs can be likened to human body parts, such as bones and teeth. The human tooth is wear-resistant from the outside and ductile on the inside to act as a shock absorber to improve fatigue life [16]. Similarly, FGMs are ideal for application in heat exchanger pipes where they can offer corrosion resistance on the tube inside the wall and wear resistance on the tube outside the wall [17]. They also reduce residual stresses experienced during the fabrication process by limiting the mismatch in material properties, which is reported to cause premature failure of heat exchanger parts during service [18].

Literature on FGMs reveals that this class of customised material offers a potential application for use in heat exchanger pipes operating in severe conditions, owing to the novel system of combining dissimilar materials. For instance, Zhang et al. [19] fabricated an FGM made of stainless steel 316L (SS316L) and pure copper (Cu) using Inconel 718 (IN718) as an interlayer using directed energy deposition (DED) technique. In an effort to increase the overall performance of component working under severe conditions, including prospective usage in heat exchangers, several material properties were combined. The SS316L/IN718/Cu FGM was made to combine the high thermal and electrical conductivity of copper, good machinability and corrosion resistance of SS316L, and high strength at elevated temperatures of IN78. Related studies have been carried out to develop FGMs for demanding environments using different material properties. This shows that additive manufacturing can be used to fabricate FGMs with combined material properties that offer potential application for enhanced resilience against degradation in HXs pipes.

Laser cladding surface modification is a promising additive manufacturing technique for applying heat exchanger coatings. At present, it is one of the most cost-effective and efficient techniques capable of mitigating corrosion through overlay coatings [10]. It employs a laser beam to melt metal powders and blends them to form a thin material film into a substrate material, as shown in Figure 1(a) [20]. It has been demonstrated to lengthen component service lives by producing coatings with good metallurgical bond and refined microstructure, see Figure 1(b). Also, manufacturers have resorted to employing this technique to fabricate high-value components because of its ability to produce high-quality parts most economically. On the other hand, improper selection of process parameters hinders its successful implementation, leading to processing defects that could lead to component failure during service. Research efforts in determining the optimum process parameters is being directed towards maximising the quality characteristics of coatings such as wear resistance and density of parts.

It is evident from the literature that there is a paradigm shift in the fabrication of HX materials, attributed to the calls for prospects and novel materials that can increase heat transfer efficiency. Thus, this review aims to provide useful insights into the selection of suitable materials and candidate coatings that can be used to overcome well-known industrial problems associated with the failure of heat exchangers, to meet current and future energy demands. The objective is to give a detailed overview of the emerging candidate materials, capabilities, and viability of the laser cladding technique with a focus on the effects of processing defects and microstructure on the performance of fabricated FGMs. This will be achieved by exploring how suitable process parameters can be selected and improved using hybrid optimisation techniques. Many researchers have not explored this area in the frame of heat exchanger application and it forms the basis of prospects for fabricating FGMs. Given this, the production of suitable materials with enhanced abilities can be realised for prospective application in the heat exchanger industry.

Heat exchangers

Boiler components are of great interest in power plants process industries because they are essential in transferring heat between two mediums (liquid or gas) [21–23]. A particular research interest is focused on boiler pipes as critical components that entail high maintenance costs due to failure when operating in aggressive conditions. Amongst the failure mechanisms that affects boiler components, corrosion is reported to be the leading [6]. Because these devices transmit various fluids, there are a number of corrosion mechanisms that weaken the pipe material. Gaseous substances in hostile conditions can cause the protective layer to oxidise and become weaker, which decreases the resistance of the pipe to attack. When boiler pipes are subjected to high temperatures, oxide layers may build on the pipe surface, resulting in deposits from chemical reactions that minimise the heat transfer surface. For example, deposits of corrosive iron oxide may develop on the surface of a steel pipe exposed to steam at temperatures lower than 560°C [24]. The effects involve a reduced cross

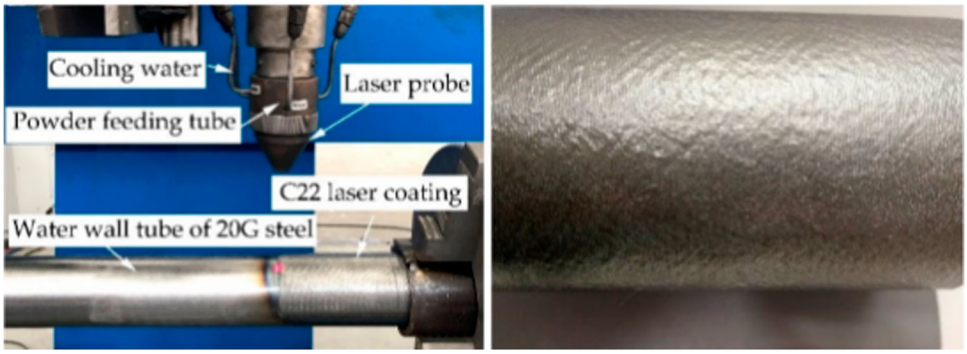

Figure 1. Photographs of (a) laser coating setup for boiler tubes and (b) 20G steel water wall tube using C22 laser coating [20].

sectional area, elevated stress levels, overheating, and pipe thinning, which hasten material deterioration.

In thermally stressed boiler pipes, intergranular corrosion can occur when the cohesiveness of a material at its grain boundaries is compromised. Therefore, the surface of a boiler pipe needs to be modified for improved resistance against stress cracking. The degree of pipe compatibility and adhesion can also be affected by the absorption of degrading gases like hydrogen. Boiler pipes can deteriorate due to hydrogen in a hydrogen sulphide atmosphere, which can lead to sulphide stress cracking, a type of hydrogen embrittlement. When hydrogen atoms enter a metal, they leave perforations in the microstructure that cause cracks to develop under applied stress during service. Additionally, manufacturing defects can allow for the entry of oxides that impair the microstructural integrity, such as the creation of porosity during fabrication [21,25–27].

The phenomenon of degradation process is elucidated further in the next section. The main focus and emphasis is on boiler pipe HX, which are the most versatile HX type due to the robust performance, affordability, broad material selection, and huge heat transfer area to volume and weight [24,28–30]. Additionally, the performance enhancement of these devices is of interest due to the increasing energy demand in a growing population, which necessitates high performance equipment to maximise output electricity [30].

Nature of degradation and its mechanism in heat exchangers

Degradation of boiler tubes due to corrosion leads to tube failure due to the formation of scales and corrosion products that lower the heat transfer efficiency [31]. Generally, corrosion involves the transformation of refined metal to a chemically stable oxide, a phenomenon that thrives in hostile mediums such as untreated industrial water, seawater, oxidation media (e.g. chromic and perchloric), reducing acids (e.g. hydrochloric and phosphoric), salt solutions, alkaline media (e.g. NaOH and KOH), and organic compounds (e.g. alcohols and ethers) [32]. Sadeghi et al. [10] revealed that corrosion in heat exchanger components is triggered by the interaction of alloys and their oxides with chlorides, sulfates, and sulfites. Wu et al. [33] also affirmed that chlorine-induced corrosion is one of the most reported cases of failure induced by chloride gas reactions with metals (active oxidation), or reaction that leads to the formation of ions (electrochemical), and the reaction occurring between chlorides (molten-salt based). Simply put, the presence of Cl-containing compounds like salt deposits formed by gaseous reactions, react with heat exchanger alloys to form alkali chlorides that penetrate through microstructural defects such as pores and cracks. Increasing temperature will increase the corrosion rate since the reaction will be accelerated. Similarly, Oska et al. [34] reported tube failure of a biomass boiler shown in Figure 2(a) due to high amounts of chlorine at the microstructural interface, as shown in Figure 2(b,c). This shows that refined microstructure with good cohesion bonding at the substrate and interface is desirable to withstand chloride attack.

Uusitalo et al. [35] investigated the susceptibility of high-temperature boiler coatings to corrosion in environments containing chlorine and salt deposits. The corrosion tests were conducted on austenitic stainless steel and low-alloy ferritic steel deposited using laser cladding and High-Velocity Oxygen Fuel (HVOF) techniques for different coatings. Of particular interest in the various materials investigated is material 3, comprising Ni-50Cr coating. It was prone to chlorine attacks which they reported to have disintegrated some individual grains along splat boundaries. Correspondingly, material 5 comprising the Ni-21Cr9Mo coating suffered a chlorine attack along the splat boundaries in 9 wt% chromium-containing portions labelled (a) in Figure 3. The presence of excess chlorine and low content of potassium and sodium were found at the coating-substrate interface and along substrate grain boundaries of the substrate where the material suffered the most severe attack. They concluded that the coatings fabricated by the

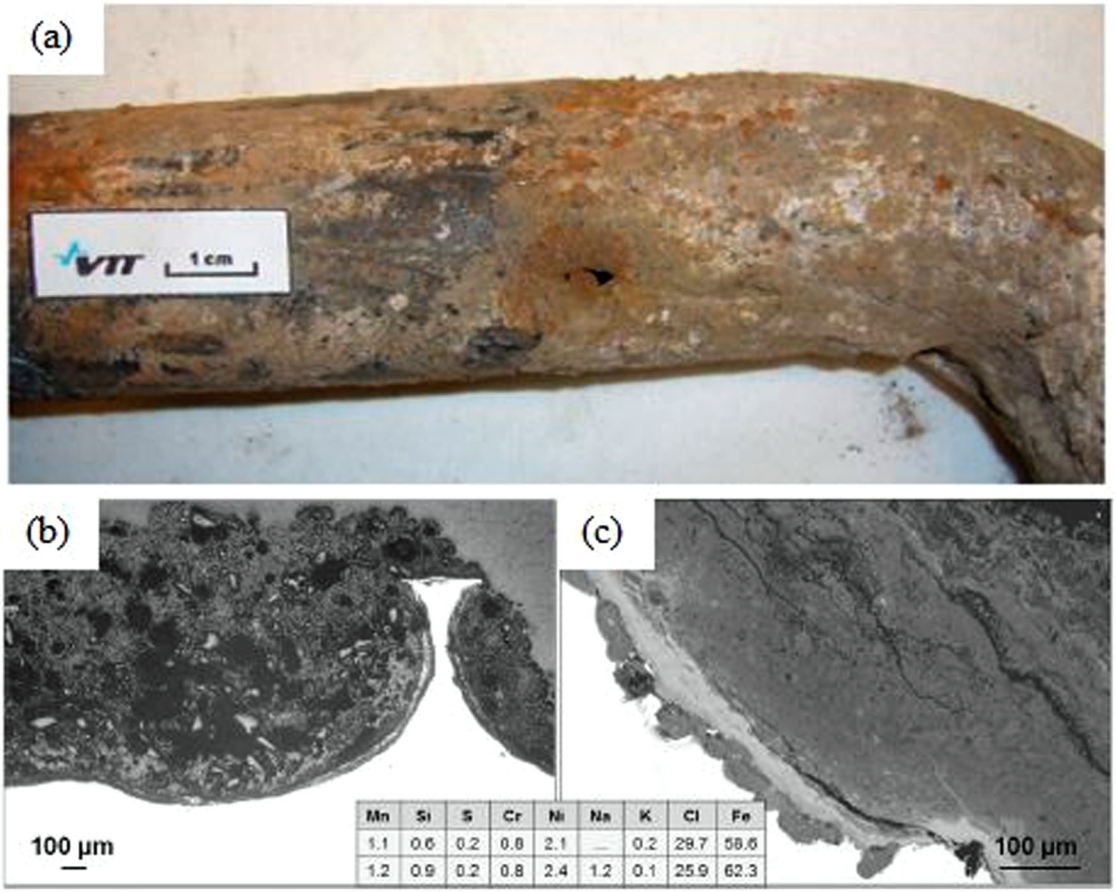

Figure 2. Tube failure (a) leakage observed using optical microscopy (b, c) SEM magnified view of leakage showing higher chlorine content that caused corrosion [34].

thermal spraying technique suffered an attack at splat boundaries, causing penetration through voids and oxide, as shown in the Figure 4(a) and Figure 3(b), respectively. This proves the general observation that chlorine-induced corrosion is the most encountered mechanism of degradation in power plants, mostly occurring through the oxidisation of metals leading to oxide infiltration. Further, they reported that laser cladded coatings did not show any form of attack at splat boundaries, nor was there any oxide penetration

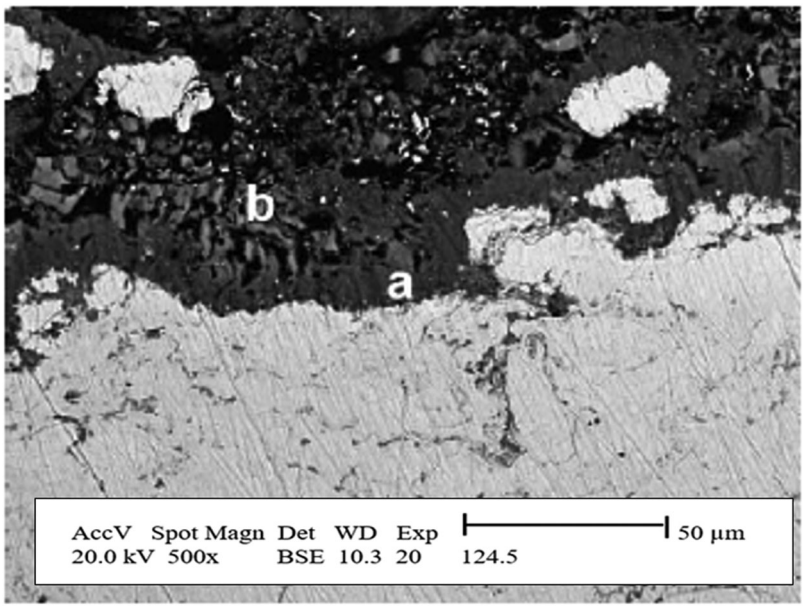

Figure 3. Corrosion attack on Ni-21Cr9Mo coating along the splat boundaries due to (a) chromium, sulfur, sodium, and (b) chlorine and potassium [35].

reported, even though they suffered chlorine attack at oxidised regions containing chromium-rich dendrites. This implies that chlorine-induced corrosion can be reduced through fabrication processes since it attacks heat exchanger coatings through penetration of the microstructure containing voids, exemplifying that coatings with enhanced microstructural characteristics can withstand diffusion of particles through the microstructure and offer better corrosion protection.

Wu et al. [33] carried out a comparative investigation concerning the influence of operating conditions and temperature fluctuations on the nickel-coating (Ni and Ni_2Al_3) performance of two boiler tubes operating at 520°C–540°C. The Randers boiler tube failed 2 times during service, leading to partial corrosion because the temperature was monitored, whereas the Maribo boiler tube corroded severely because it was reported to have failed 213 times due to temperature fluctuations. Figure 5 shows the microstructural grains of the coating under attack, leading to severe corrosion of the latter tube. This further proves that materials with good microstructural quality characteristics are desirable in fabricating heat exchanger components to prevent the diffusion of particles through defects in severe operating conditions.

Usman & Khan [36] investigated the premature failure of heat exchanger tubes made of ASTM A213 grade T-11, operating in an environment containing high levels of hydrogen, nitrogen, and carbon monoxide. They found that the tubes failed due to thermal fatigue at elevated temperatures leading to circumferential crack formation, water leakage, and inadequate cooling (Figure 6). They attributed that to manufacturing defects, implying that the cracks encountered during fabrication initiated crack growth that led to fatigue failure as a result of cyclic loading. Panahi et al. [37] also investigated a failed shell and tube heat exchanger using microstructural analysis. They concluded that the presence of chloride caused penetration of corrosive substances into the subsequent tube material (Figure 7a), leading to pitting corrosion when oxides penetrate the passive protective film (Figure 7b). The exchanger tubes made of stainless steel 304L, are reported to have failed after six years of operation, leading to gas leakages. They attributed the gas leakage to the cracking caused by chloride reactions in the presence of hydrogen sulphite (H_2S) and carbon dioxide (CO_2). This shows that corrosion problems arise due to chemical reactions in hostile environments, leading to oxide formation, which penetrates the layer causing pits in the microstructure. It also confirms that heat exchanger coating materials must be fabricated with good material properties to withstand failure aggravated by processing defects, which cause penetration of oxides and depletion of protective films at the surface.

Allahkaram et al. 's [38] investigation of a failed shell-and-tube heat exchanger with Inconel 625 tubes revealed fluid leakages that had an impact on the operation of a gas cooler. They established that it was due to crevice corrosion at tube-to-shell, and tube-to-baffle contact regions caused by harmful deposits, showing that corrosion-resistant materials are also prone to attack if not used in their actual application environment. This also calls for enormous research efforts on the development of HXs with suitable material properties which are economic, cost-effective, and efficient by carefully selecting materials that can withstand failure. In a similar study by Panahi et al. [37], a shell-and-tube heat exchanger having tubes made of stainless steel 304L also failed due to crevice corrosion resulting in cracking and reduced tube walls. They recommended the use of resistant alloys to mitigate such failures. The reason is that alloys have material properties that can be adjusted to offer better corrosion and wear protection, and contain additional elements that improve overall thermo-mechanical properties.

Another study conducted by Faes et al. [6] revealed that the shell and tube, and plate heat exchangers are the most affected by corrosion effects. They reported that corroded heat exchangers can endanger many lives due to environmental risk factors such as explosions and hazardous effects due to contamination. Jin et al. [23] also stated that corrosion degrades the performance of shell and tube HX causing unwanted failures. Moreover, corrosion is reported to reduce the system's overall performance due to pressure drops. For instance, Albanakis et al. [39] found in their study that pressure drops were attributed to fouling, a process involving undesirable deposits of substances on the heat transfer surface. Faes et al. [6] also pointed out some common corrosion attacks experienced by heat exchangers, including uniform corrosion, stress corrosion cracking, intergranular corrosion, intergranular corrosion, galvanic corrosion, fatigue corrosion, and erosion-corrosion.

Uniform corrosion is one of the prevalent forms of corrosion in the heat exchanger industry. It is mostly experienced when corrosion spreads over the entire heat transfer surface because of chemical reactions triggered by ammonium, chlorine, and hydrogen ions [40]. When the protective film coating of a metal surface degrades, pits are formed and deepen on the entire surface, resulting in pitting corrosion. Davíðsdóttir et al. [41] studied the corrosion resistance of four metals in geothermal power plants (Inconel 625, 316L stainless steel, 254SMO, and titanium grade 2) using in-situ geothermal testing. They revealed that uniform corrosion is influenced by the type of material used, after In625 was found to be the only material not attacked by this corrosion upon testing, implying that it can be overcome by selecting the proper materials and coatings.

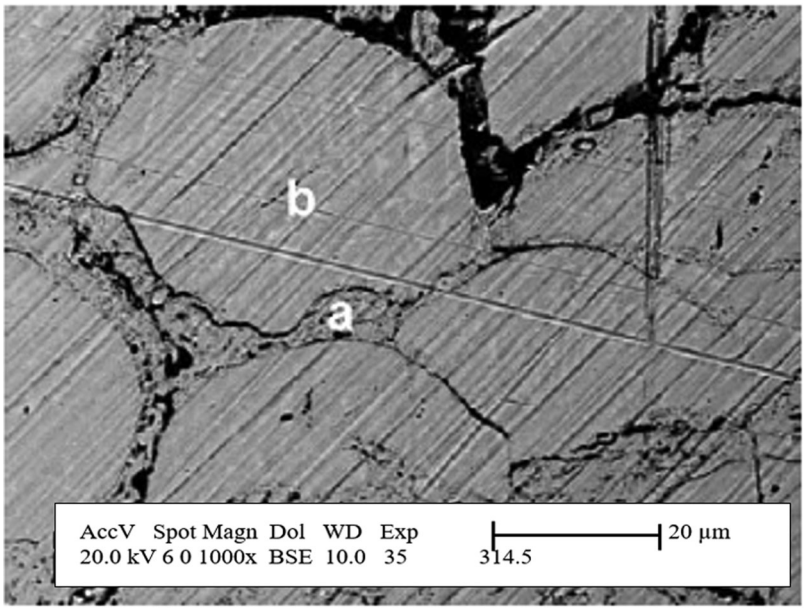

Figure 4. A chlorine attack on Ni-21Cr9Mo coating at (a) splat boundaries (b) causing penetration through microstructural voids and oxide [35].

Erosion-corrosion is one of the deterioration mechanisms that led to the failure of many heat exchangers. It is normally propelled by turbulence or turbulent conditions in fluids, which leads to the erosion-wear of the metal tube thinning. This is often experienced under high pressure and velocity environments, fluids with deposits, ledges, and where water changes directions like in U-curves of design, leading to attack at curves and the entrance of the tubing. In addition, the division of the incoming fluid as it enters smaller tubes leads to metal wearing, leaving what seems like a horseshoe shape [8,42,43].

Galvanic corrosion is another form of corrosion between two metals coming in contact in a conductive solution leading to electrical flow. This electrochemical process happens in dissimilar metals and is often encountered in heat exchangers, especially at joint interfaces [44]. In addition, it often occurs with chemically induced corrosion when there are chemical interactions between heat exchanger material and fluids. Mousavian et al. [45] conducted a failure analysis of a shell and tube oil cooler used in geothermal power plants and found that the cause of failure was due to chemically induced corrosion triggered by the entrance of impurities and the increased chlorine content in fluid. They further recommend careful selection of gasket material because a material that cannot withstand attack will be prone to attack under aggressive conditions.

Stress corrosion cracking (SCC) is encountered when three conditions are present; a corrosive media (e.g. sulfide-rich environment), the presence of vapour, and stresses induced in the material. For instance, when the material has higher tensile residual stresses introduced during manufacturing, it can become defenceless against SCC [31]. SCC usually leads to material fatigue and cracking. This was also proved in the work of Corleto & Argade [46], who investigated a failed heat exchanger and pointed out

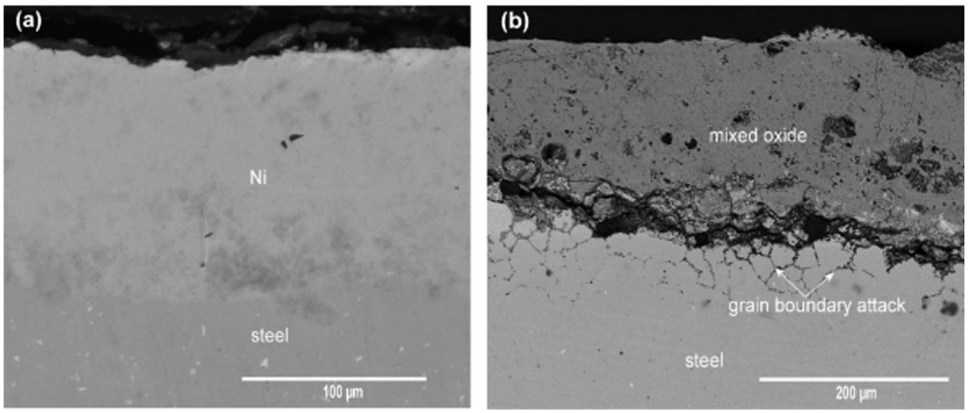

Figure 5. Corrosion morphology of exposed boiler tubes due to excessive thermal cycle in nickel coated (a) Randers tube and (b) Maribo tube [33].

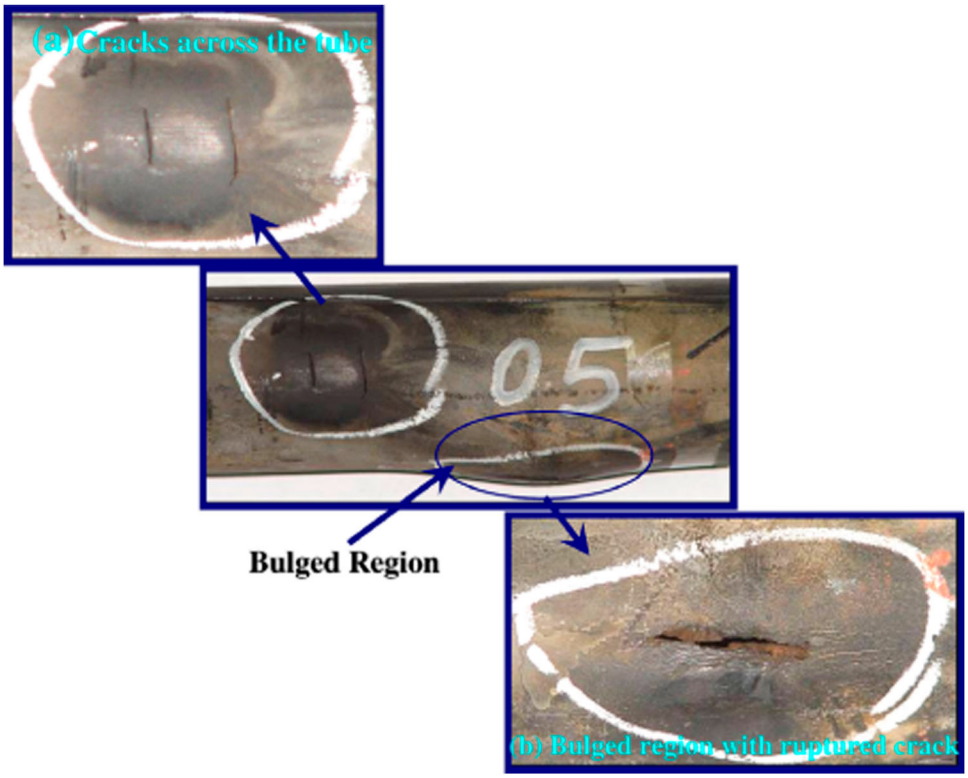

Figure 6. Cracked and ruptured portions of heat exchanger tube due to manufacturing defects [36].

that was prone to crack development when joining Duplex SS and Carbon steel, worsened by crack deformities introduced to the material during fabrication, leading to corrosion. Vasauskas & Baskutis [47] also stated that the presence of tensile stresses and a corrosive media makes heat exchanger tubes susceptible to SCC, leading to the formation of cracks. They further reveal that the cracking mechanism varies in SCC, it can be in the form of inter-granular crack propagation, creep, rupture, or stress rupture. This shows that SCC can be avoided through microstructural enhancement by reducing cracking deformities during fabrication, which drives the growth of cracks.

Summary of findings

It can be asserted that there is a relation between material characteristics, failure mechanisms, and how these affect heat transfer efficiency, as shown in Figure 8. This demonstrates the importance of thoroughly evaluating and correlating the selection of suitable materials with working conditions to reduce the occurrence of failure. Material choice enhances the efficiency, equipment life, return on investment (ROI), and heat exchanger performance. Hence, this article expounds more on material selection in the next section.

Material selection for heat exchangers

Material selection is an important factor to consider when improving heat exchangers' performance. According to Permatasari & Yusuf, [48] the efficiency of the heat transfer process is affected by the material selection criterion. They indicated that using suitable materials in heat exchangers, such as shell and tube heat exchangers will help avoid any possible failures due to corrosion. Also, they showed that material selection determines the heat transfer rate as it influences the pressure drop. Collins et al. [49] also studied the heat transfer process of a gas-cooled reactor that uses an intermediate heat exchanger and concluded that it must withstand critical pressure drops for maximum efficiency. Of great importance in these studies is their emphasis on material selection, implying that it should be made the apex priority in the design and fabrication process for any type of heat exchanger.

Kapranos and Priestner [50] reviewed the most common materials used in heat exchangers, summarised as aluminium, copper-nickel, stainless steel, and titanium alloys. However, Lazić et al. [42] also reviewed boiler pipe materials and revealed that steel is the most dominant metal utilised for boiler pipes. On the other hand, Saito et al. [43] explained that Ni-based alloys and advanced ferritic steels are the ideal candidate materials for power generation boilers because they can withstand severe working conditions. Meanwhile, Lister [51] showed that copper is another important and commonly used material for power plant boilers which can be combined with Ni to form more corrosion-resistant cupronickels. Based on these findings, this article limited its review to steel, nickel, and copper alloy substrates and coatings. Their resistance to degradation is

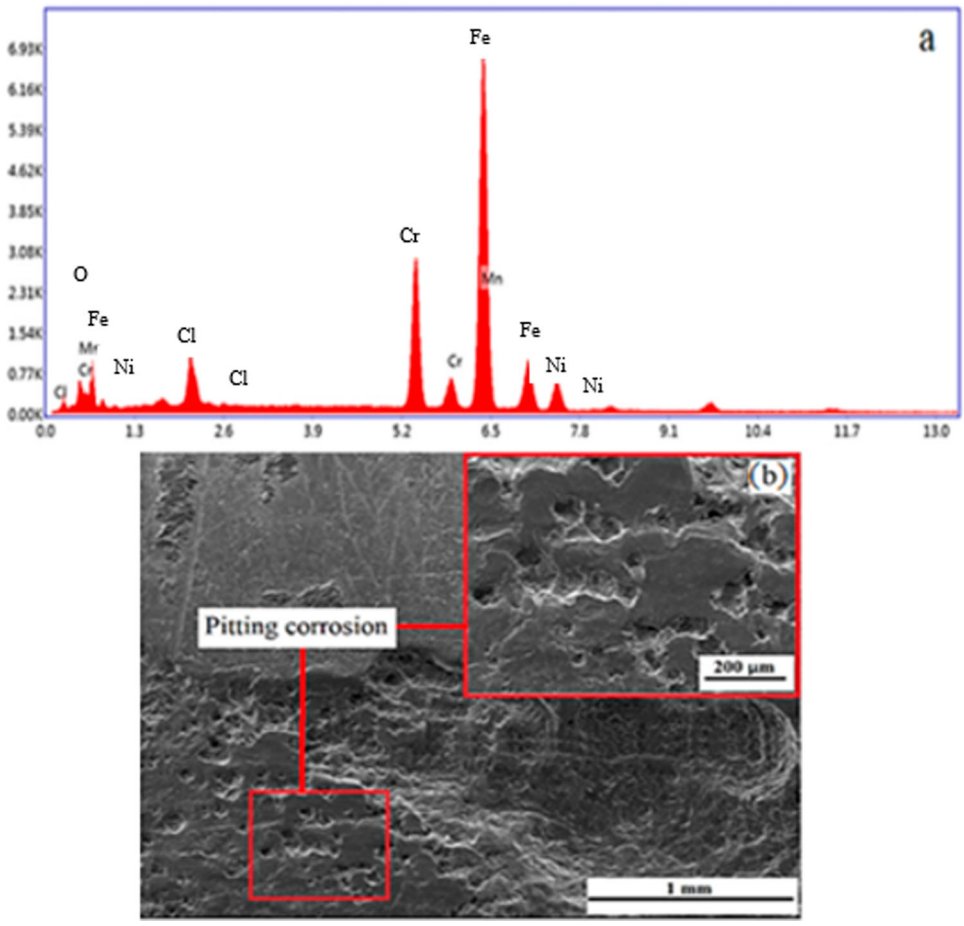

Figure 7. Corrosion failure analysis of failed exchanger tubes (a) EDS analysis showing the presence of Cl peaks (b) SEM micrographs showing pitting corrosion [37].

further elucidated with a focus on microstructure and phase transformation and how these influence performance characteristics.

Ferrous-alloy substrates and coatings

Ferrous-based alloys constitute the largest group of materials used in heat exchanger coatings and substrates owing to their durability against degradation. The most commonly utilised in the heat exchanger industry are stainless steel and carbon steel since they offer better corrosion resistance and limit the presence of deposits. Notwithstanding, several other types of metals including cast irons, alloy steels, and tool steels belong to this group of metals.

Stainless steels (SS) are iron-based alloys that play a significant role in fabricating coating materials for heat exchangers. The increased chromium and nickel

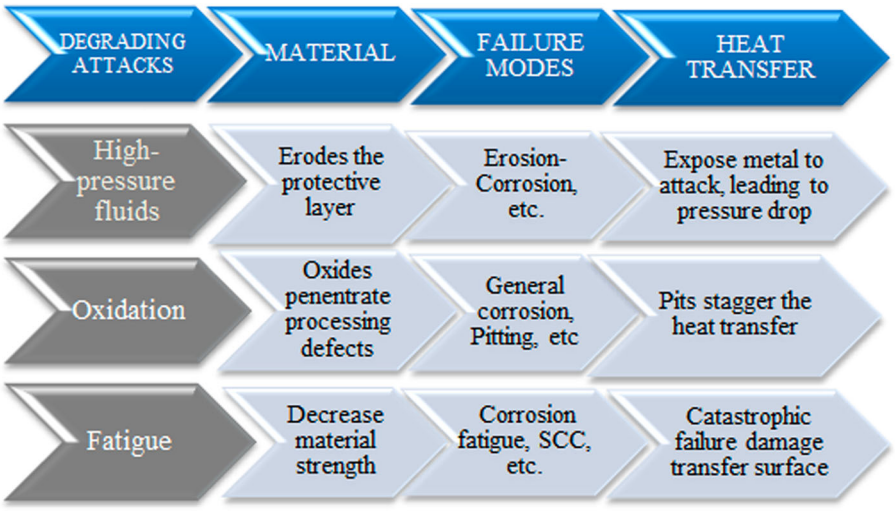

Figure 8. Relationship between material qualities, failure modes, and heat transfer.

content gives them good thermal and corrosion resistance. The iron-based alloys are classified according to the AISI stainless steel numbering series of 200, 300, and 400. They can further be grouped according to the type of hardening they undergo to improve their material or microstructural properties. This refers to austenitic, ferritic, duplex, and martensitic [52].

The austenitic is a widely known group of SS identified by the 300 series and a few belonging to the 200 series, having good material characteristics (e.g. excellent corrosion resistance, good strength, high thermal coefficient, heat capacity, and excellent formability), making them stand out amongst the other series. For example, type 304 stainless steel (SS304) and SS316 belonging to this group are used to manufacture heat exchanger tubes owing to their ideal material properties that can also be enhanced by heat treatment and annealing. According to Lima et al. [53], adding molybdenum to these steels can transform their microstructure to improve resistance to pitting corrosion in severely corrosive environments. However, sensitisation is reported to occur to these SS types when operating at higher temperatures ranging between 400°C to 850°C, a phenomenon that involves depletion of chromium and carbide precipitation at the grain boundaries. This often exposes SS to intergranular stress corrosion cracking of boiler tubes.

To overcome these challenges, carbon content can be reduced to values not exceeding 0.3 wt%, leading to the realisation of an improved version referred to as SS304L and SS316L. Nevertheless, these latter types may be prone to sensitisation when operating at higher temperatures for a prolonged time. Yoo et al. [54] revealed that SS304L contains Cr- element that offers significant corrosion resistance, but it often precipitates along the grain boundaries when exposed to temperatures reaching 870°C, which they attribute to the depletion of Cr along the zone close to the grain boundary, causing inter-granular corrosion in heat exchanger tubes. For instance, Rezakhani [55] analysed the corrosion behaviour of FeCrAl coating deposited on SA213-T11 steel via the thermal spray technique for boiler tubes operating at elevated temperatures. They found that salt deposits attacked the steels due to the scale composition formed, which shows that scale formation is an industrial problem degrading components. The corrosion products were observed after exposure at 550°C. Figure 12(a) shows the microstructural cross-section of the coating that suffered an attack at boundaries (grain and splat), as well as the interface of the substrate and coating, as shown in Figure 12(b). This could be attributed to the spallation of oxide layers and depletion of chromium-protecting elements at the grain boundaries due to excess chlorine, sodium, and sulfur reactions, leading to the destruction of corrosion attacks at grain boundary zones and weak interfaces. The attack confirms that a proper bond with good consolidation of the substrate and coating is desirable for enhanced corrosion resistance.

Voisin et al. [56] also studied the susceptibility of SS316L to corrosion attack and found that they form a primary barrier comprising Cr_2O_3 film that enables it to operate in severely corrosive environments, which is why 316L is resistant to pitting corrosion. Despite the excellent corrosion resistance of SS316L due to the high content of Cr present, it is also susceptible to corrosion when degrading agents penetrate the oxide film, forming a nucleation site. This is influenced by processing defects, including phases, grain boundaries, and crystal dislocations in the microstructure, implying that controlled and optimum process conditions can mitigate the prevalence of pitting corrosion in heat exchanger tubes. Voisi and co-investigators revealed that Manganese-rich sulfides (MnS) that normally initiate pitting were not found in their material fabricated using 316L by Laser Powder bed Fusion process, owing to good cooling and rapid solidification mechanism that led to the formation of a good microstructure without cracks and pores. In addition, they also highlighted that the formation of a higher melt pool can be an initiation site of pits, which could be attributed to the crack propagation along the cellular structures. Research on the influence of melt pools on pitting corrosion is still scarce. Thus, studies are needed on the pit nucleation of SS316L and how adding Cr can mitigate heat exchanger failures.

Therefore, it can be inferred that increased Cr in stainless steel improves its corrosion resistance since it forms an anti-corrosion passive layer when it reacts with oxygen. Because of that, stainless steel 304L and 316L types are most utilised in heat exchanger tubing due to reduced carbon precipitation attributed to the lower carbon content and higher chromium content ($\geq$ 10.5%), which enhance their corrosion resistance and mechanical properties. The austenitic SS-types also exhibit an austenitic microstructure that forms a columnar dendritic morphology during directed energy deposition that often forms uniform grain distribution. It is worth noting that the formation of microstructure also depends on the processing technique used, meaning the same microstructure may not be obtained with other techniques such as selective laser melting (SLM) [57]. Several studies have also demonstrated that microstructural formation during processing affects the heat exchanger performance characteristics (e.g. wear, corrosion, oxidation). For instance, Pokhmurskii et al. [58] investigated the erosion-corrosion behaviour of boiler tubes and stated that the most important attribute of a coating that determines its oxidation resistance is the microstructure of the coating. They studied the addition of alloying elements (Ti, Mn, B, Mg, Ni, Si) to the Fe-Cr-Al

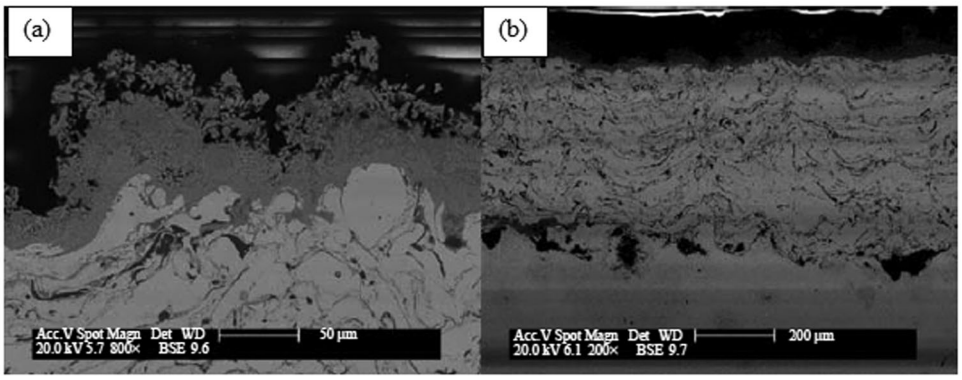

Figure 9. Microstructural cross-section of FeCrAl coating deposited on SA213-T11 steel showing corrosion attack at (a) boundaries (grain and splat), and (b) the interface of the substrate and coating [55].

system and reported that for arc-sprayed coatings. They attributed the wear resistance to the precipitation of hard surface particle of chromium-alloyed iron borides in the coating. This can be explained by the homogeneity of the elemental powder distribution with good consolidation that influences the coating characteristics in offering protection.

Reddy et al. [59] deposited FeCrAl on stainless steel substrate using laser cladding technique for application in boilers. The microstructural changes were investigated when HCL and KCL are introduced. As a candidate coating for HX surface in commercial power plants, FeCrAl was found to produce preformed alumina scales when the temperature was set at 450°C but suffered chlorine-based corrosion. This could be because chlorine reduced the amount of chromium in the coating, causing a significant mass change as shown in Figures 9 and 10. Yoo et al. [54] also mentioned that 304L stainless steel is often used in heat exchangers because it contains Cr and Ni, which are responsible for high corrosion resistance due to the Cr oxide formed on the surface as a passive layer. They further revealed that this Cr could be eroded when operating at elevated temperatures at hostile environmental conditions, leading to corrosion attacks in severe environmental conditions. They used the laser surface cleaning (LSC) method to solve the corrosion problem in 304L stainless steel by increasing

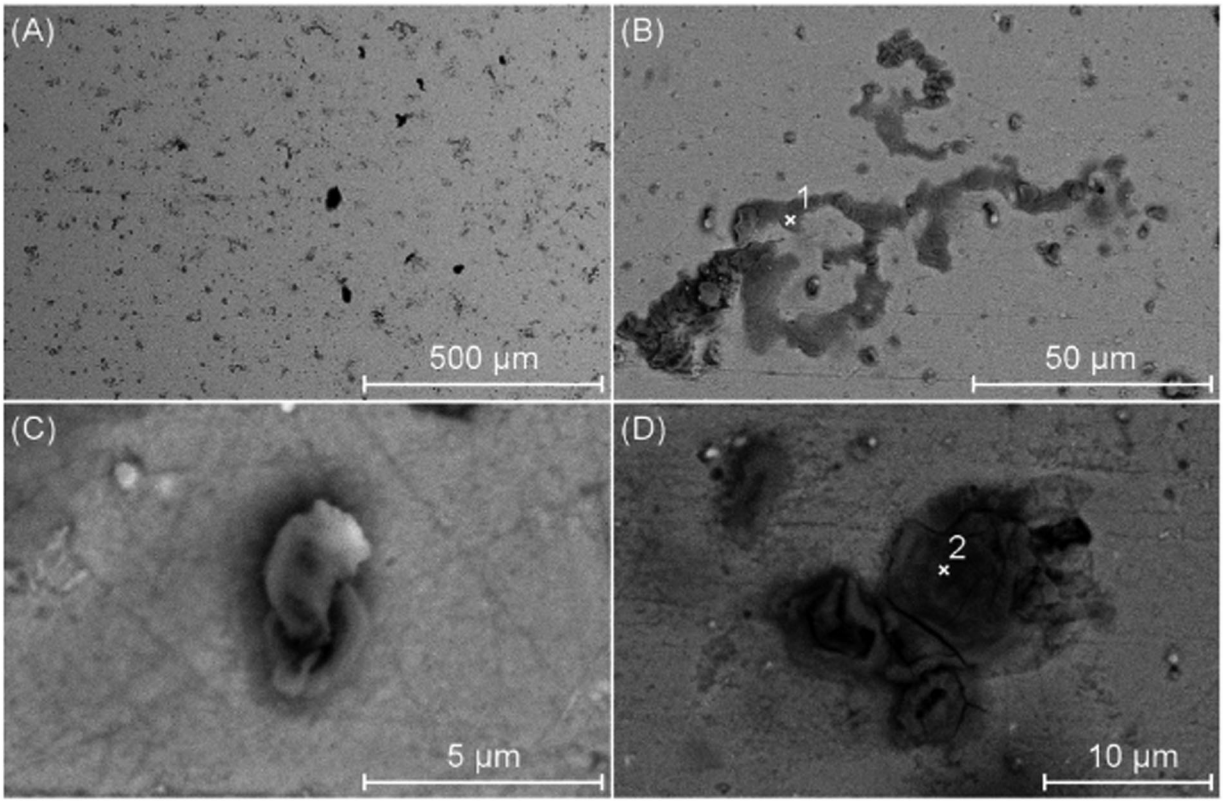

Figure 10. Oxide formation on the microstructural surface after exposure to HCL (A) Thin oxide (B) other morphology deposits (C) Structure in the form of plume (D) other surface morphology [59].

Table 1. Material properties of some commonly used copper-based alloys.

Copper-based alloys	Designation	Thermal conductivity (W/m-k)	Tensile strength (MPa)	Density (10^{-3} Kg/m^3)
Cu-Ni 90/10 [68]	C70600	50	320	8.9
Cu-Ni 70/30	C71500	29	420	8.95
Cu99.9	CDA14410	391	221	8.89

the surface temperature from 447.2°C to 611.6°C and subjecting the coating to NaCl solution spraying every 12 h. The hatch distance was varied for two parameters (0.1 and 1.8 mm) and the number of repetition (1 and 18) to create three specimens (LSC 1.8/1, LSC 1.8/18, and LSC 0.1/1). Heat accumulation was suppressed when laser surface cleaning (LSC) was used with a large hatch distance of 1.8 mm compared to a lower hatch distance of 0.1. The LSC 1.8/18 (1.8 hatch distance, 18 repetitions) resulted in improved microhardness from 224.1 HV to 270.4 HV, and they recommended a relatively low energy input LSC process with several iterations that can cause the least modifications to the microstructure and mechanical properties after LSC. The removal of the corrosion products using the LSC parameter of 1.8/18 and 0.1 demonstrates the effectiveness of LSC as a surface cleaning approach for removing impurities from a variety of industrial components vulnerable to corrosion attack.

Hussain et al. [60] also studied FeCrAl, In625, NiCr, and NiCrAlY as candidate materials for coal/biomass Co-fired power plants deposited on the T91 steel substrate. The samples were investigated for corrosion resistance together with the quality of the microstructure. The coatings made of FeCrAl and NiCrAlY were found to be more porous than those of In625 and NiCr. In addition, the FeCrAl microstructure is reported a porous layer on the microstructure, which could be due to inadequate melting. FeCrAl followed NiCr in ranking, showing less metal damage underexposure, which is attributed to the protective chromium oxide layer, proving that the amount of chromium in the material determines the resistance level against corrosion and the ability to withstand failure in hostile environmental conditions.

On the other hand, stainless steel including SS316L and SS304 are suitable substrate materials due to the Cr oxide-passive layer formed on its surface, improving its corrosion resistance [54]. Because of this, stainless steels are chosen by researchers as substrate materials during laser deposition. Losada et al. [61] also investigated the performance of carbon steel and low alloying stainless steel as base materials in heat exchanger coatings against fouling and corrosion when used in geothermal energy involving brines. For carbon steel, they selected type EN 10028:2 P265G which they report as good for high-temperature applications. 316L is also selected as a suitable coating due to its relatively low cost. The coatings on steel proved to have excellent adhesion with no damage observed, whereas some blisters and rusting on the coating surface were observed for carbon steel. It can be concluded that stainless steel is good base material compared to carbon steel because it is prone to rust.

On the contrary, low-carbon steels are suitable for depositing corrosion-resistant heat exchanger coatings. They form good interfacial bonding with most alloy coatings. Ideally, their corrosion resistance is improved by protective layers formed by coatings to inhibit corrosion attack [62]. For instance, Chanda et al. [63] electrodeposited a crack-free chromium-based alloy coating (Ni-CR-P) on AISI 1020 low carbon steel at pH 3.0 and room temperature of 25°C to improve its corrosion resistance. The improved corrosion resistance is attributed to the presence of Cr, which forms a protective layer normally consisting of Cr_2O_3 and CrO_3 oxides, leading to increased

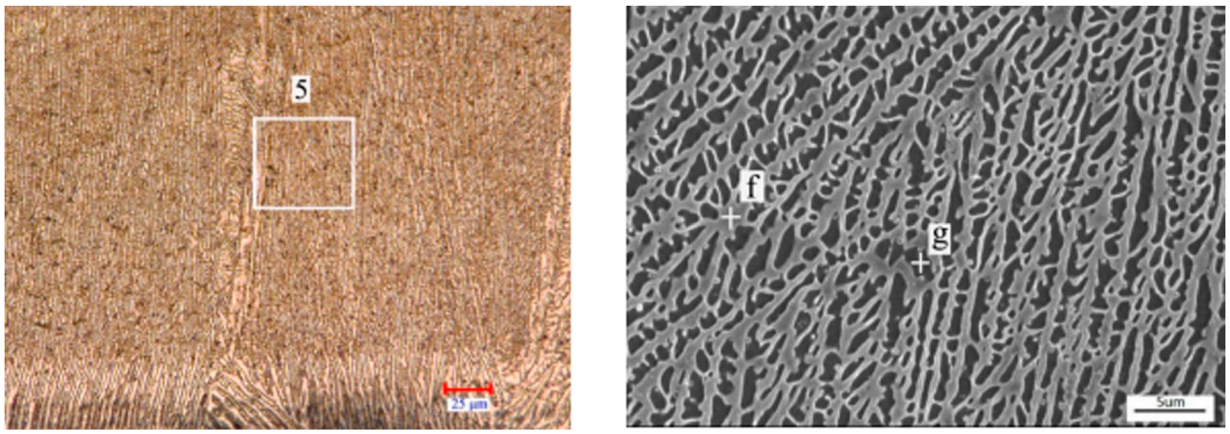

Figure 11. Enhanced microstructure of laser cladding Ni-Cr-Si coatings deposited on copper substrates (a) dendrites and columnar grains formation (b) magnified view of the square labelled 5 [71].

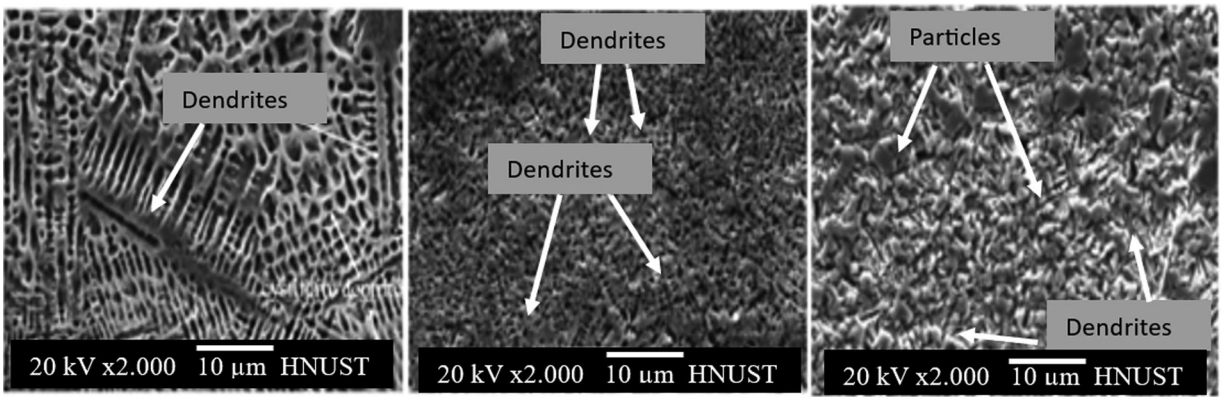

Figure 12. Microstructural transformation of laser cladding Ni–Cr/TiB_2 coatings on copper substrate (a) dendrites formation with the addition of 5 wt% TiB_2 (b) 10 wt% TiB_2 (c) 20 wt % TiB_2 with particle formation [71].

formation of interfacial contact resistance. The research results also showed that these oxides improve corrosion resistance but suffer attack by hydrated oxides in humid environments leading to the formation of pits on the surface. To improve on this, they increased the Cr content to alter the composition and microstructural properties of the coating to withstand pitting corrosion. This indicates that low-carbon steels are good substrate materials but suffer pitting degradation if the Cr content is reduced. In addition, the incorporation of Cr elements into the coatings can alter the microstructure to form anti-corrosion stable oxides upon exposure to severe environmental conditions. It is worth noting that a higher carbon content is not desirable because it lowers the material ductility and weldability, which can pose a significant challenge during laser cladding of heat exchanger coatings. Low-carbon steels are therefore used instead because they have lower carbon content. In addition, they are ideal as base materials during laser cladding because they don't require additional preheating, especially those characterised by ferrite and pearlite.

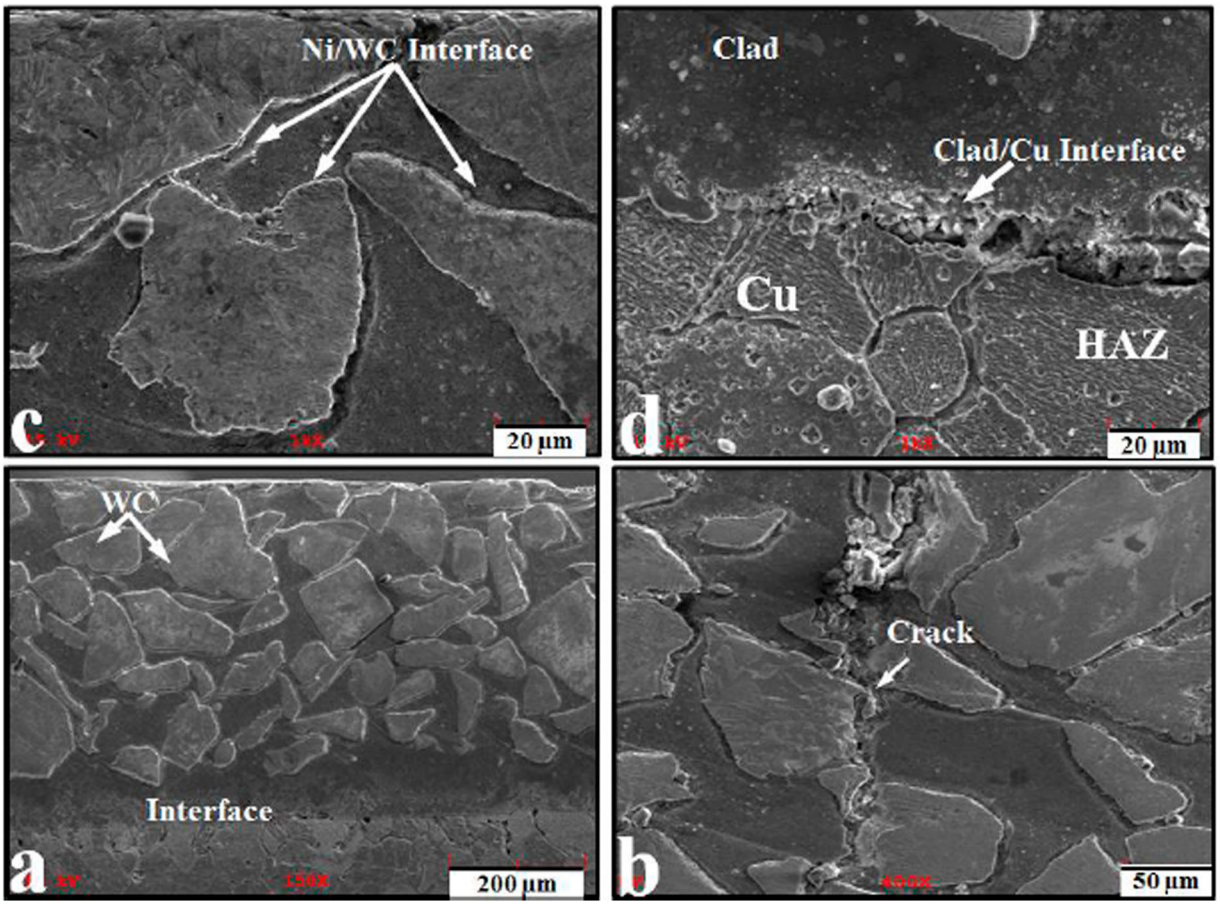

Figure 13. Microstructure of Ni-C-B-Si-W alloy cladded on a copper substrate with (a) good substrate/coating metallurgical bond (b) some cracks viewed at high magnification (c) large Ni/WC Interface and (d) good bond viewed at the clad/Cu interface [73].

This is attributed to the phase transformation that occurs when the laser beam interacts with the substrate causing pearlite to dissolve and form a martensitic structure in the heat-affected zone. Cracking can also occur in the HAZ if the laser power is low because segregation of impurities will be hindered during deposition [64,65]. This confirms that heat exchanger tubes made of carbon steel excel in corrosion resistance due to the presence of chromium, iron, and manganese.

Copper-alloy substrates and coatings

Copper alloys are noble ductile metals with outstanding characteristics such as good corrosion resistance and high electrical and thermal conductivity. For this reason, it is an indispensable material in fabricating heat exchangers, and heat sinks, where high thermal resistance and good heat transfer are required [63]. Moreover, copper forms oxide films that are anticorrosion protective layers when they react with water. Mahmood et al. [66] investigated the thermal performance of copper coatings for heat exchangers using an experimental thermal system and showed that the surface characteristics of copper could be improved by increasing microstructural grain size, which enhances heat transfer. This implies that material selection affects corrosion resistance and heat transfer efficiency. It also shows that the surface-to-volume ratio plays a significant role in the heat transfer efficiency of copper coatings. For this reason, they chose copper in their study because of its good thermal conductivity that reaches up to 62%, which is higher than that of aluminium and stainless steel, the two materials reported to be alternatives to copper. In addition, they revealed that the anodised copper coating can be instrumental in the design of heat exchangers through equipment size reduction. This can help in reducing material waste and costs. However, its low strength, poor corrosion resistance, and low hardness limit its industrial application due to reduced service life as a result of surface degradation, amongst other factors. Hence, its alloys continue to be explored by researchers to attain superior material properties with combined functionalities in heat exchanger applications.

Schleich [67] also stated that CuNi 90/10 alloy is a candidate coating material for piping material, especially in seawater subsystems. However, they state that it is susceptible to erosion-corrosion and corrosion damage when operating in polluted waters, indicating the need for careful design considerations and material selection before design. Also, they state that a cuprous film produced during chemical reaction protects against corrosion attack, showing that copper-nickel alloys such as CuNi 90/10 are resistant to some attacks, such as localised corrosion crevice corrosion and can be successfully implemented in the fabrication of high-temperature devices such as heat exchangers. Table 1 summarises its material properties and other commonly used Cu-based alloys.

Jin et al. [69] argued that even though copper has good thermal properties, it is often difficult to perform laser cladding on copper and its alloys. They attributed that to its poor wettability with other metallic, and high reflectivity, reducing the energy input required for a stable molten pool. This leads to pore and crack formation due to inadequate particle melting. Because of this, Jin and co-investigators revealed that Ni-based alloys are suitable candidate materials for cladding with copper because of their good wettability with the substrate. In agreement with Jin`s group, joining Ni and Cu is desirable because of the formation of Ni-Cu solid solutions and phases that can enhance the hardness, corrosion, and wear properties of heat exchanger tubes. For example, the laser cladding technique enhanced the microstructural properties of Ni-Cr-Si coatings deposited on copper substrates by Zhang et al. [70]. The findings revealed the formation of Ni_2Si dendritic phases at the top and columnar grains at the bottom, having an average microhardness of 900 HV0.1 (Figure 11). The dendrites are formed due to rapid solidification of the laser cladding technique leading to the growth of columnar grains, showing that copper alloys can be successfully fabricated via laser cladding to produce desirable phases that influence microstructural properties.

labelledFurthermore, reinforcement materials (e.g. Ti, C, and W) have been found to improve the microstructural properties of copper and its alloys. For instance, Yan et al. [71] added TiB_2 and CaF_2 to Ni-Cr coating produced by laser cladding on Cu-Cr-Zn alloy substrate to improve the tribological properties. The addition of TiB_2 from 5 wt% (Figure 15a), then 10 wt% (Figure 12b), and 20 wt % (Figure 12c) resulted in a microstructural transformation from martensitic structure to cystic form-dendrites, and reinforced particles. This is attributed to the improved microhardness reaching 946 HV0.1, and improved wear resistance that was 6.32 times better than that of the copper substrate, showing that coatings can improve the poor wear resistance of copper and other properties which are dependent on the microstructural development.

Balu et al. [72] cladded copper substrate with nickel-based alloy to improve its wear resistance properties. The substrate was preheated at 300°C to prevent processing defects caused by poor laser beam coupling, which could also be related to avoiding thermal shock. The Ni-C-B-Si-W alloy is reported to have an improved hardness of 572 HV which was 7 times higher than the substrate hardness of 84 HV. The coating had different microstructures at different regions analysed due to varying cooling rates as a function

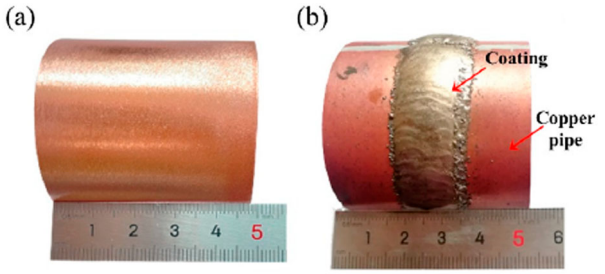

Figure 14. Laser cladding Ni60A on copper pipes Original copper pipes before deposition [73].

of time. The SEM micrographs at the cross-section exhibited a uniformly distributed nickel matrix containing large particles of tungsten carbide (WC) (Figure 13c), having some few cracks (Figure 13b) and a rough carbide particle surface (Figure 13d), with a good substrate/coating metallurgical bond (Figure 13a). Interestingly, it can be seen that copper and nickel-based coatings can form a good metallurgical bond with the substrate, which is desirable when modifying the surface of copper heat exchanger tubes.

For example, Lv et al. [73] successfully deposited Ni60A coating on heat exchanger copper tubes and obtained (Figure 14) using the plasma cladding technique. The phase composition was characterised by CrB phases having a grey dendritic phase. However, their hardness and wear resistance is reported to have reduced at temperatures exceeding 850°C. These undesirable properties, which reduce the component's service life, can be improved through the addition of intermetallic to improve the wear resistance and hardness properties.

Ng et al. [74] illustrated the use of intermediate layers in joining dissimilar materials. Cu and Mo are dissimilar materials with different materials properties, thus it is not easy to join them. To overcome these limitations, they employed Ni as an intermediate layer because it is compatible with Cu and Mo. The

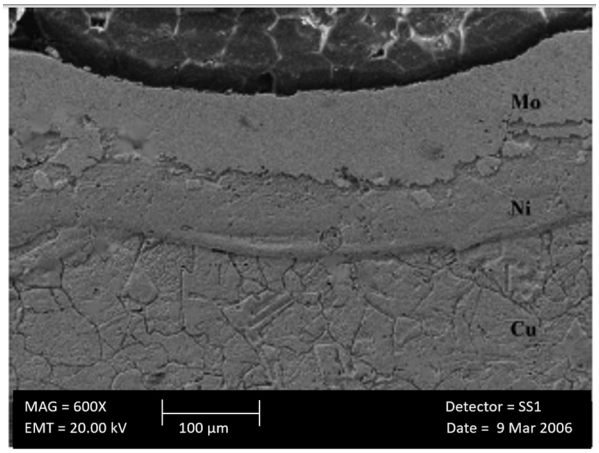

Figure 15. Strong interfacial bonding between Mo-clad and Cu-substrate, via Ni intermediate layer [74].

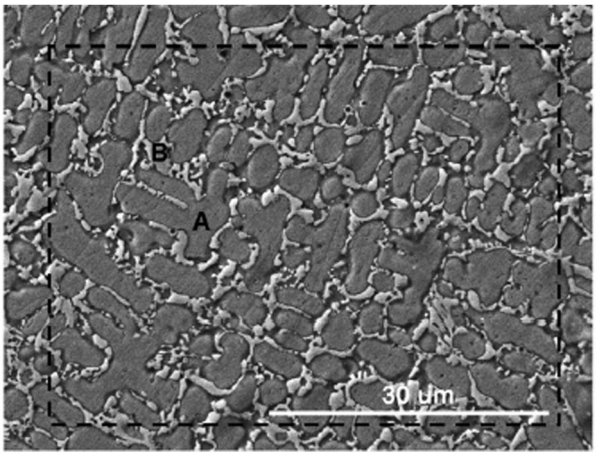

Figure 16. Nickel-based coating SEM morphology (a) dendrite (b) interdendritic phase [78].

SEM morphology in Figure 13 illustrates the strong interfacial bonding obtained between the three materials, showing that intermetallic is desirable in alloying dissimilar materials to improve the microstructural properties. They reported a 7 times increase in the hardness of Mo-clad more than the substrate Figure 15.

Nickel-based substrates and coatings

A superalloy is an alloy consisting of nickel, cobalt, or iron as base elements, making them possess excellent oxidation resistance, creep, corrosion, and erosion at elevated temperatures above 648°C. Nickel-based superalloys are the best-preferred candidate for heat exchanger applications because they contain essential solutes characterised by titanium and/or aluminium. The same is reported to have a Face Centred Cubic (FCC) austenitic crystal structure that retains the gamma (γ) equilibrium microstructure and the gamma prime (γ'), which is responsible for the high strength and creep resistance at high temperatures. Some nickel-based alloys include NiCrAl, NiCr, NiAl, and NiCrMo because they form aluminium-rich oxide scales, which enhance the rate of corrosion protection during service.

Nickel-based coatings have also found application as boiler tube overlays because they offer good resistance to dry gases e.g. carbon dioxide. Conversely, the coatings suffer attacks when operating in environments having chlorine. Literature does not show how chlorine and metal oxides penetrate the nickel coatings. This article, therefore, elucidates how cracks and pores introduced during fabrication affect the microstructural resistance against corrosion attack. Ahmad [75] indicated that adding elements that form scales such as Cr and Al can improve nickel coatings' corrosion resistance and the parts' life span. This is attributed to the stable oxide layer produced by Cr. As such, an increase in Cr content leads to an increase

in corrosion protection of nickel coatings. For instance, Chanda et al. [63] showed that the increase in Cr content improved the resistance against pitting corrosion of Ni-Cr-P coating when deposited on AISI 1020 low-carbon steel by forming a layer of protection at the surface. Due to good material properties, the research focus of heat exchanger manufacturers is to utilise nickel-based coatings in boiler tubes to mitigate degradation.

Researchers have made several attempts to deposit other nickel coatings on different substrate materials due to their ability to operate at high temperatures while maintaining their excellent mechanical properties, good corrosion, and wear resistance properties [76]. Wang et al. [77] employed the laser cladding technique to deposit Ni-based alloy as a coating on ductile Cast Iron. They obtained dendrites composed of a eutectic structure that was bright white between the dendrites and a dark-grey solid solution phase found in the dendrites. They also observed less segregation of the C element in both structures and increased microstructure size. Alternatively, an intermetallic can be introduced to the substrate before cladding the coating to overcome this challenge. This was seen in the work of Wang and co-investigators [78], who introduced n-Al_2O_3/Ni interlayers to the copper substrate before laser cladding the Ni-Co Duplex coating. A defect-free microstructure was therefore obtained with enhanced microhardness properties reported to be 8.2 times better than that of the copper substrate. Moreover, they carried out X-Ray Diffraction (XRD) and Scanning Electron Microscopy (SEM) analysis illustrated in Figure 16 and found out the microstructure comprised of the γ-nickel solid solution having some metallic silicates and carbides. The γ-nickel solid solution was formed due to a dendrite composition that exhibits higher content of Cr and Ni, whereas the carbides and silicates were a result of interdendritic phases rich in Mo, W, and Ti elements.

Yinghua et al. [79] showed that the microstructure and mechanical properties of Ni-based superalloys can be improved by changing the composition through the in-situ synthesis of hard phase particles or by direct addition. They reviewed laser cladding of Ni-based alloy coating and found that improving the size and particle distribution of TiC, TiB_2, and TiB, significantly improved the wear resistance and hardness of coatings, which could be attributed to the reaction of Nb particles with C particles in the melt pool to refine the microstructure, thus avoiding the prevalence of defects such as pores and cracks. Also, adding Ti results in the realisation of the eutectic phase comprising the γ and laves phase that changes the morphology for improved properties such as microhardness. For instance, Qunshuang et al. [64]. fabricated Ni60/WC composite coating using the laser cladding technique to investigate the effects of adding Ti to the microstructure. Figure 17(a) shows the presence of Cr_5B_3 ceramic particles and $M_{26}C_6$ carbide laminar.

They further report that the addition of Ti particles resulted in the formation of Ni60-20WC-2Ti with an improved wear resistance that was 2.6 times better than the Ni60/WC original coating. This could be attributed to the added TiC particles that suppressed and restricted the growth of $M_{26}C_6$ carbides when synthesised, thus refining the microstructural grains responsible for increased wear resistance. Therefore, it can be inferred that adding Ti elements to nickel alloy coatings improves their mechanical properties, such as wear-resistance which are essential characteristics of heat exchanger parts.

On the other hand, In625 is also reported to perform best in waste-to-energy-fired boilers, especially in the temperature range of 400°C–650°C. It effectively

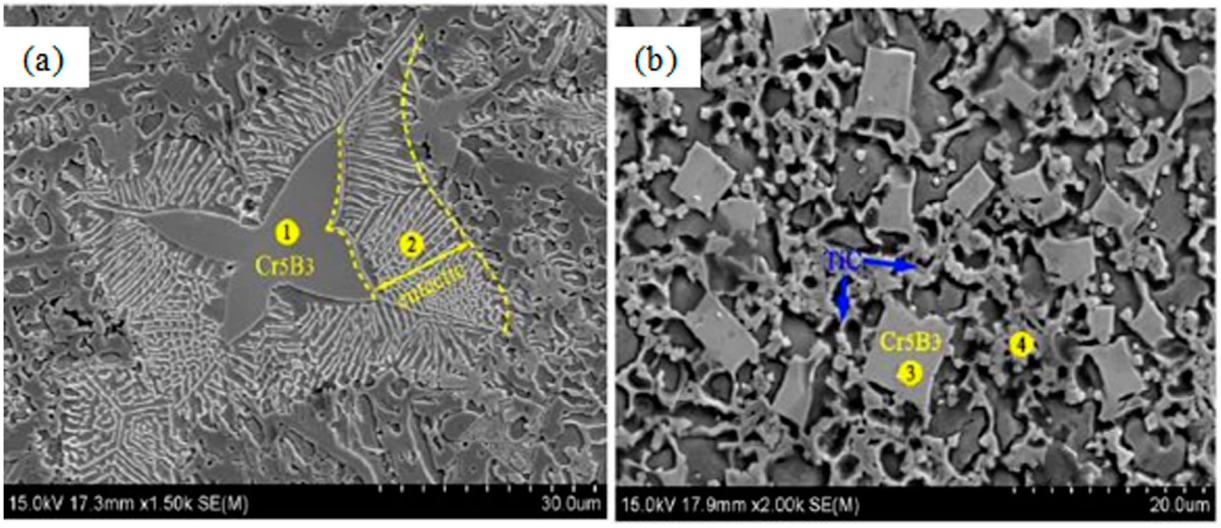

Figure 17. Microstructure of in-situ synthesised ceramic particles in (a) Ni60/WC coating and (b) Ni60-20WC-2Ti coating [64].

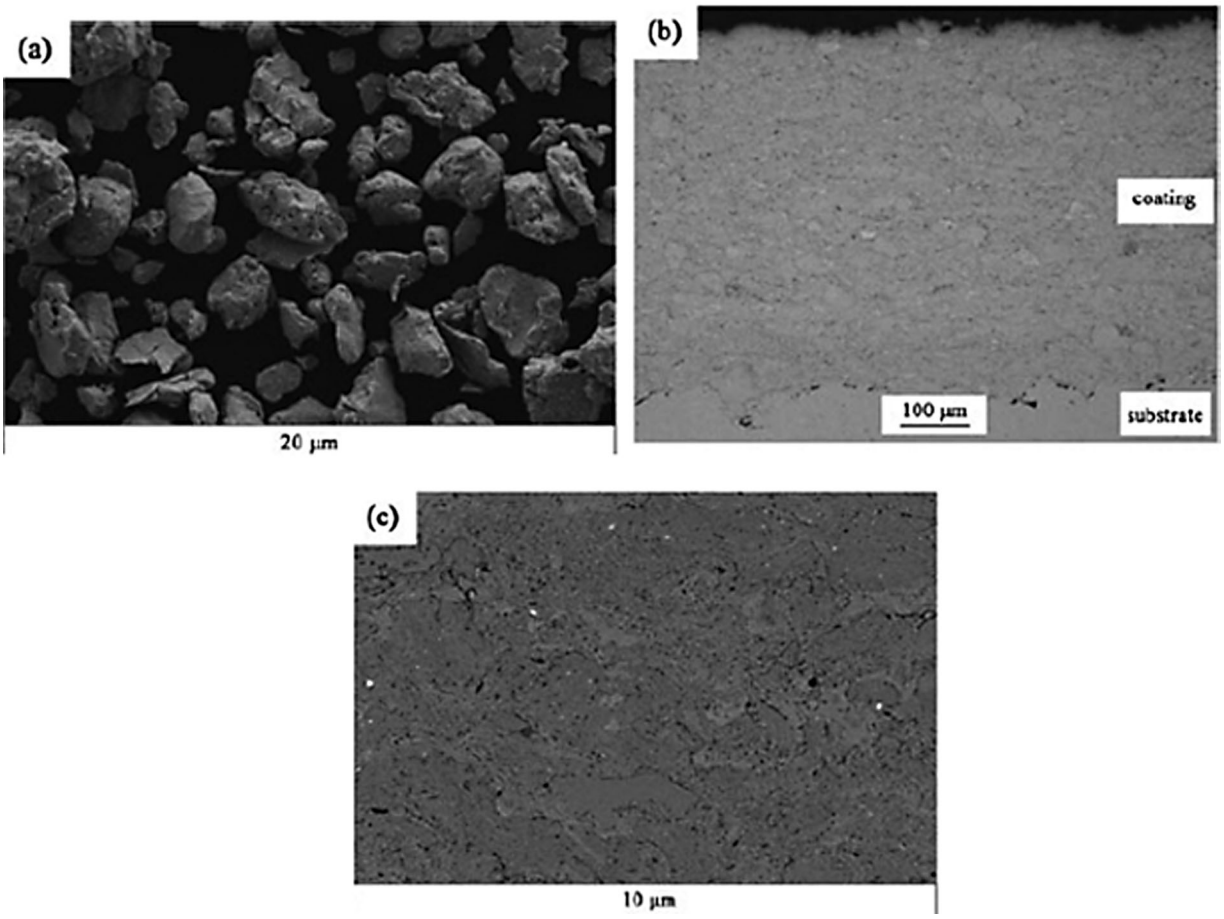

Figure 18. Microstructural transformation of NiCrC coating showing (a) course morphology and microstructure (b) good substrate and coating bond (c) cross-section of refined microstructure [81].

prevents high-temperature oxidation and corrosion when operating at elevated temperatures due to high content concentration of Nb, Mo, and Cr, which often form a protective layer of Cr_2O_3, including NiO, Nb_2O_3, and $NbCrO_4$ [65]. Hruska et al. [52] investigated the corrosion behaviour of nickel-based coatings at elevated temperatures. Two base materials that are reportedly candidates for use in biomass boilers were tested for 5000 h in an atmosphere that contained HCl and SO_2. Both low alloyed steel $16Mo_3$ and austenite stainless steel AISI 310 showed good corrosion resistance without any porosity or oxidation observed, proving they are suitable candidate materials. A similar study was also conducted by Dhaiveegan et al. [80] in which the corrosion behaviour of stainless steel 316L and 304 were investigated for 3 years of exposure in an industrial–marine–urban environment.

Tao et al. [81] successfully prepared NiCrC alloy coating to protect boiler tubes against corrosion attack using the HVOF technique. The corrosion resistance was tested using a thermogravimetric method, and the coating exhibited good corrosion resistance. This could be attributed to the dense, compact, and uniform microstructural properties obtained, which bonded well with the substrate forming a homogeneous bond. The micrographs in (a) show irregularly shaped particles, but the grain particles were refined during crushing and welding, leading to a refined microstructure seen in Figure 18. It can be seen that grain size can influence microstructural formation and transformation, causing a homogenous structure responsible for enhanced corrosion resistance. In addition, a low porosity level of 0.09% is reported, which could have improved the bonding strength that enhanced the microhardness to the average value of 727.5 HV0.3.

However, nickel-based superalloys are prone to attack and embrittlement in the presence of sulfur gases, mostly when operating at elevated temperatures. Despite the limitations, it is observed that they have found application in heat exchangers due to their corrosion resistance, implying that their level of resistance can be improved for a specified application in heat exchangers. Some commonly used nickel-based alloys include Incoloy 825, Inconel 600/625, Chlorimet, Cast nickel, and Hastelloy [82–88]. Similarly, in the work of Reddy et al. [59], pitting corrosion was found in the stainless steel samples, and they used Inconel 625 to protect it through the laser cladding technique, owing to the excellent corrosion resistance of Inconel 625. This shows that Inconel can be blended

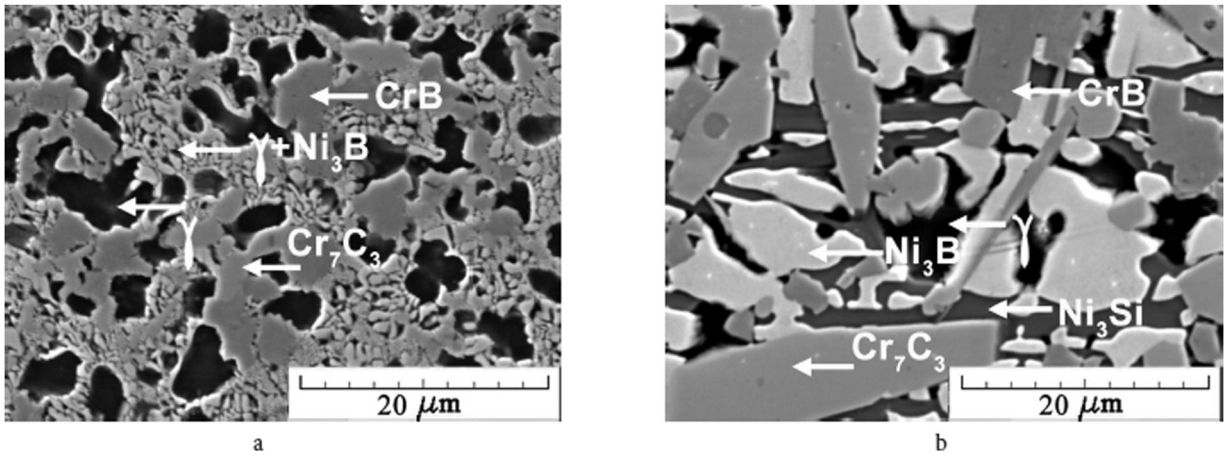

Figure 19. NiCrBSi coating on CuCrZr substrate (a) before annealing (b) after annealing with large chromium carbides (Cr_7C_3) and chromium borides (CrB) phases that improved the wear and hardness properties [90].

with many materials to produce high-grade HX application coatings. Nickel superalloys are reported to have a complex composition and have new interlayer bonding properties in the field of research, which Reeks et al. [89] argued should be studied in-depth for optimised performance.

Due to declining performance characteristics, nickel-based coatings are often limited in their application at high temperatures. For instance, NiCr-based coatings deposited via laser cladding and plasma spraying were reported to lose hardness and wear resistance at temperatures exceeding 700°C, making them prone to degradation [90]. Makarov et al. [90] stated that tungsten carbide phases can be used to improve the microstructural properties of Ni-based coatings to enhance their wear resistance at elevated temperatures. NiBSi-WC composite coating deposited on CuCrZr substrate by laser cladding was also investigated. When NiCrBSi coating is deposited with subsequent annealing, a microstructure possessing uniformly distributed structure is obtained having γ-Ni solid solutions relating to the 400–450 HV0.05 microhardness obtained (Figure 19a). Of special interest is the secondary phase transformation that takes place during precipitation and cooling, leading to the formation of strengthening phases comprising chromium carbides (Cr_7C_3) and chromium borides (CrB), with microhardness of 1650–2400 HV. Moreover, these phases improved the resistance to wear and hardness properties of the coating due to the increased size of strengthening phase particles (Figure 19b). They attribute the formation of large particles to the reaction of boron and WC carbide. This shows that annealing nickel-based coatings can cause the formation of large strengthening phases that enables coatings to perform at high temperatures, as well as improved performance characteristics such as hardness and wear, which are desirable in withstanding degradation, especially for heat exchangers operating at elevated temperatures and cyclic loading. By contrast, copper alloys can form a good bond with Ni-based alloys in producing coatings meeting the

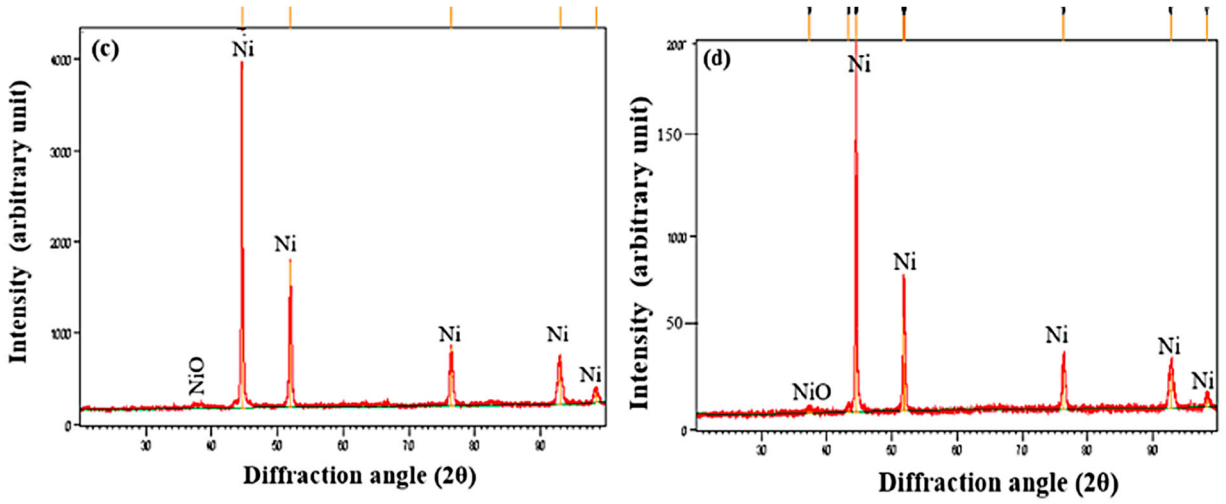

Figure 20. XRD analysis of Ni-Cr-Ti and Ni-5Al coatings deposited via wire arc spraying technique on T22 and T99 boiler steel showing the presence of NiO phases [91].

requirements for high temperature, wear, and corrosion resistance of heat exchangers.

Sharma et al. [91] investigated the high-temperature oxidation performance of Ni-Cr-Ti and Ni-5Al coatings deposited via wire arc spraying technique on T22 and T99 boiler steel. The XRD analysis showed the presence of NiO phases in excess (Figures 20 and 21), which could have improved the microhardness and corrosion resistance properties since the microhardness of the coating was reported to be 428 and 355 HV, respectively, higher than that of T91 steel (194 HV) and T22 steel (171 HV). They pointed out the increase in microhardness to the high impact velocity of the powder particles (Ni, Ti, Cr, Al), which could have caused increased cohesion strength and oxidation resistance accredited to the Cr content. The research results also showed a good metallurgical bond between the substrate and coating, characterised by splat-like microstructure with porosity levels of less than 6%, due to good adhesion properties during the melting of particles. It can be seen that higher levels of Cr content offer significant oxidation resistance, which is desirable for heat exchanger applications to mitigate the degradation initiated by oxidation reactions.

As summarised in Table 2, the surveyed literature clarifies that steels are the most popular tube material because of their superior mechanical properties and corrosion resistance. This makes them reliable in severe operating conditions due to passivation, which involves a thin protective oxide layer formed when chromium in steels reacts with oxygen to safeguard against corrosion and maintain strength at extreme temperatures. Furthermore, other elements such as nickel and molybdenum can enhance the formation of the protective oxide layer, which implies that stainless steel types with higher content of molybdenum and nickel will be more resistant to corrosion attack as compared to other types. Thus, increasing their content in the microstructure significantly enhances their microstructural properties and resistance to penetration. However, the depletion of chromium content in steel makes them vulnerable to corrosion attack when the iron in stainless steel reacts with oxygen in the presence of moisture. In addition, steels are disadvantaged when used for a prolonged time at elevated temperatures, leading to distortion of the protective film. This long exposure can also lead to attack at the grain boundary and grain boundary sensitisation, which the article found to be the main cause of failure in most heat exchanger pipes. Therefore, it is clear that stainless steel alloys are desirable for use in heat exchangers but still suffer in some operating conditions.

On the other hand, using nickel-based alloys is advantageous due to their high strength, attributed to the addition of chromium and molybdenum, which makes them retain their corrosion and oxidation resistance because it takes them longer to oxidise in aggressive media. Moreover, nickel-based alloys can form intermetallics that enhance their microhardness and mechanical strength in several operating conditions. Alloying elements can also form protective scales, solid-solution, and carbide strengthening, significantly improving their microstructural properties and characteristics to withstand degradation. Nevertheless, it is also evident that nickel alloys are not entirely resistant to degradation. In severe operating conditions, they still suffer intergranular cracking, fatigue, and tube rupture since the alloys are normally insufficient to meet the unique operational requirements.

The excellent thermal conductivity of copper alloys makes them ideal for heat exchangers. Additionally, it complements reinforcing materials effectively, greatly enhancing corrosion resistance. However, copper is a soft metal, so its alloys are vulnerable to condensation, wear-erosion, and rupture attack when exposed to oxygen, carbon dioxide, and ammonia. Furthermore, copper-related failures also come from deposits, where an abrupt loss in mechanical strength causes pitting and cracking.

Based on the given literature, it has been established that individual alloys are preferred as surface

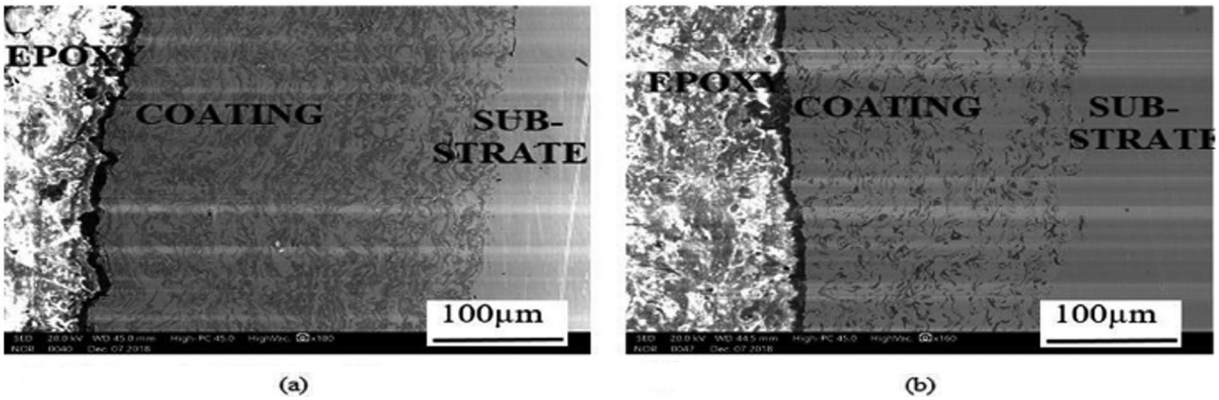

Figure 21. Plasma sprayed (a) NiCrTi coating on T91 substrate with (b) good substrate/coating bonding [91].

modifiers of boiler pipes due to their superior material properties. However, individual alloys have limited resilience in aggressive environments. Thus functionally graded materials are recommended to improve on the drawbacks [11,16,99,100]. This is because they can utilise the combination of different material properties to withstand degradation. Stainless steel, nickel, and copper are the main materials of interest in this article for the production of FGMs because they are the most often utilised tube materials.

Hence, the phase change and microstructural evolution of these groupings of materials are fully examined in the next section.

Functionally graded coatings for heat exchanger applications

Functionally graded materials (FGMs) are a new generation of multifunctional materials that can be utilised as surface modifiers to mitigate the degradation of heat exchanger parts [101]. This is due to their compositional grading and microstructure, which can be altered to perform the desired function [102–105]. Figure 22 illustrates how two materials with different compositions and properties can be varied linearly to achieve tailored properties in a specific direction. To date, the grading of dissimilar materials is a challenge to the materials research fraternity because of conflicting requirements and a lack of clear understanding of the material's thermal, chemical, mechanical, and tribological properties, which are affected by the microstructural-phase transformation during manufacturing [106]. For this reason, this section discusses the substrate and FGM interaction using findings from the literature, focusing on the influence of material properties on the FGM microstructural transformation to elucidate how it influences performance characteristics such as resistance to corrosion, wear-erosion, and oxidation.

FGMs can be employed in various industries utilising heat exchangers (Figure 23). Power generation is one of the growing energy industries that demand components with superior material properties able to withstand severe working conditions. For instance, boiler tubes are subjected to high temperatures, abrasion due to solid particles, corrosion during chemical reactions, and high pressures, causing wall thinning and ultimate failure. As such, it is impossible to obtain an individual alloy with all favourable material properties to withstand degradation conditions, except in the context of material combination FGMs. Individual coatings used on boiler tubes are susceptible to premature failure because they cannot satisfy the demand for combined material properties, showing the eminent industrial need for joining alloyed materials intended for tube coatings. According to Polat et al. [107], using FGMs is important because they reduce residual-interfacial stresses and cracking that aggravates the prevalence of calamitous failure effects caused by poor bond strength of coatings. They further revealed that FGMs are advantageous because they reduce the thermal mismatch between substrate and coating, which is influenced by factors such as thermal conductivity, coating thickness, bond strength, elastic modulus, and thermal expansion. A similar conclusion was reached by EL-Wazery & EL-Desouky [108], who stated that functionally graded coatings could be fabricated using dissimilar materials, such as ceramic-metal combinations, and produce grading's with a reduced thermal mismatch at the interface. It can be concluded that FGMs are indispensable materials for combating failures such as stress-corrosion cracking that are aggravated by thermal stresses in boiler tubes.

Repeated thermal cycles can result in the formation of thermal cracks, which degrade the quality of manufactured components. Significant residual stresses induced by thermal cycles are a key mechanism that can contribute to the formation of a cracked network. This could be a result of thermal fatigue spurred by temperature variations, regional temperature gradients, and high temperatures under confined thermal transformations. Additionally, the rapid cooling rates associated with the laser deposition process can introduce cracking mechanism spurred by high residual stresses [109]. This shows that heat input must be controlled during deposition to avoid formation of thermal cracks developed at the grain boundaries during solidification. Molobi et al. [110] also stated that the high initial thermal gradient can lead to susceptibility of crack formation due to precipitation on grain boundaries, and this could be reduced by using substrate preheating. Pellizzari et al. [111] studied the thermal crack behaviour of AISI H13 tool steel fabricated using direct laser metal deposition. They found that as the number of cycles increased from 500 to 1500 cycles, the crack length and magnitude of thermal cracks increased, as shown in Figure 24(a). This implies that high laser power must be controlled in multi-pass laser cladding to avoid multi cracks caused by large thermal temperature gradients between the substrate and coating layers [112,113]. Additionally, the thermal cycle controls the kinetics of precipitation, phase transition, and grain shape. Therefore, it must be controlled, and post-processing must be ensured to reduce the creation of defects [102,114].

The exploitation of FGMs made up of dissimilar materials has attracted far-reaching research interest due to the demand for high-performance heat exchanger components. Another reason is to solve some of the challenges encountered during FGM processing. Nam et al. [103] fabricated an FGM using Fe and SS316 powders via laser metal deposition. They reported many pores and cracks at the interface

Table 2. Summary of microstructure and property relationship of different material systems used in modifying heat exchanger parts.

	Substrate	Coating	Technique	Microstructure/Property relationship	Application	Comments	Refs
Fe-based	SA213-T11 steel	FeCrAl	Thermal spray	Protective layer containing chromium at the microstructural surface enhance corrosion properties	Boiler tubes	Steels contain chromium which enhances their corrosion resistance. Scale formation at microstructural grain boundaries of steels can lead to corrosion attack at boundaries and interface through spallation	.[55]
	Stainless steel	FeCrAl	Arc-sprayed	Homogeneity of the elemental powder distribution influences the microstructural evolution, improving the wear resistance.	Boilers	Steels containing Cr perform better at elevated temperatures.	[59]
	SS304L	Haynes 282 Ni-alloy	HVOF	Large grain size particles with good bond strength without porosity enhanced high-temperature protection of the substrate	Power plant boiler tubes	The high content of ni in steels improves oxidation resistance at elevated temperatures.	[92]
	SA213-T11 steel	Metco 41C alloy	HVOF	Carbide phases formed improved the wear and harness properties	Power plants	The introduction of SiC in the microstructural matrix can significantly improve the wear resistance properties due to perfect particle distribution	[93]
	AISI 1020 Low carbon steel	Ni-Cr-*P*	Electro-deposition	The Cr_2O_3 and CrO_3 oxides contained in the protective layer can improve the corrosion resistance but can suffer attack by hydrated oxides in humid environments leading to pitting formation	Electro-deposition	The oxide layer prevents corrosion by forming a hard surface barrier that prevents reaction with oxygen.	[63]
Cu-based	CuCrZr	NiCrBSi	Laser cladding	Secondary phase transformation due to chromium carbides and chromium borides strengthening phases improved wear and hardness properties	Heat exchangers	Formation of large particles of strengthening phases by annealing significantly improved the high-temperature wear and corrosion resistance.	[90]
	Cu-Cr-Zn alloy	Ni–Cr/TiB_2	Laser cladding	The addition of TiB_2 reinforcements is responsible for the improved hardness and wear properties.	Casting molds	Properties of copper alloyed coatings can be enhanced through the addition of reinforcements.	[71]
	Pure copper	Ni-Cr-Si	Laser cladding	Formation of Ni_2Si phases enhanced the microhardness properties.	Metallurgical and electrical industries	Solidification process influenced the formation of phases which enhanced the microstructural properties.	[70]
	Cu	Mo coating	Laser cladding	Strong interfacial bonding owing to the NI-intermediate layer, leading to 7 times microhardness improvement	Electrical contact components	Intermediate layers are useful in joining dissimilar materials to overcome the limitations in a mismatch in material properties.	[74]
	Cu:Cr (99.9:0.1)	Ni-Co coating	Laser cladding	Formation of reinforced hard phases increased the microhardness by 7 times more than the substrate	Casting and rolling	Increase in microhardness improved the wear resistance of the coating	[94]
Ni-based	16Mo3 steel	Inconel 625	Cold Metal Transfer	The secondary phases including laves phases and carbide/nitrides improved the hardness properties.	Boiler Tubes	Solidification process influenced the formation of the microstructure having a cellular-dendritic structure, as well as the segregation of dendritic regions having Ni, Cr, and Fe.	[95]
	Ductile cast iron	Ni-Cu alloy	Laser cladding	Eutectic structure and dark-grey solid solution phase, as well as less segregation of the C element, increase the size of the microstructure.	High temperature environments	Microstructural diffusion is obstructed by the low solubility of carbon present in nickel alloys. The application of ductile cast iron is hindered by the costs associated with preheating and post heat treatment.	[96]
	Ductile cast iron	Stellite 6	Laser cladding	Carbide formation that dispersed in the solid solution of Co-based matrix.	Machine tools	The presence of carbides enhanced the microstructural properties, leading to higher microhardness.	[97]
		NiCrC	HVOF	Grain boundaries as a function of grain size influenced the homogeneity of the microstructural formation that improved the hardness	Boiler tubes	Corrosion resistance was enhanced by the transformation of the grain size from coarse morphology to refined microstructure, due to adequate melting	[81]
	2.25Cr-1Mo steel	Ni-20Cr + TiC	Cold spray technique	Enhanced hot corrosion resistance due to oxide formation and the presence of Cr	Boilers	The corrosion attack on boiler steels was significantly reduced by adding TiC to the coating.	[98]

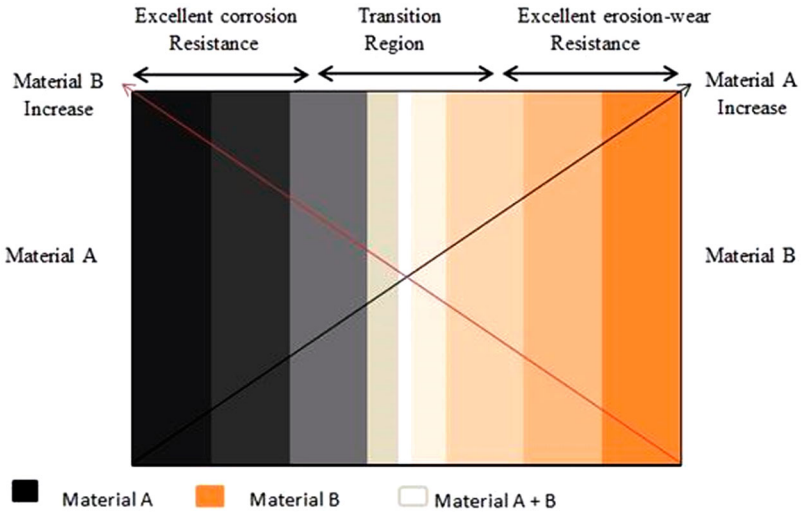

Figure 22. Variation of FGM material properties in a specific direction.

between the mild steel substrate and the directly deposited SS316, even when introducing Fe powders to the SS316. The cracking at the substrate might have been caused by the thermal shock normally overcome by substrate preheating while cracking at the interface might have required an interlayer to transition between dissimilar material properties. Olakanmi et al. [14] revealed that intermetallic coatings are useful, provided the nature of the intermetallics formed and their amount can be controlled at the desired level. To ascertain the influence of energy density on the microstructural consolidation using intermetallics, they deposited titanium aluminide (Ti-Al) blended with TiC using the laser cladding technique on the Ti6Al4V substrate. An important conclusion that can be drawn from their work is that intermetallics can be useful in refining the developing desirable phases (Figure 24) and enhanced microstructural properties as energy density is varied (Figure 25). Further, they can enhance the microhardness characteristics of FGM coatings, which is desirable for heat exchanger overlays in preventing oxide penetration. Of equal importance is that processing parameters can influence the microstructural reaction responsible for initiating good quality characteristics such as

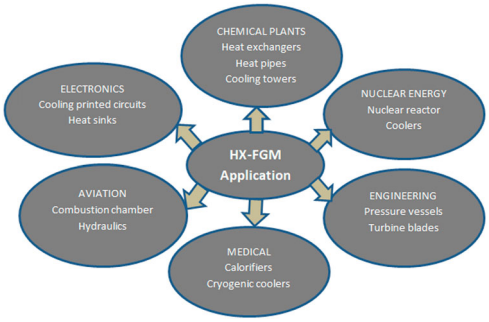

Figure 23. Potential fields of FGM application in the heat exchanger industry.

microhardness, which are desirable performance characteristics for heat exchangers.

A significant amount of data about FGMs has been developed with continuous material property discrepancies, [11,105,115–119] especially on stainless steel, copper, and nickel.

Liang et al. [120] used a laser-engineered net shaping process to develop two different functionally graded SS316L and Inconel 718. The structure varied gradually from 100% layer of SS316L to 100% layer of In718. Of importance in their study is the microstructural evolution observed that was rich in columnar dendritic growth, which occurred in both the transverse section and the normal section. They concluded that the columnar to cellular microstructural transition in the first FGMs (FGM1) resulted in decreased microhardness (0–50 v/o) between substrate and SS316L due to the rate of solidification occurring between ferrite and austenitic structure during deposition. However, when Inconel 718 was added to the grading, the microhardness of the second FGM was significantly increased because of the Cr, and Mo elemental reinforcements that led to solid solution strengthening, as illustrated in Figure 26. The wear resistance of FGM2 was also investigated and found to exhibit excellent wear resistance for both 100% layers of SS316L and In718. It can be seen that the addition of strengthening elements such as Cr and Mo content can significantly improve the hardness of FGM coatings which is desirable for erosion-wear and corrosion resistance in heat exchanger boiler tubes.

Zhang et al. [19] fabricated an SS316L/IN718/Cu functionally graded material on SS304L substrate by joining dissimilar materials having different material properties, using SS316L as the first layer build-up, followed by IN718, and then pure copper. They developed the FGM to combine the high thermal conductivity of copper, the high-temperature

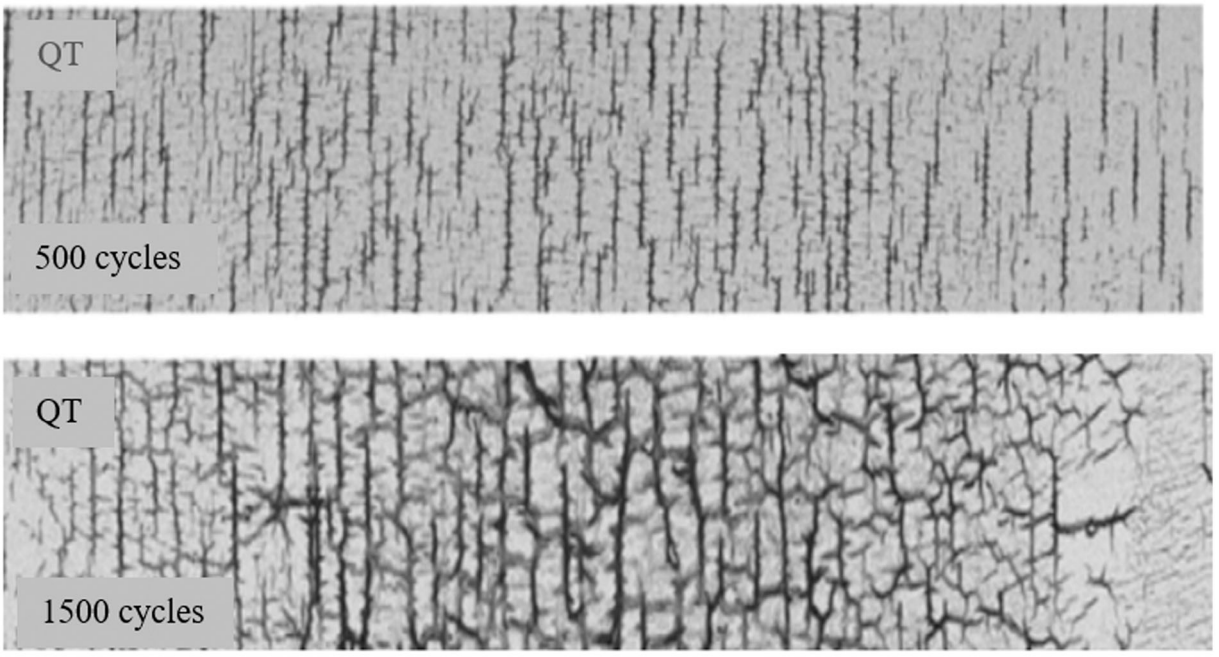

(a)

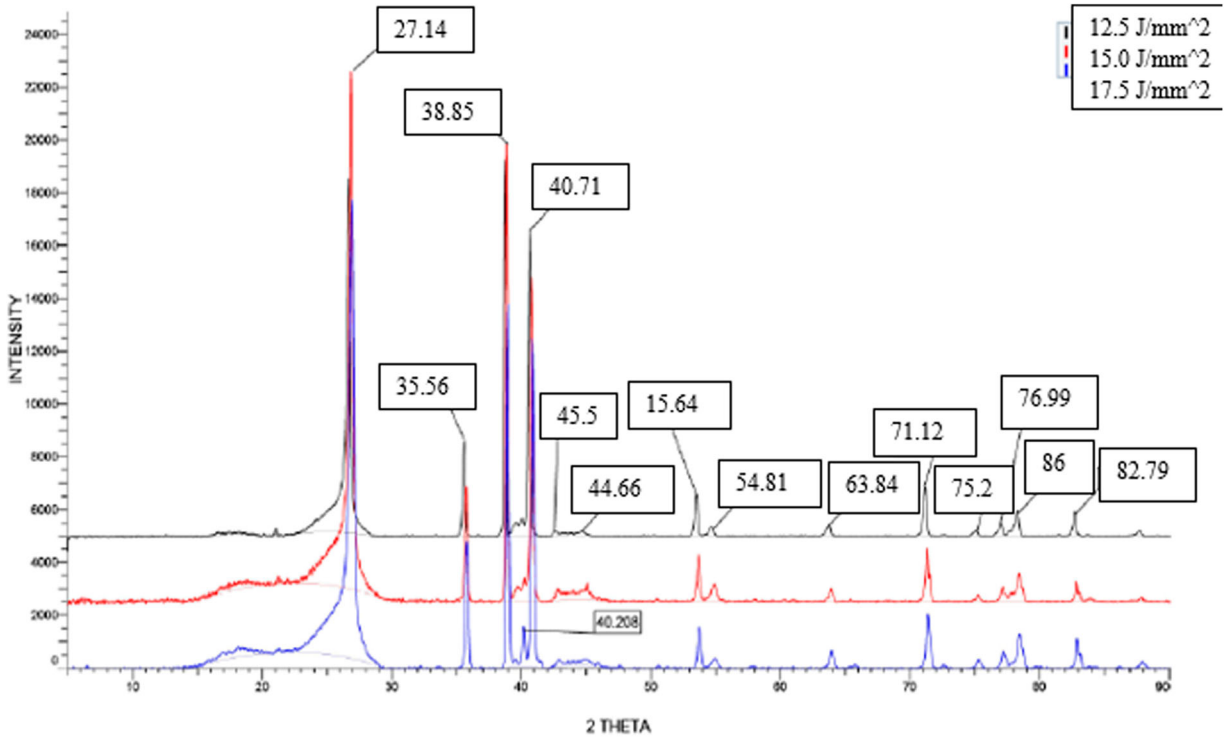

(b)

Figure 24. (a) Thermal crack frequency due to thermal cycles. XRD analysis of functionally graded Ti-Al, showing enhancement of phases formation with increasing LED [14].

strength of In718, which was also an interlayer, and the excellent corrosion resistance of SS316L, for parts subjected to harsh environmental conditions such as elevated high pressure and corrosion. The microstructure obtained was defect-free, with a 125% improvement in thermal conductivity which could be attributed to the excellent interfacial bonding achieved with combined material properties. A good consolidation between the SS316L/IN718 interface was observed, as shown in Figure 27. Of particular interest in their study is the phase transformation that occurs in the SS316L layer, which initially had columnar dendrites in the vertical direction Figure 27(a) and changed to an equiaxed structure upon blending with In718, see Figure 27(b,c). A refined microstructure with a good consolidation was also observed at the Cu and IN718 interface, as shown in Figure 27(d,e). Zhang and co-investigators [19] did not vary process parameters in their study, a process that can be further investigated to enhance

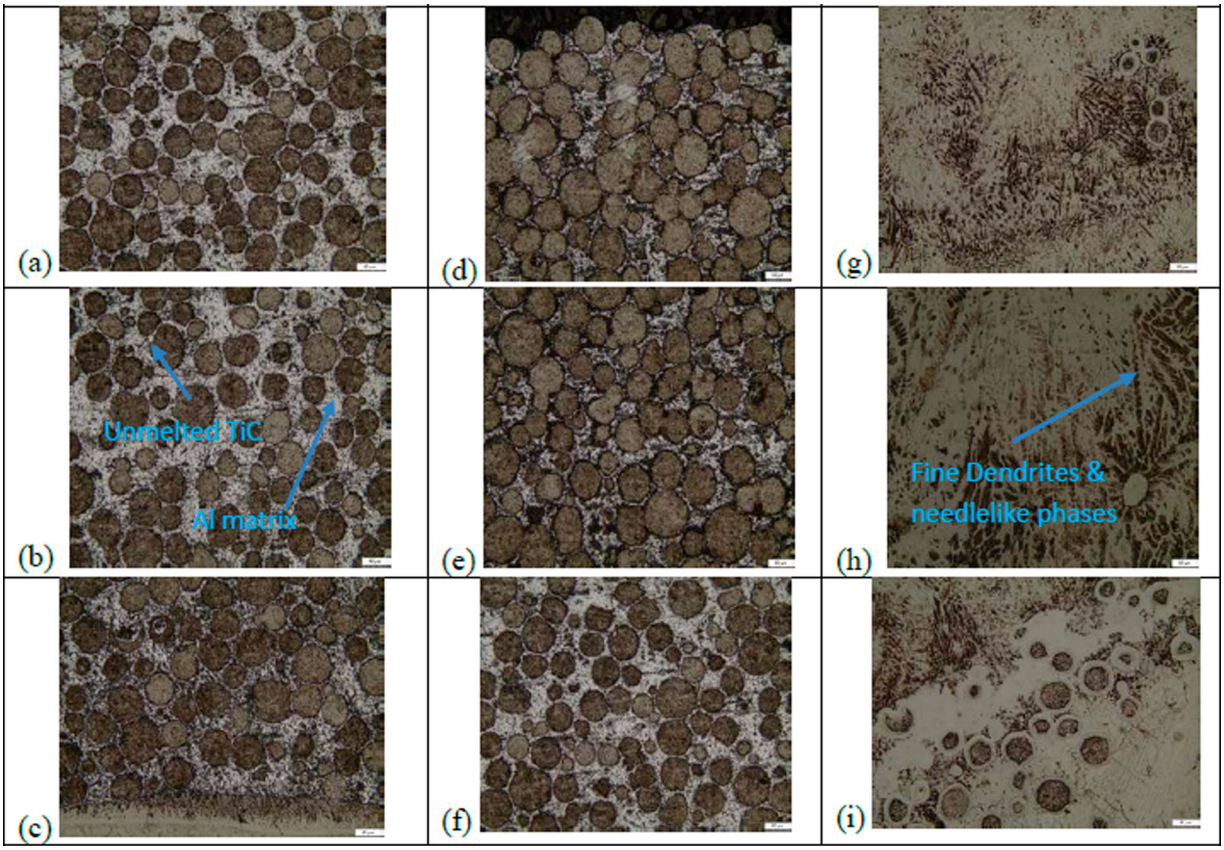

Figure 25. Optical micrographs showing the level of particle melting with 12.5 (a,b,c); 15.0 (d,e,f), and 17.5 J/mm^2 (g,h,i) [14].

the material properties by determining the optimum parameters. Also, certain alloys which are of interest to the heat exchanger tubing industry, such as Inconel 625, can be used when joining stainless steel 316L and pure copper to exploit their resistance to degradations, including pitting corrosion, erosion-wear, and stress-corrosion cracking.

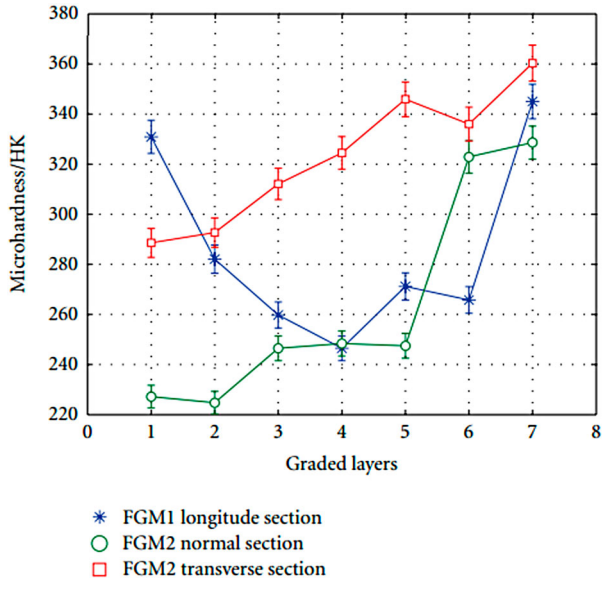

Figure 26. Variation of the microhardness along the direction of SS316L/In718 grading [120].

Luo et al. [121] investigated the hot corrosion behaviour of functionally graded Inconel 718/Haynes 25 with a 75% Na_2SO_4 and 25% NaCl molten salt coating at 700°C and 900°C. Figure 28(a–f) illustrates the micrographs obtained showing a microstructural transformation from coarse columnar dendrites in 100% Inconel to uniformly distributed fine equiaxed grains in 100% Haynes 25. They attribute the uniform transformation occurring to Inconel 718 as a consequence of increasing Haynes 25 content, causing a dense oxide layer that enhances the hot corrosion resistance because of the finer equiaxed grains formed with an increase in Cr content. This might be since Haynes 25 is a Cobalt–Nickel-Chromium-Tungsten alloy. Generally, Cr tends to form passivation on surfaces, suppressing the corrosion-anticipated reactions and penetration of corrosion products through the material surface. This shows that FGMs can be adopted as heat exchanger coatings to augment the properties of another material towards enhancing their corrosion resistance.

Ben-Artzy et al. [122] joined dissimilar materials comprising SS316L and C300 maraging steel to develop a grading using directed energy deposition. They chose C300 steel because of its wear resistance and high strength since it is a cobalt-containing alloy with properties strengthened by hardening intermetallic precipitates containing molybdenum (Ni_3Mo & Fe_7Mo_6). The corrosion resistance nature of SS316L

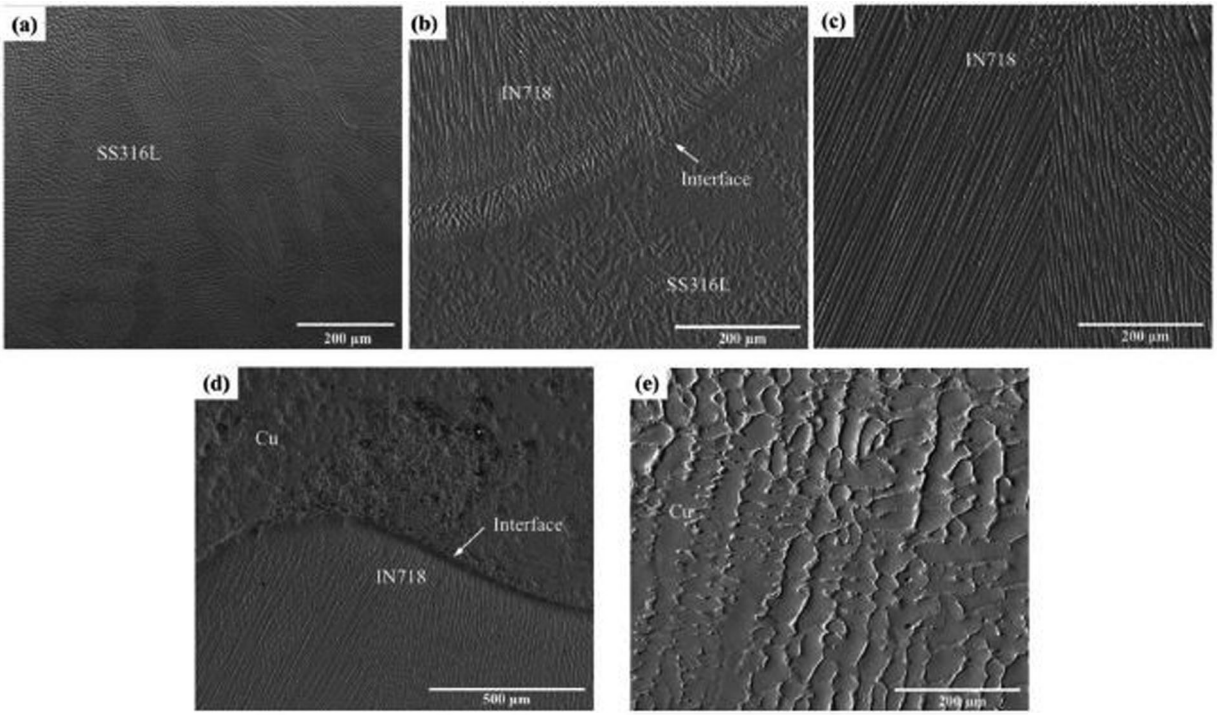

Figure 27. (a) Microstructural transformation of laser SS316L/IN718/Cu functionally graded material (a) SS316L columnar dendrites (b) good bonding at the interface (c) In718 equiaxed structure (d) good blending between Cu and In718 (e) Transformed Cu microstructure [19].

qualified it for grading since their idea was to develop a graded material with high wear and corrosion resistance. They reported that the graded coating did not have intermetallic, which they attribute to having been suppressed by the formation of the $TiCr_2$ phase. In particular, when the Cr and Mo alloying elements in SS316L are depleted in harsh environments, some intermetallics can produce intermetallic precipitation, making heat exchanger coatings susceptible to localised corrosion. Their work thus represents a successful grading of dissimilar materials.

Sun et al. [123] fabricated a functionally graded coating comprising Ti6Al4V and Inconel 625. They attributed the microstructural refinement to the nucleation rate that was significantly increased by the alloying elements. This resulted in a

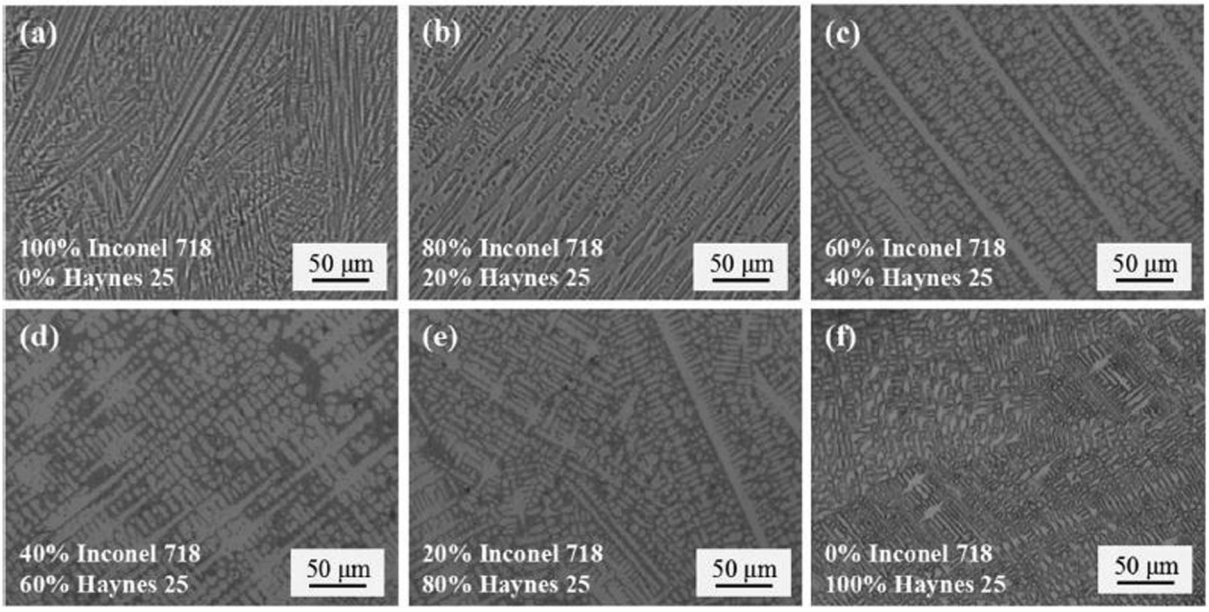

Figure 28. Microstructural variation with different compositions (a) Inconel 718 at 100%, (b) Inconel 718 at 80% and 20% Haynes, (c) 60% Inconel 718 and 40% Haynes, (d) 40% Inconel 718 and 60% Haynes, (e) 205 Inconel 718 and 80% Haynes, and (f) 100% Haynes [121].

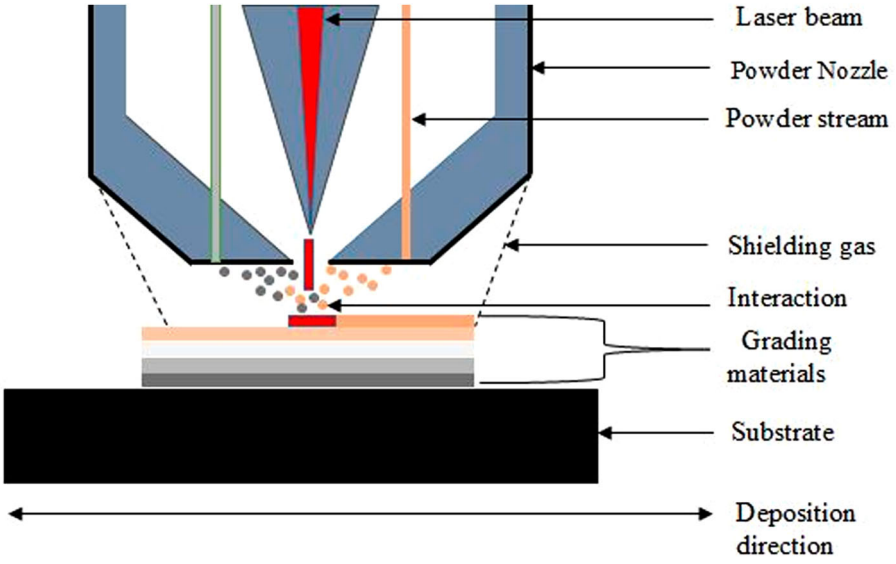

Figure 29. Laser cladding beam interaction with functionally graded material.

microstructural transformation from a laminar structure characterised by laminar phases (α and β) to an equiaxed structure as a function of compositional variation. Because of the refined microstructure, the hardness of the coating was significantly increased, which they attributed to the formation of solid solution hardening, Ti_2Ni precipitates, and $CrNi_2$ compounds. However, they encountered some cracks at the intermediate layer due to brittle phases. It can be seen from their findings and conclusion that the presence of cracks deteriorates the material performance, a processing challenge that can accelerate stress corrosion cracking in heat exchanger pipes.

Consequently, research interest is increasing to fabricate FGMs of dissimilar materials that meet the ever-increasing demand for improved system performance, lightweight and hybrid structures, and functionality that can overcome other industrial challenges. Another advantage of FGMs is the ability to join dissimilar materials, which involves joining materials with different thermo-physical properties. Hence, they have

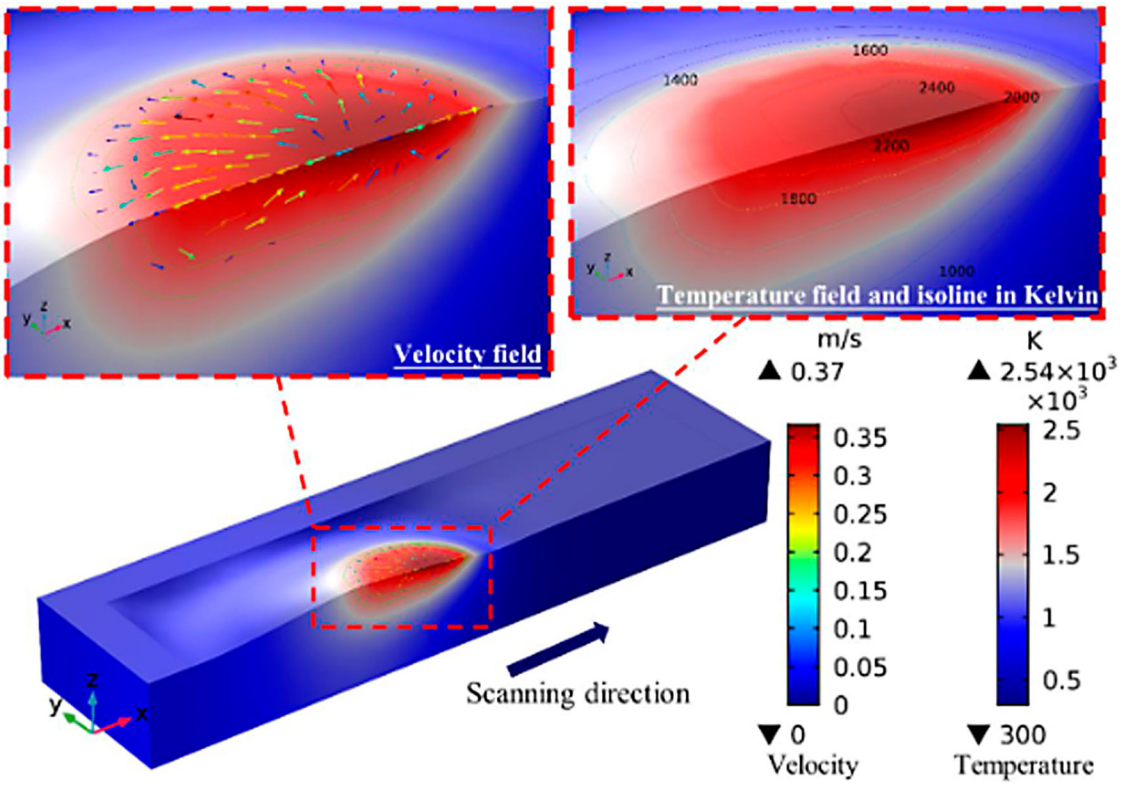

Figure 30. Laser cladding temperature field and velocity distribution [138].

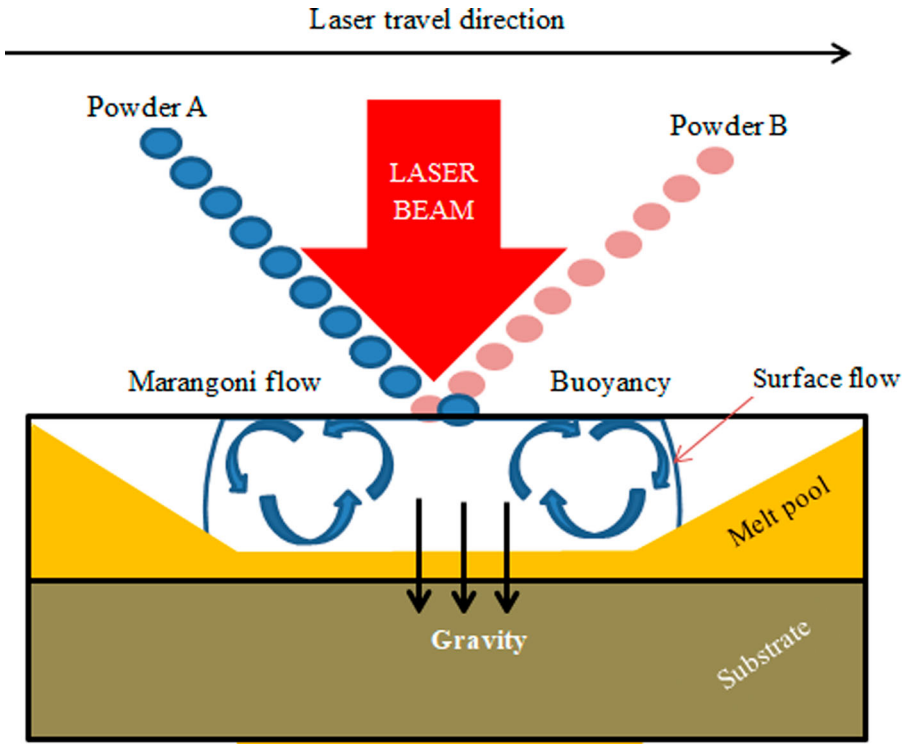

Figure 31. The phenomenon of Marangoni convection and Buoyancy (driving force) during melting laser cladding of functionally graded materials.

found applications in fabricating heat exchanger tubes. Moreover, careful material selection is critical when joining dissimilar materials to avert processing deformities. For instance, Meng et al. [124] observed that the direct joining of Ti alloys and stainless steel dissimilar materials resulted in brittle Fe-Ti intermetallic, which is the main cause of cracking. They indicated that the use of an interlayer that acts as a transition material could significantly reduce these reported cracks. Adesina et al. [125], in agreement with Pardal et al. [126], elucidated further that such intermetallics and reactive oxides experienced during deposition can influence the corrosion behaviour of coatings and even hinder the joining of materials. On the other hand, it is worth noting that some intermetallics have good properties such as NiTi intermetallics having good corrosion resistance, wear, and oxidation resistance [127]. Furthermore, dissimilar materials can be joined successfully without experiencing any intermetallics. Ben-Artzy et al. [122], successfully joined dissimilar metals of SS316 and C300 maraging steel through the DED technique without experiencing the formation of undesirable intermetallics. This indicates the joining possibilities of fabricating heat exchanger components using dissimilar materials. Several material combinations are employed in the fabrication of FGMs [128]. This includes metal–metal, [115] and metal-ceramic [108,129].

In conclusion, FGMs exhibit superior material properties and benefits compared to conventional alloys and composite materials. The increased heat transfer efficiency, [130] reduced residual stresses, and ability to join dissimilar materials makes them ideal for heat exchanger applications. Until recently, conventional manufacturing methods have been used in fabricating FGMs (e.g. plasma spraying, powder metallurgy, and vapour deposition techniques). Consequently, laser cladding has emerged as a promising coating technique that circumvents the limitations of conventional manufacturing methods. This is credited to its capability to produce fully dense FGM coatings with reduced thermal distortion and minimum dilution [131]. Thus, it can produce graded materials that reduce the corrosion and wear effect in severe environmental conditions such as exchanger tubing. On the other hand, the implementation of laser cladding has suffered significant drawbacks due to processing deformities, such as cracking, porosity, and delamination, encountered during the processing of FGMs. It remains unclear in the literature how the laser cladding process and material parameters affect the performance characteristics of heat exchangers concerning laser beam interaction and microstructural/phase transformation. Hence, this review provides a detailed analysis of laser cladding of functionally graded coatings in the next section. Micrographs are used to expound the effects of process and material parameters on the functional performance of steel-nickel-copper FGMs for HX applications.

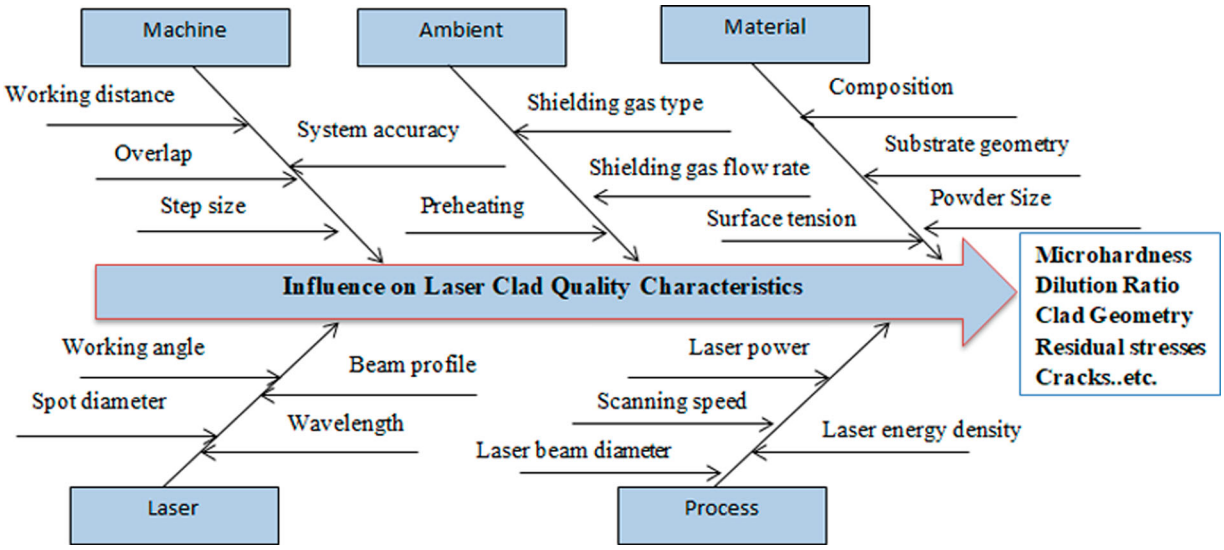

Figure 32. Ishikawa diagram showing effects of laser cladding parameters on clad quality characteristics for heat exchanger applications.

Processing of functionally graded coatings for heat exchanger applications via laser cladding

Laser-based additive manufacturing (LBAM) techniques have evolved since the late 1990s to extend the component`s lifespan through distinctive manufacturing processes such as laser cladding of heat exchanger tubes [132]. Laser cladding employs the same concept as laser metal deposition (LMD), also called directed metal deposition (DMD), directed laser fabrication (DLF), and laser-engineered net shaping (LENS) [133]. Laser cladding as an AM technique is a promising technique that finds application in process industries such as power generation and petrochemical plants due to its efficiency and ability to develop surface quality coatings with great process flexibility and provide desirable economic benefits. It melts metal powders using a laser beam to form a thin film into a substrate material to achieve a homogeneous powder mixing [134]. When the laser beam interacts with the powders, melting occurs, resulting in the solidification of the molten material presented in Figure 29. During this process, a microstructural transformation occurs as particles fuse on a substrate material to form a coating. Owing to this, functionally graded coatings can be produced with fine-grained microstructures through rapid solidification.

Despite short interaction time being desirable during laser cladding, it can lead to processing defects if the process conditions are not properly controlled. For instance, porosity due to trapped inert gas, partial penetration influenced by low heat input, and cracking because of a large thermal gradient between the substrate and the powder/laser beam can be experienced. Moreover, tensile residual stresses are normally generated during the laser cladding process due to the highly concentrated energy input and rapid fabrication velocities [135], which could lead to accelerated failure in heat exchanger parts through spallation and cracking. Normally, they occur in the transition zones of tubes leading to stress corrosion cracking [136]. However, the fabrication of functionally graded materials via laser cladding is reported to reduce the residual stresses in the material due to the interlayers responsible for expansions [19]. This indicates that FGMs can minimise the combined effect of residual stresses formed in the material during fabrication. The next section elucidates the laser beam interaction with the functionally graded materials to avert microstructural distortions and alteration of material properties.

According to Elijah [137], the heat induced during the laser cladding process causes melting and fluid flow, influencing the microstructure's phases and grain structure, dislocations, and residual stresses, which then affect the quality of fabricated parts. This might be explained by the Marangoni effect, which is a mass transfer caused by surface tension, driven by thermos-capillary forces and elemental diffusion. As shown in Figure 30, this causes a shallow melt pool to develop as the surface tension changes from low to high, suggesting that the deformation of the molten pool grows as the laser power increases [138]. They further revealed that the variation of velocity during deposition could result in unstable powder interactions with substrate, which often leads to processing defects such as cracks or pores if the movement of heat source is not controlled.

The surface tension forces, which [137] reported to have a direct relationship with temperature, prompted the elemental flow in different directions along the boundaries, forming different melt-pool shapes. Le & Lo [139] stated that surface tensions depend on the

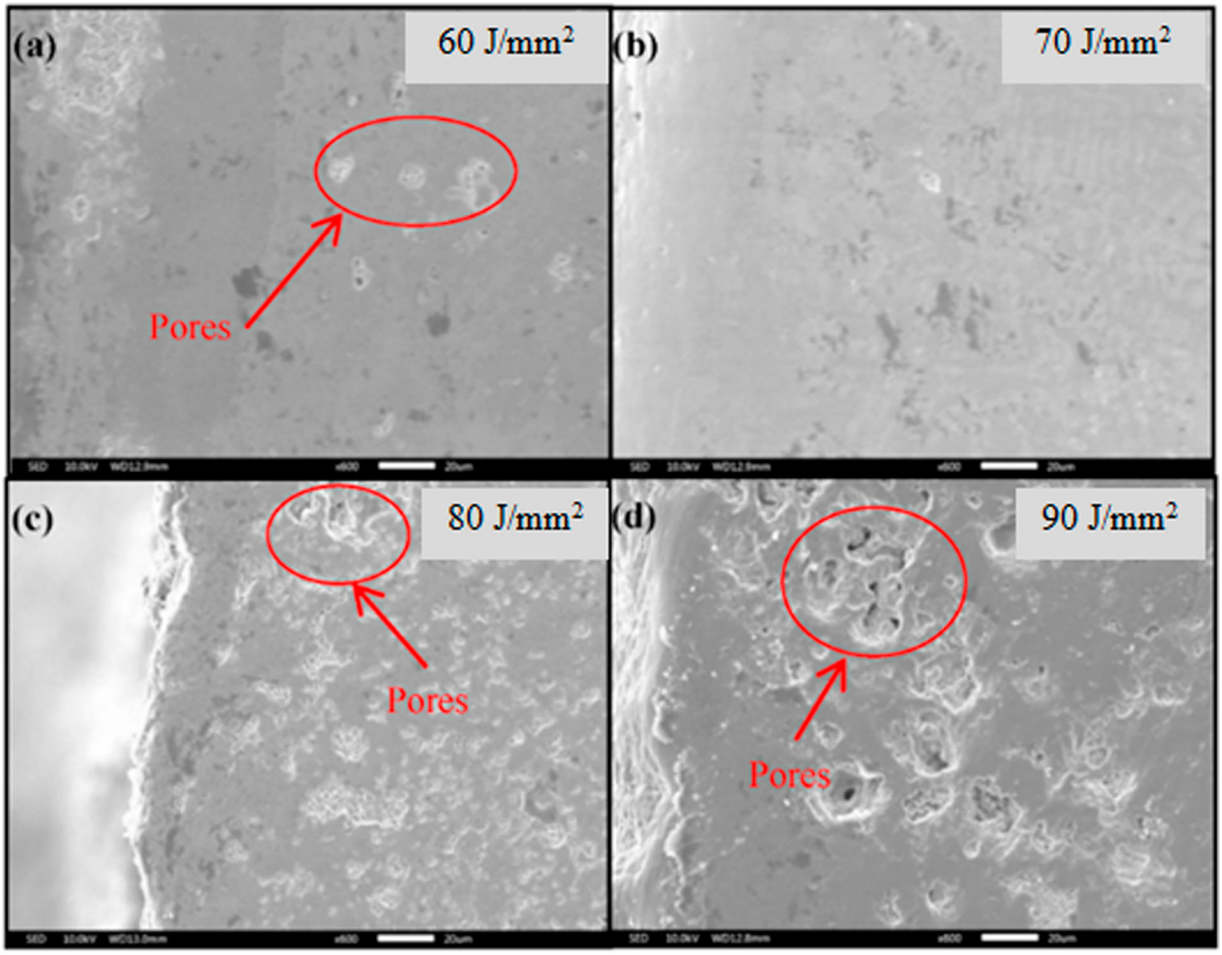

Figure 33. Morphology of HA-TiO_2 graded coatings showing effects of varying LED [148].

metal composition. This shows that a higher content of an element present (e.g. sulfur) in a material can increase the surface tension and the melt pool, because surface tensions control the flow pattern that forms in the melt pool. Equation 1 is based on the dilution rate method, indicating that X_{mix} represents the properties of the melt-pool material containing a mixture of powder and substrate materials. It is demonstrated that the melt pool generated during laser deposition is a mixture of melted powders and melted substrates, where the powder and substrate properties are depicted numerically as (X_{pow}) and (X_{sub}), respectively [138].

$$X_{mix} = \alpha X_{sub} + (1 - \alpha) X_{pow} \quad (1)$$

Where α is the mixture fraction governed by the dilution.

Figure 31 shows the movement of fluids in the Marangoni convection. When melt pools form, a transition mechanism occurs from regions with low surface tension to regions with higher surface tension. This implies that varying melting temperatures in the form of laser power can control the melt pool characteristics, affecting the fabricated component's quality characteristics. Unless et al. [140] explained that surface tension can cause the segregation of dissimilar materials within layer build-up. They attributed that to different material densities. Simply put, higher heat input is experienced during laser beam melting at the centre of the deposited material, which lowers its density. Simply put, the material at the edge will be cooler and have higher density because of the buoyancy driving force. Because of this, an increase in temperature lowers the surface tension, implying that varying deposition and pre-heating temperatures can improve the consolidation mechanism of the fabricated FGMs. Similarly, substrate preheating can reduce thermal shock during deposition, especially in dissimilar materials, and control surface tensions.

In conclusion, it is evident from the cited literature that the laser material interaction of the copper substrate and SS316L-In625 has not been explained. As a result, this study lays the groundwork for the experimental work that will address this largely unexplored area of required research.

Laser cladding process parameters

Control parameters affect the microstructure and quality of functionally graded materials during laser cladding. Numerous factors can influence the quality of the clad, which is why they are categorised.

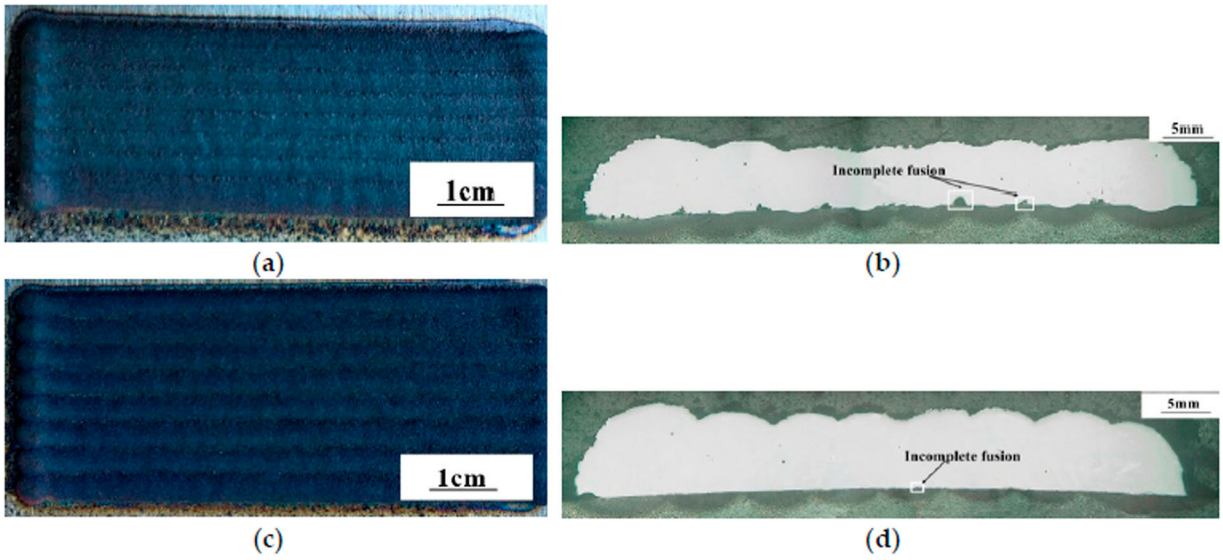

Figure 34. Comparison of clad morphology obtained using parameters from (a,b) orthogonal design and (c,d) optimal GRA values [154].

The Ishikawa diagram, often known as the fishbone or the cause-and-effect diagram is a well-known classification scheme. Therefore, the parameters affecting the clad quality during FGM manufacturing for heat exchanger surface modification are categorised in Figure 32 using the Ishikawa diagram.

Goodarzi et al. [141] posited that while various LC process parameters exist, the laser power, scanning speed, and powder flow rate have the most influence. To address the poor clad quality characteristics formed due to poor processing conditions, this section combines and elucidates four important parameters and their consequences on heat exchanger part performance using research from the literature. This includes (i) the laser energy density, (ii) the composition and particle size distribution of coating powders, (iii) shield gas type and velocity, and (iv) the substrate pre-heat temperature. Laser energy density is selected as the most important parameter because it influences the melt pool and solidification mechanism, which determines the microstructural properties that affect the performance characteristics of heat exchangers. The nature of the powder composition and particle size distribution also influences the rate of melting and consolidation mechanism. Due to some intrinsic process defects, such as porosity,

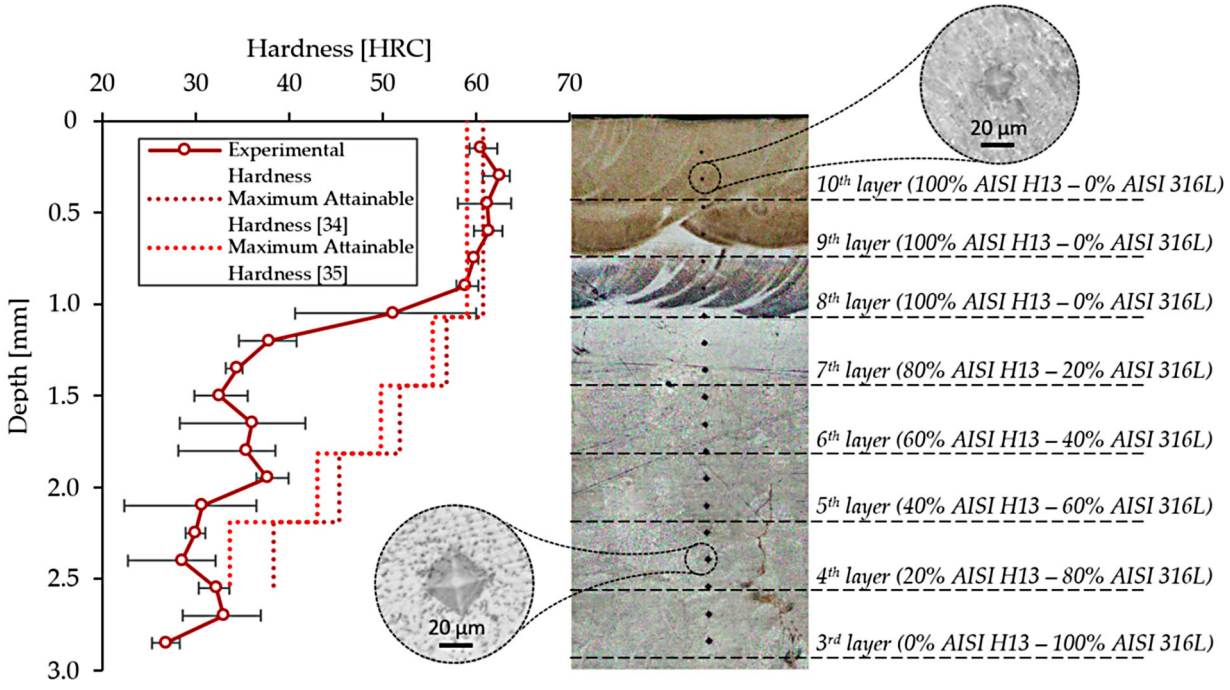

Figure 35. Variation of hardness in functionally graded AISI 316L and AISI H13 attributed to variation in composition [155].

which affect FGM clads intended for boiler tubes' resistance to oxide penetration, shielding gas was selected as another crucial parameter because it can protect the material from the atmospheric reaction during LC processing. Another important factor explored is substrate preheating, which lessens thermal gradients that can prevent fusion between the surface of boiler pipes and the deposited coating layers during surface modification. Further investigation is carried out into their impact on three qualitative characteristics. This refers to corrosion and wear, aspect ratio, and microhardness because the most frequently documented failure mechanism in heat exchangers is due to corrosion cracking, fatigue, and erosion, which are accelerated by poor clad quality and geometrical features [142].

Laser energy density

The laser energy density (LED) is measured in J/mm^2 and has a directly proportional relationship with laser power (P) as well as an inverse relationship to speed (V) and beam diameter (d), as shown in equation 2 [15]. Simply put, the energy dissipation rate as a function of time determines the molten pool size, which influences the solidification process, the morphology of the grain structure, and the geometrical characteristics of the FGM clads [143,144]. Further, an increase in scanning speed will reduce LED because the duration of laser metal interaction will be shortened since the laser beam cannot dwell longer during deposition, leading to a smaller melt pool. Moreover, the type of microstructure formed is significantly influenced by the size of the laser spot diameter, also referred to as beam diameter. Due to a reduction in the rapid cooling process attributable to the energy density, an increase in laser spot diameter will also decrease the melt pool temperature [145].

$$LED = \frac{P}{V.d} \tag{2}$$

The relationship between LED and wear properties has been investigated previously. The smaller melt pool caused by a lower LED can undoubtedly result in smaller, uneven grains, which frequently have higher porosity and less wear resistance [146]. Additionally, a rise in suitable values for LED can result in a desirable melt pool that improves FGMs' resilience to wear and corrosion due to good microstructural formation. However, if the LED exceeds a certain threshold, there may be an excessive melt pool that takes longer to solidify, allowing for the creation of pores and cracks in the microstructure [147]. As a result, the cladding quality can be compromised, causing heat exchanger pipes to exhibit poor wear and corrosion characteristics because oxide can penetrate the FGM clad easily.

For instance, Jing et al. [148] used laser cladding to fabricate HA-TiO_2 functionally graded layer on a Ti6Al4V substrate and varied LED between 20 J/mm^2 and 100 J/mm^2. At LED of 20 J/mm^2, there was pore formation, but when LED increased, they observed a good consolidation mechanism that produced flat surfaces with strong bonds at LED of 60 J/mm^2, and smoother surfaces with no cracks or pores at LED of 70 J/mm^2, which is attributed to the uniform particle consolidation upon melting. This can also enhance the corrosion resistance because the lower the surface roughness, the greater the corrosion resistance. However, as the LED was increased to 80 J/mm^2 and 90 J/mm^2, there was an increase in defects formation, including the formation of thermal stress cracks, pores, and uneven/loose clad surface, as shown in Figure 33. They attributed the existence of cracks in FGM clads to the gasification-induced depletion of W, Ti, Co, and P enrichments, which led to higher tensile stress. A strong bond might also indicate that the LED was just right to generate a sufficient melt pool to consolidate with the substrate [14]. In contrast, a higher LED produced an excessive melt pool that slowed down the solidification process and caused pores to form, which can compromise the performance of heat exchanger parts under high-pressure loading and result in stress corrosion cracking [86]. Additionally, it was found that the corrosion resistance increased at 70 J/mm^2 with a lesser corrosion rate of 0.062 mm.a^{-1}, but decreased at 90 J/mm^2 with a higher corrosion rate of 0.211 mm.a^{-1}. This shows how the morphology and surface quality of graded coatings are affected by LED and how this significantly affects wear and corrosion behaviour, a vital quality characteristic needed to extend the service life of heat exchanger parts operating in demanding environments.

The relationship between LED and microhardness has been previously studied. Generally, an increase in energy density leads to higher microhardness properties due to grain refinement, microstructural enhancement, solid solutions, and precipitated phases [149]. Sufficient particle melting during high energy input promotes microstructural grain growth, leading to strong metallurgical bonds or structures responsible for increasing the mechanical properties of heat exchanger coatings [150]. Cheng et al. [151] produced Inconel 718 FGM and stainless steel 316L FGM and discovered that higher LED increased dendritic structure. Typically, as LED increases, fewer lave phases are precipitated, creating a dendritic structure that alters the microhardness properties. This might be the consequence of undercooling, which affects the mechanical characteristics, and rapid dendritic growth, demonstrating that using the appropriate LED parameters is essential to obtaining desirable grain struc-

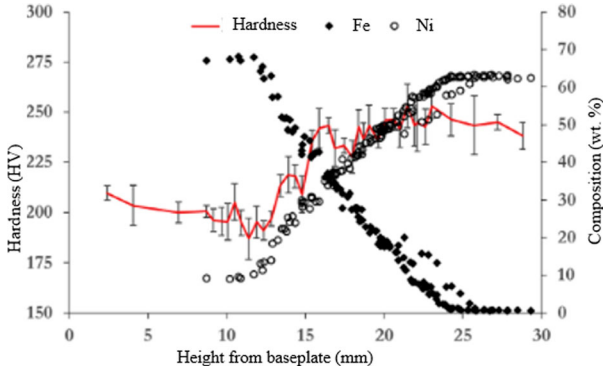

Figure 36. Variation of microhardness of SS304L/Inconel 625 FGM due to variation of the Fe and Ni composition [156].

ture, better deposition quality, and enhanced material performance.

Ocylok et al. [152] employed the laser cladding technique and built a crack-free Stellite 31 and Marlok-graded layer to improve corrosion and wear resistance properties. The authors reported an increase in hardness that varied linearly across the transition layers. They attribute the enhanced microstructural properties to the LED processing conditions, as they argued that the porosity level decreased with an increase in LED. Olakanmi et al. [14] studied the influence of LED on microstructural properties, which influence the microhardness properties. Three different values of laser energy density (12.50, 15.00, and 17.50 J/mm^2) were used to fabricate the titanium aluminide (Ti-Al) blended with TiC that was deposited on Ti6Al4Vsubstrate. They obtained a good bonding when the LED was set at 17.50 J/mm^2. Figure 27 shows optical micrographs of fabricated samples illustrating good melting of TiC particles, as shown in Figure 25(g–i), whereas, at an energy density of 12.50 and 15.00 J/mm^2, there was inadequate melting except for aluminium, which they attributed to insufficient energy input capable of initiating a metallurgical reaction. This led to the formation of intermetallics, including Ti_2AlC, γ, and α_2 shown in Figure 24 of the XRD analysis. An increase in the LED enhanced the formation and intensity of the matrix phases. The same intermetallics are reported to have influenced the FGM-clad microhardness to be higher than that of the Ti6Al4V substrate. Because of that, the microhardness for the LED set at 12.50 and 15.00 J/mm^2 was lower since the reaction was not sufficient enough to form intermetallics. This shows a need to optimise the LED parameters to reduce process defects.

Mahamood & Akinlabi [17] compared the performance of optimised functionally graded Ti6Al4V/TiC with that fabricated with fixed process parameters. They revealed that the wear resistance and the microhardness were significantly enhanced at optimum LED parameters to 1200 VHN, which was four times better than that of the substrate, showing that clad quality resistance to wear and optimised parameters can improve the microhardness.

The LED also influences the FGM clads' aspect ratio and dilution. In Eq. 4, the clad track width and height can be used to calculate the aspect ratio, while the deposit height and penetration depth calculate the dilution (see Eq.5).

$$Aspect\ Ratio = \frac{w}{h} \tag{3}$$

$$Dilution = \frac{D}{D+H} \tag{4}$$

As LED increases, so do the aspect ratio and dilution [153]. This is because higher energy densities cause more melting, which allows the base material and the FGM cladding material to mix more. Specifically, as the LED increases, the clad height decreases. On the other hand, when the LED increases, the FGM clad width also increases. This could be attributed to the melting force and flow viscous force of the Marangoni convention phenomenon that leads to suppression of the deposited layer upon melting. This leads to reduced clad height, while the melt pool volume expansion on the surface worsens the melted area, which in this case, increases the FGM clad width [143,144]. Therefore, it is without a doubt that the clad height must be smaller during the surface modification of boiler tubes to improve cost efficiency and reduce clad weight because it depends on the amount of FGM powders introduced to form layers during deposition. However, the clad width is preferred to be larger because it increases the surface area of the coating's effectiveness in protecting against various degrading attacks.

Lian et al. [154] optimised the flatness ratio and cladding efficiency using the multi-response Grey Relational Analysis (GRA) method. The laser power and scanning speed varied between 1.2 and 1.5 kW, and 5 and 8 mm/s, respectively. They compared the clad morphology of samples fabricated using parameters from Taguchi L_{16} orthogonal experimental design and those manufactured using optimal GRA values of 1.5 kW. Results showed defects in the clad morphology of non-optimised samples, as illustrated in Figure 37(a,b), but there was a reduction in clad reduction in flaws of incomplete fusion between the substrate and cladded layer when using optimal parameters, as illustrated in Figure 34(c,d). Further, the method had a negligible 0.97% prediction error, showing that optimal processing parameters can enhance the clad geometry and clad efficiency.

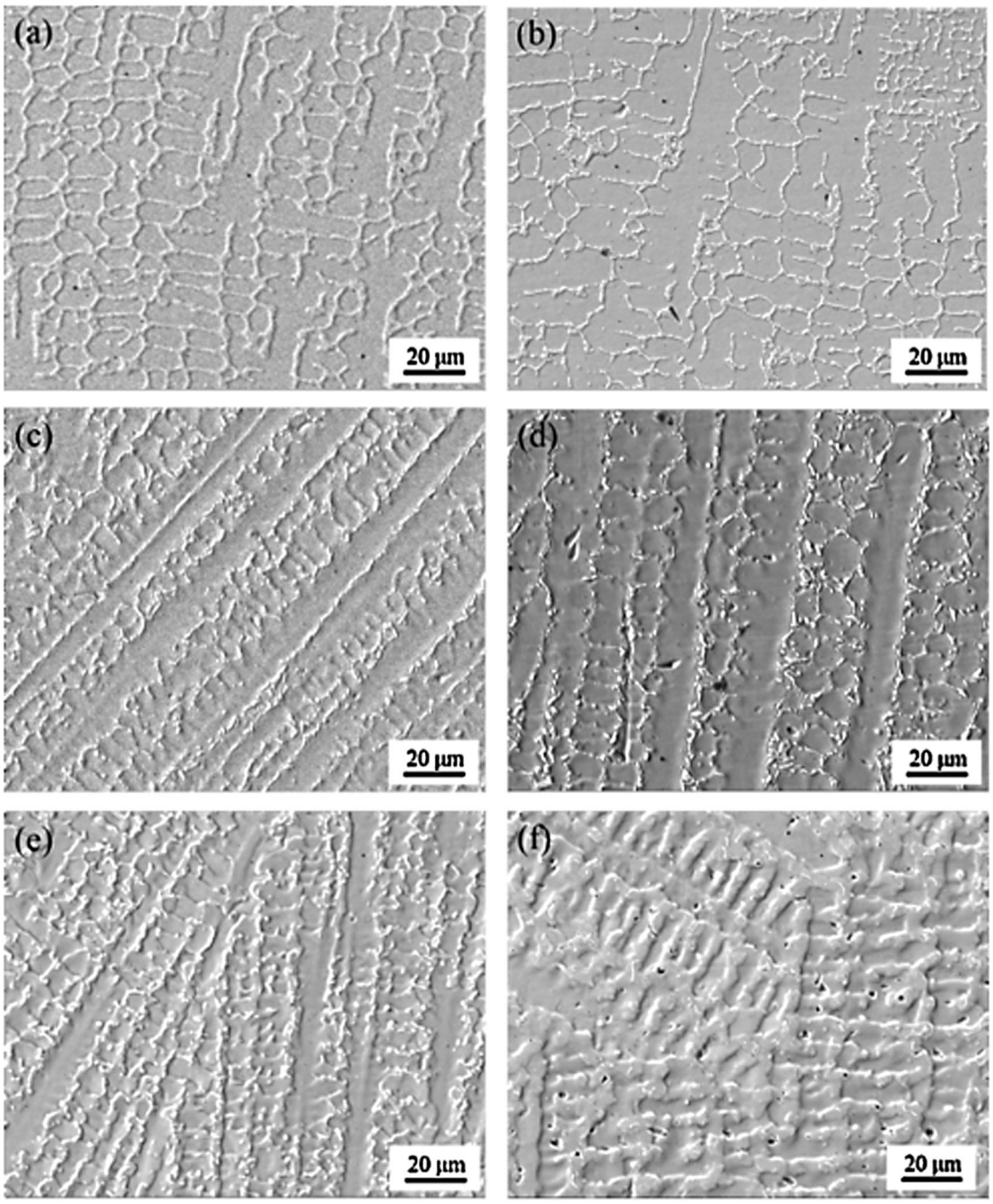

Figure 37. Microstructural variation with varying composition in functionally graded 316L/Inconel 718 fabricated via LMD technique [161].

Composition & powder flow rate

The changes in material composition as the powders are varied during the cladding of FGMs can cause microstructural variation, influencing the clad mechanical properties. As an example, Ostolaza et al. [155] investigated the clad quality characteristics of functionally graded AISI 316L and AISI H13 produced by the DED method on AISI 1045 mild steel substrate as the material composition was changed. The first layer was initially deposited with 100% AISI 316L, then the composition was changed at intervals of 20 wt% until the top layer with 100% AISI H13, as shown in Figure 35. They observed an austenitic with ferrite microstructure at the lower 316L layer and a gradual change to martensite and austenite microstructure at the H13 top layer. Consequently, the microhardness property was enhanced because it increased sharply from the lower to the upper layer by adding H13 powder, which they attributed to the increase in carbon content. This shows that carbon content is a hardening element that causes a sharp increase in microhardness of the FGM clad when its content is increased during deposition.

Carroll et al. [156] also concluded that variation in composition can alter the FGM microhardness properties along the length of the gradient zone, as depicted in Figure 36. They employed the DED method to deposit 20 layers of SS304L followed by nineteen layers

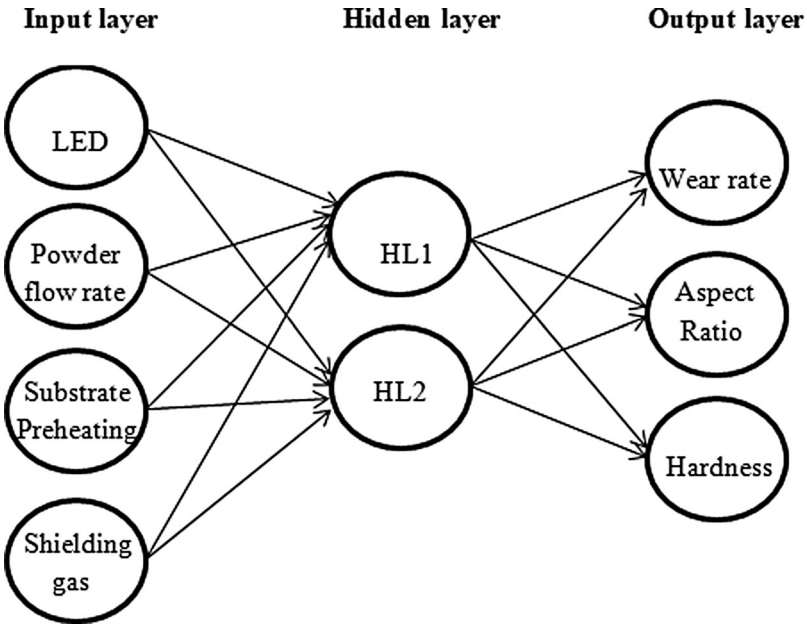

Figure 38. ANN structure for laser cladding parameters and clad characteristics.

of Inconel 625 through a gradient zone. Cracks in the region having 79 wt% SS304L and 21 wt% IN625 were observed due to compositional and microstructural variations. The formation of a secondary phase having micro-sized particles containing carbides in Nb and Mo content is what they accredited to crack initiation. This shows that when the composition of elemental powders is not varied properly, clad quality can be compromised by defect formation, leading to susceptibility of poor strength, hydrogen cracking, and embrittlement in various regions of the coated heat exchanger part. Luo et al. [121] studied the hot corrosion resistance of the IN718/Haynes 25 FGM as the composition was varied. The microstructure was characterised by columnar grains, which changed to equiaxed as the content of Haynes 25 was increased. This demonstrates compositional variation during FGM fabrication can lead to microstructural transformation, which directly impacts the FGM clad properties.

Furthermore, variation in composition also affects the wear and corrosion resistance of FGMs, as seen in the work of Ostolaza et al. [155]. The corrosion resistance was reduced when the composition was varied from SS316L to AISI H13 because 316L contains higher chromium content of 16% and makes it have higher corrosion resistance, but it is reduced due to the increase in H13 content which has a lower chromium content of about 5%, leading to poor corrosion resistance at the top layer [157]. Besides, the FGM had cracks and a lack of fusion defects at the interface that reduce resistance to erosion-corrosion, which they attributed to the inherent brittle sigma phase of stainless steels formed by subsequent cooling and heating

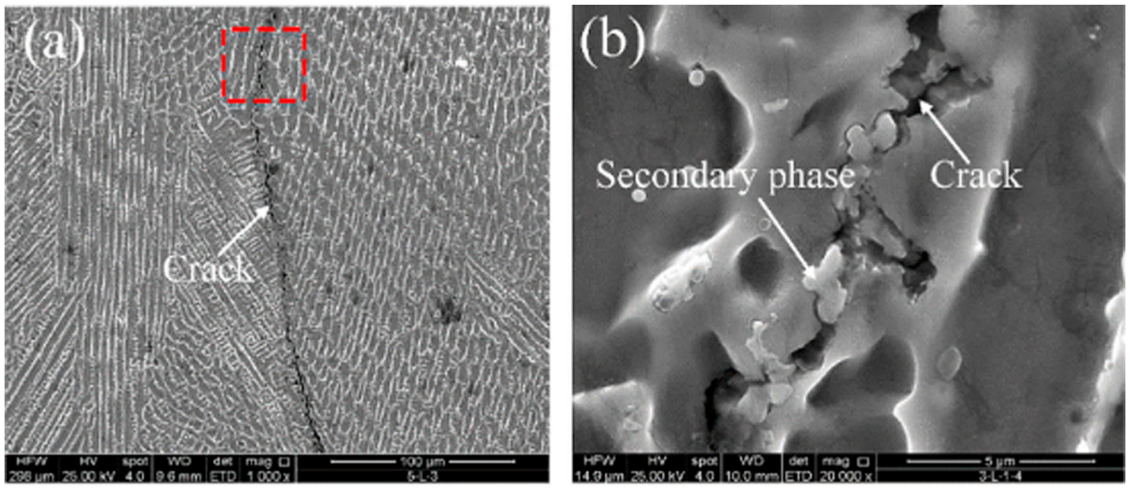

Figure 39. Solidification cracking due to lack of preheating causing (a) intergranular cracking along grain boundaries (b) cracks in precipitated areas [169].

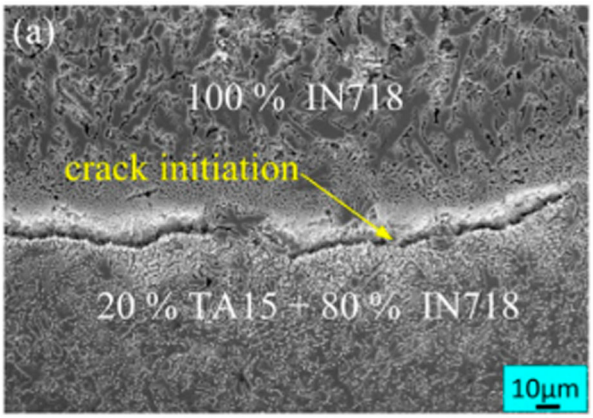

Figure 40. Crack initiation in the microstructure gradient zone of TA15-IN718 FGM due to lack of substrate preheating [172].

cycles. Chromium can be blended with SiC to enhance the surface properties of coatings. Jagdheesh et al. [158] modified the surface of AISI-type 316L stainless steel using Cr-SIC. This was done to improve the hardness qualities by laser surface alloying. They attained a higher microhardness of 1300 HV at the laser-processed zone that enhanced the wear resistance. The enhanced quality characteristics were attributed to forming M7C3 (M = Fe, Cr) carbides following the dissociation of Cr_3C_2 during melting and the integration of the Cr-SiC mixture in the melt zone. This demonstrates that increased Cr concentration can improve mechanical properties because of the solid solution strengthening mechanism and the finer grain crystal structure, which is desirable for boiler tube applications under demanding operating conditions. In a related study, Jagdheesh et al. [159] employed laser surface alloying of AISI grade 316L using Ni-SiC to increase the surface hardness. The microstructure was characterised by γ-austenite, M_7C_3, and δ-ferritic phases. The higher microhardness (733 HV) was largely due to the Si concentration in the LSA region, due to the microstructural reinforcement capabilities upon dissolution [160].

Chen et al. [161] also studied the effects of varying composition on microstructural transformation when fabricating 316L/Inconel 718 FGM on 304L substrate. The composition gradients having 5% of component A, 10% of component B, and 20% of component C were varied linearly with pre-alloyed 316L being deposited prior on the substrate. The microstructure of the fabricated FGM varied with increasing composition. It was mostly dominated by the columnar dendrites as well as the fine equiaxed grains (see Figure 37). Of particular interest is that when the content of Inconel 718 was increased above 40%, there was laves phase precipitation at the interdendritic regions due to heat accumulation that led to the formation of coarse grain. The presence of laves phase also increased the tensile and wear properties of the FGM at a composition gradient of 10% In718 but reduced gradually when the composition was reduced to 5%, leading to thermal cracks. It is clear that laves phases, which are intermetallic, can be formed during the combination of dissimilar powder compositions and can be both beneficial and detrimental in a way if present in the FGM microstructure [162]. Therefore, the composition gradient should be controlled to ensure they are successfully utilised for functional applications such as increased wear and corrosion resistance, which are desirable for boiler pipes.

The rate at which the powder flows into the laser beam powder melting region, referred to as the 'powder flow rate,' is another parameter that significantly impacts the properties of the fabricated FGM clads. For this reason, the powder flow rate parameter has been studied by several researchers to investigate its influence on the FGM-clad surface attributes. It is reported that the quality of surface finish during laser cladding improves when the powder flow rate is reduced, [163] implying that the powder flow rate should be controlled, especially in the heat exchanger industry, to reduce secondary finishing operations that can be costly. Additionally, an increase in powder flow rate causes an increase in clad height, and it reduces the clad width, which leads to a reduction in the aspect ratio [164]. The clad geometry can be explained by the excessive build-up that occurs when powder flows into the matrix in bulk proportions, but the width decreases since much of the energy per unit area is required to melt the much powder introduced to the matrix. It is evident that powder flow rate is an important parameter that governs the clad geometry, implying that optimisation techniques must be utilised to obtain sound surface clads.

For instance, Tiwari et al. [164] employed the hybrid optimisation approach utilising the artificial neural network (ANN) and particle swarm optimisation (PSO) to optimise the laser power, scan speed, and powder feed rate to improve the aspect ratio quality characteristics. The developed ANN-PSO model had an 8.68% error, demonstrating that the ANN-PSO model is suitable for predicting and optimising quality characteristics during laser cladding since the simulation results agreed with the experimental results. A general ANN structure comprises an input, hidden, and output layer to correlate function between process parameters and output parameters/performance characteristics, [165] as depicted in Figure 38.

Substrate preheating

Before laser irradiation of the deposited FGM layer, the base material can be heated in a 'substrate preheating' procedure to minimise processing defects that occur when FGMs are fabricated [166]. The process

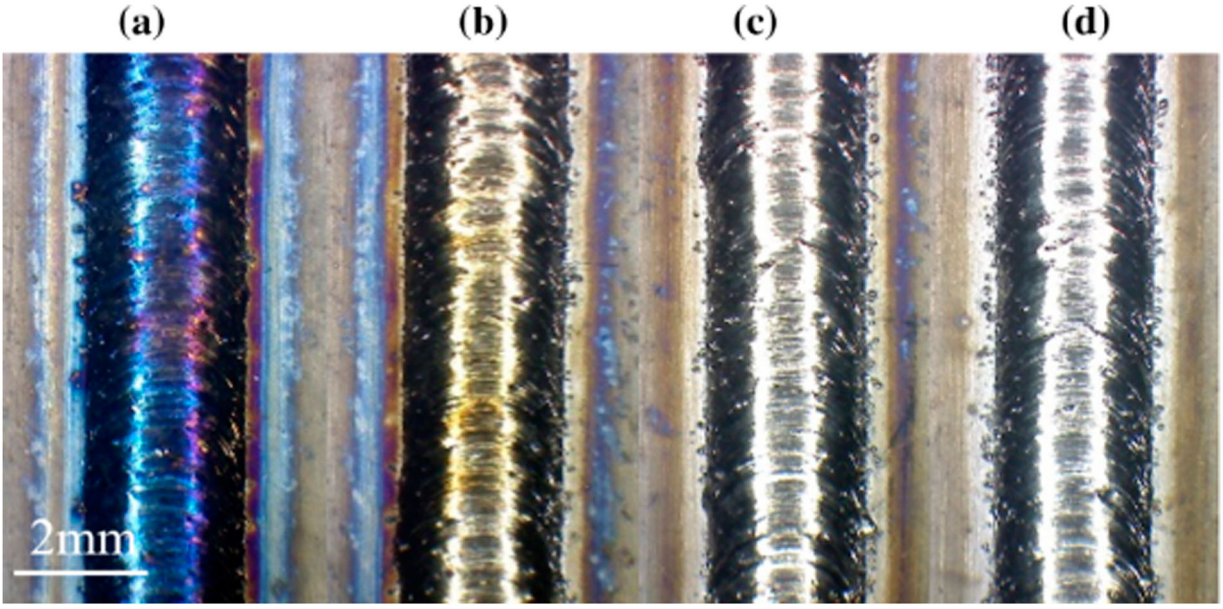

Figure 41. Discolouration of clads due to oxidation as shielding gas velocity is varied [175].

of substrate preheating can be carried out to reduce undesirable factors such as thermal mismatch between the substrate and the deposited layers and residual stress build-up. Large thermal gradients build up between the substrate and the FGM clads, and rapid cooling rates are reported to influence crack formation [167]. Substrate preheating is, therefore, a crucial parameter for mitigating premature failure of boiler pipes in severe operating conditions by suppressing the internal stresses and cooling rates. This is because an increase in temperature reduces the build-up of residual stresses, lowering the cracking probabilities [168].

Studies have been carried out to ascertain the effects of substrate preheating when manufacturing FGM and its influence on the clad quality characteristics such as corrosion and wear behaviour, aspect ratio, and microhardness properties. For instance, Meng et al. [169] performed synchronous preheating for 5 min on a 100 mm x 100 mm substrate to reduce the thermal gradient and residual stresses of functionally graded 316L/Inconel 625 manufactured by LMD. The change in the thermal gradient of the molten pool affected the grain morphology through a microstructural transformation from columnar to equiaxed structure. They further revealed that the thermal gradient reduced as the FGM-deposited layers increased. Meanwhile, there was a segregation of elements such as Nb and Mo eutectic along grain boundaries that led to solidification cracks in the middle for non-preheated deposition (See Figure 39). Meng et al. [169]. also encountered crack formation in the transition zone for the non-preheated samples when grading Inconel 625 to Ti6Al4V. They attributed that to the formation of Cr- and Mo-enriched phases, while synchronously preheated samples suppressed the cracking. This demonstrates that preheating affects FGM layers' phase formation and solidification process. It also enables the development of strong interface adhesion to lessen processing flaws like crack formation and residual stresses. This is because laser beam reflectivity and thermal mismatch can make clads susceptible to poorly clad quality traits that impair performance under difficult operating circumstances [170]. Thus, it's possible to argue that the likelihood of crack development decreases as preheating temperature increases.

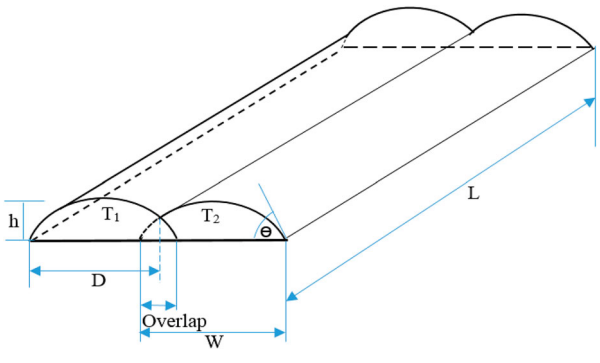

Figure 42. Schematic illustration of laser clad overlap.

Preheating can significantly improve the microstructure and internal stress build-up when fabricating FGMs because it impacts the rate of cooling of the deposited layer by avoiding locked-in stresses that can initiate crack formation and residual stresses, leading to grain refinement and enhancement of microhardness properties. It enables the realisation of homogenous FGM clads with defect-free microstructures [95,97,98]. For instance, Banait et al. [171] employed preheating the substrate to 400 °C before directed energy deposition of Ni-Cr-B-Si and SS316L functionally graded layers. They pointed out that

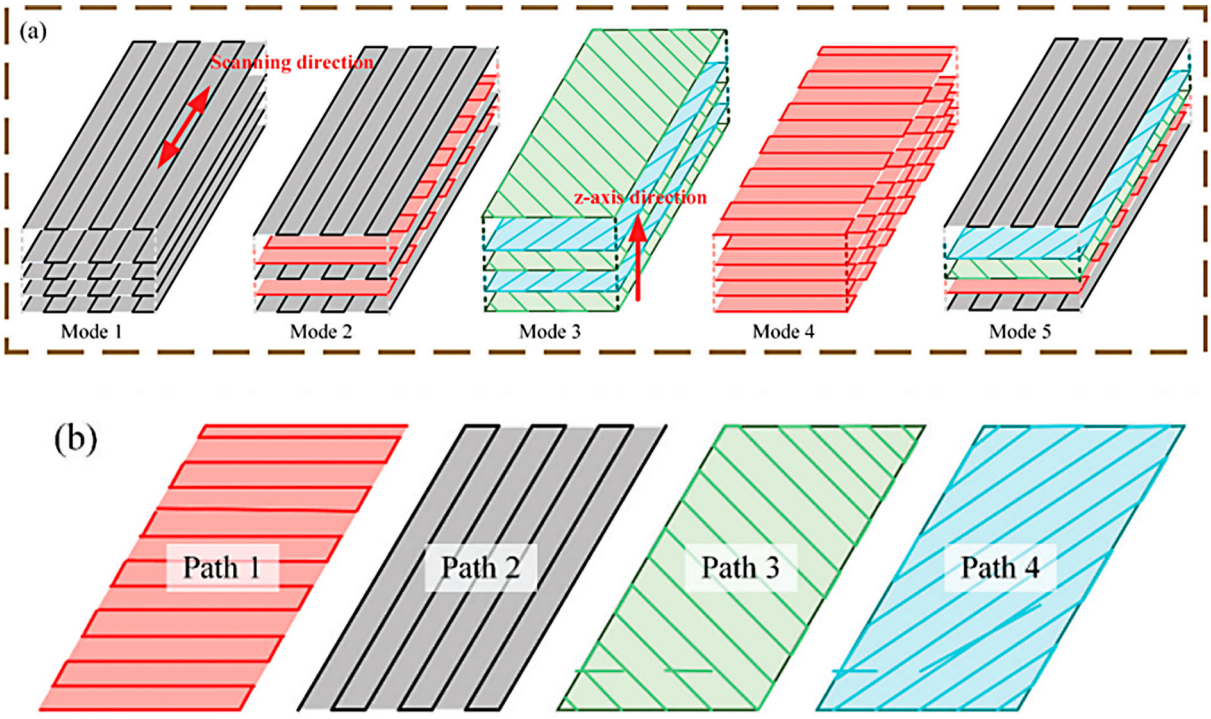

Figure 43. Laser track overlap using different configuration (a) mode 1–5 (b) path 1–4.

preheating was designed to offer slower cooling to avert the development of cracks. Shang et al. [172] also demonstrated that preheating can help prevent crack formation when fabricating TA15-Inconel718 FGM. They carried out a comparative study of preheated and non-preheated samples and observed that no cracks were present when preheating was carried out at 500°C. This also led to the suppression of internal stresses, which they reported was below the yield strength with a tensile strength of 207 MPa. It shows that preheating can increase the tensile strength, which enhances the microhardness properties because the yield strength and tensile strength typically correlate with microhardness properties. Contrarily, the non-preheated FGM exhibited cracks in the region between 80% and 100% of the Inconel 718 layer (see Figure 40), demonstrating the significance of substrate preheating in the prevention of defects since these flaws can impair the performance of coated boiler pipes and cause crack initiation under high fluid pressure.

Preheating can be employed as a way of process optimisation to mitigate substrate warping and distortion because an increase in preheating temperature increases total accumulated substrate distortion due to thermal contractions [173]. The substrate temperature differences could also explain this since the top of the surface is normally hotter than the bottom during laser cladding, implying that preheating reduces substrate distortion for thin but increases substrate distortion for thick substrates. Furthermore, a rise in preheating temperature results in an increase in the rate of deposition. This implies that the clad height increases with increasing preheating temperature. However, more study on the effects of substrate preheating on overall FGM aspect ratio is required because the effects on aspect ratio, wear, and corrosion quality characteristics have received scant attention.

Research shows that pipes operating in severe conditions can be preheated before surface modification for improved wear and corrosion resistance. For instance, Liu et al. [174] preheated copper alloy and successfully deposited a defect-free Ni60-WC cladding coating. This enabled the formation of the γ (Fe, Ni), M_7C_3, and WC reinforcement phases which improved the copper substrate wear resistance since the wear rate was $9 \times 10^{-5} mm^3 \cdot N^{-1} \cdot m^{-1}$, constituting 1.14% of the substrate material. Higher corrosion resistance was also obtained with a corrosion current density of $2.34 \times 10^{-7} mA \cdot mm^{-2}$, which was better than the substrates. This demonstrates how preheating can enable the formation of reinforcement phases, which are responsible for improved wear and corrosion resistance.

Shielding gas type and velocity

Shielding gas, measured in L/min, employs an inert gas environment to prevent the deposition from oxidising due to interacting with atmospheric gases (refer to Figure 32). The most utilised shielding gas in laser cladding is argon gas. The existence of harmful

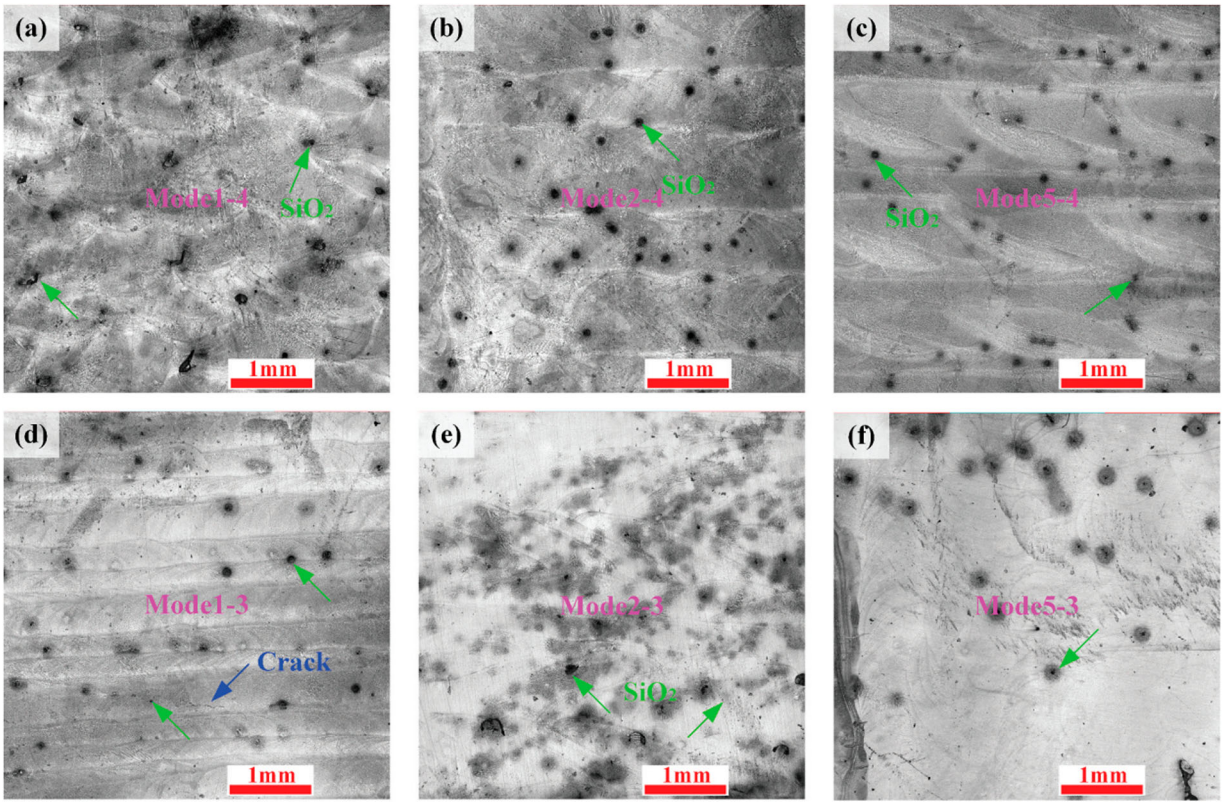

Figure 44. Micrographs formed using different modes of laser overlap (a) mode 1–4 (b) mode 2–4 (c) mode 5–4 (d) mode 1–3 (e) mode 2–3 (f) mode 5-3.

gases can lead to the oxidation of clads, which lowers the quality of the cladding and their resistance to deteriorating attacks in heat exchangers, making shielding gas a crucial parameter [175]. For instance, Li et al. [175] deposited bulk components of 4 clads with varying external shielding gas rates, labelled Q1 (14 L/min), Q2 (18 L/min), Q3 (30 L/min), and Q4 (50 L/min). They observed that at lower shielding gas values of Q1, there was oxidation that led to bluish discolouration, which became yellowish in Q2, and silver in Q3 and Q4, as shown in Figure 41. It can be seen that oxidation damage the surface integrity of clads, which can make the FGM clads meant for surface modification of boiler pipes succumb to corrosion attack including galvanic corrosion.

Furthermore, the high reactivity at lower shielding gas values can result in oxide formation and inclusions in the microstructure. For instance, oxides rich in Si and Mn can be introduced when steels react with oxygen, which ends up affecting the stress corrosion cracking behaviour [57]. This is because intergranular Si-rich oxides in the microstructure weaken the material's corrosion resistance, leading to the degradation of heat exchanger components. This shows that the melt pool should be protected using oxides to reduce reaction with the atmosphere since it can increase the presence of oxide content on the FGM clad. The shielding gas also impacts the mechanical characteristics of laser-clad FGM because it can be linked to one of the most fundamental porosity issues. When the atmospheric reaction is suppressed, the phases decarburise, increasing their microhardness properties while reducing porosity. As a result, the microhardness of clads increases with rising shielding gas velocity [143].

Track overlap

Laser cladding (LC) track overlap is another process parameter that influence clad properties. LC involves the deposition of relatively thick coatings (50 μm to 2 mm), which necessitates overlapping of clad tracks to cover a large surface area [144]. Clad overlap is calculated by dividing the difference between clad width (W) and distance (D) by clad width (see Figure 42). Studies have shown that overlap percentage, strategy, and dimensions affects the clad quality characteristics, such as surface roughness, clad geometry, hardness, wear resistance, surface morphology, and corrosion resistance [176–178]. Tanigawa et al. [176] deposited Ni-Cr-Si-B alloy coating on SS304 using a single cladding layer. The study varied overlap ratio from 30 - 90% to explore the effects on surface roughness. Results showed that surface roughness decreased as the overlap ratio increased. Additionally, they asserted that a flatter surface results from a higher overlap ratio. This might be explained by the bead profile forming a homogeneous structure as a result of uniform overlap distance. However, this is not always

the case because a higher overlap ratio might cause surface disorientation by creating an irregular structure at the overlap area, which lowers the surface's flatness. For instance, Li & Ma [179] studied the overlapped single layer clad tracks of stainless steel on mild steel substrate. They observed surface roughness to have an inverse relationship with overlapping ratio in an oscillating manner. This suggests that surface roughness was at its highest at certain points and at its lowest level at some point due to variations in the overlapping ratio. Thus, it can be concluded that the control of clad overlap is essential to obtain a smooth clad surface, which is desirable for boiler tube surface to avoid pressure loss.

This is because a higher overlap ratio can increase the clad dilution, resulting in reduced performance attributes such as lower microhardness, wear resistance and corrosion resistance. Li and Ma [179] applied NiCrBSi hard coating on AISI 5140 grade steel utilising In718 as a buffer layer to enhance the surface characteristics. They pointed out that reducing the degree of clad overlap is crucial when attempting to lessen dilution and avoid coarse carbide precipitation. This is because a high melt pool generated with increasing heat input can have a detrimental effect on corrosion resistance because it produces microstructural precipitates that are vulnerable to intragranular corrosion, especially in boiler tubes. Tuominen et al. [180], in agreement with Stanciu et al. [181], showed that laser clad overlapping can influence the microstructural properties and enhance the microhardness properties. In their study, areas with overlapping passes were found to have had sufficient re-melting of particles due to overlapping, resulting in improved hardness values of 60 $HV_{0.3}$ that was higher than the non-reheated zones. Because of this, Li & Ma [179] recommended an overlap ratio that is between 29.3% and 59.2%, which they argued is the desirable value range to minimise defects, as an overlap that is greater than 70% can give rise to inter-run porosity. The pore formation can be attributed to the gap formation between successive layer deposited, leading to gas entrapment. This shows that track overlap must be maintained at optimum values to avoid defect formation that can affect fracture toughness, mechanical strength, and mass transfer properties of boiler tubes at high pressures owing to the random air voids.

Zhao et al. [178] demonstrated that overlap rate ratio is responsible for enhancing the mechanical properties. Moreover, they noted that the large thermal and residual stresses, which are not desirable for boiler tube application, can be reduced by employing the overlap ratio at optimum level. This is because appropriate engagement of overlap can improve the temperature distribution, distribution of heat at the overlap region, temperature gradient, and grain growth orientation [151]. In FGMs, different overlap modes and paths can generate different re-melting modes on the solidification layer, which rebuilds the position of the metallurgical bonding zone (see Figure 43). Hence, a good metallurgical bond due to sufficient melting with result in obtaining quality interlayered structures. Additionally, small black spot corresponding to silicon oxides were found in the clad overlap area, showing that sufficient re-melting temperatures is required to melt oxides to obtain a quality coating (see Figure 44).

Summary of findings

The microstructural formation and quality of FGM clad meant for surface treatment of boiler pipes are established to be influenced by the laser cladding parameters, including LED, composition and powder flow rate, shielding gas, and substrate preheating. A higher LED causes more melting of the particles, which increases the melt pool and Marangoni convention effects that refines the grain size and improve wear resistance. In contrast, when the LED is low, there is typically insufficient melting, and raising it above a certain point can result in defects, which can be harmful and result in process deformities like cracks that lower the quality of the clad. Due to the poor grain morphology, this can result in low microhardness and poor wear and corrosion protection. Additionally, there is a direct correlation between aspect ratio and laser energy density. This is not the case with powder composition and flow rate because an increase in powder flow rate reduces clad width and aspect ratio.

Additionally, as the composition changes, so do the powder contents, such as chromium, which increase corrosion resistance but decrease wear and corrosion resistance when depleted. Likewise, this is governed by the precipitation of laves phases, sigma phases, and refined grains, which change as layer build-up varies. The formation of undesirable phases which can lead to crack formation can be suppressed by substrate preheating. This also implies that when substrate preheating is performed, internal stress-build ups and thermal mismatch are reduced, enhancing the microstructure and increased tensile properties that improve the microhardness properties due to reinforcement phases. Because there haven't been many studies done in this field, the effects of substrate preheating and shielding gas on the FGM-clad aspect ratio are still unclear in the literature.

Meanwhile, it is evident that at lower shielding gas flow rates, there will be oxidation which can result in inclusions in the microstructure, lowering the surface integrity of FGM clads. This is because the presence of pores in FGM clads meant for surface modification of boiler pipes can lead to penetration of

deposits through the protective layer, potentially leading to pitting corrosion and stress corrosion cracking. This shows that laser cladding parameters influence the performance of clad quality characteristics and must therefore be controlled for improved service life.

This section has also demonstrated that clad quality characteristics can be predicted and optimised using statistical and numerical techniques. However, there haven't been many efforts made to improve the qualities of the FGM clads through hybrid optimisation of laser cladding parameters. This approach is suitable for simultaneously combining the abilities of the statistical and numerical models. By using the experimental matrix, the Taguchi method, for instance, offers reliable methods for reducing experimental data, but it can only optimise a single performance characteristic. It is, therefore, frequently used in conjunction with Grey Relational Analysis (GRA) method because it can combine and address various performance characteristics. However, because it only works with linear data, it has some limitations and requires prior knowledge of the relationship between input and output. This is not the case with other artificial intelligence paradigms, such as neural networks, which use nonlinear models and don't require prior knowledge.

Future work

The literature study results demonstrate that FGMs' use as surface modifiers is receiving significant attention and will continue to experience significant growth in the heat exchanger industry because they can overcome the shortcomings of individual alloy coatings. In particular, it has been shown that substrates made of Fe and Ni respond favourably when Fe/Ni FGM coatings are deposited on them. On the other hand, there hasn't been any research done on developing Fe/Ni FGM on copper substrate. Despite this, copper is one of the most frequently used materials for heat exchanger tubing but is still prone to corrosion-related failures. Further work is therefore required to fabricate the Fe/Ni FGM on copper substrate and comprehend the consolidation mechanism in order to avoid degradation of copper pipes operating in severe conditions due to process-induced deformities. Therefore, this serves as the foundation for the necessary laser cladding experimental work to develop Stainless steel 316L/Inconel 625 FGM on copper substrate for heat exchanger applications.

Additionally, it is clear in the surveyed literature that the use of hybrid algorithms, which exhibit more outstanding performance than single optimisation methods, is still in its infancy with regards to optimising FGM clads. Therefore, hybrid optimisation techniques such as the Taguchi-grey relational artificial neural approach can be employed in the future to determine optimal laser cladding settings for multi-response optimisation of FGM quality characteristic problems. This is a much-needed area of study that can also help to understand how laser cladding parameters affect the aspect ratio quality characteristics. This area has not been adequately studied even though it affects the process efficiency and weight reduction efforts during surface modification of heat exchanger parts. Furthermore, research is required in future to analyse the hybrid optimisation of laser track overlap and determine its effect on clad quality characteristics.

Conclusions

This article reviewed ways of mitigating the failure of heat exchanger components using functionally graded materials processed via laser cladding technique, and the following conclusions have been reached:

1. Corrosion, oxidation, erosion-wear, and fatigue are the most prevalent forms of attacks that deteriorate the material properties of heat exchanger parts, leading to premature failure and pressure drops. Surveyed literature has revealed that the failure emanates when protective oxides are eroded or penetrated by degrading agents (chlorides, sulfates, ammonia), due to poor processing conditions that lead to the formation of defects such as pores and cracks. Understanding the modes of these material failures can inform material selection criteria to obtain quality coatings that prolong heat exchanger service life.
2. Some of the materials that are most commonly used in the manufacture of boiler tubes include copper alloys, nickel-based alloys, and stainless steel alloys. According to the results of a thorough analysis of the pertinent literature, it can be concluded that single alloy materials experience attacks at extreme working environments. As a result, the significance of using functionally graded materials, which offer materials with customised material properties, was highlighted.
3. Laser cladding was evaluated as a potential surface modification technique that can apply functionally graded coatings due to the variation in microstructural properties and the capability to join dissimilar materials with minimum distortion and residual stress accumulation. Furthermore, four laser cladding parameters of laser energy density, composition and powder feed rate, substrate preheating, and shielding gas have been identified to affect the clad quality characteristics that influence heat exchanger resilience to degradation, specifically wear and corrosion, microhardness, and aspect ratio.

4. It is also clear from the reviewed literature that laser cladding parameter optimisation for FGMs has not been sufficiently investigated or applied; although the few studies conducted had published results that suggested it could improve the clad quality characteristics for enhanced heat exchanger performance.

Acknowledgements

The authors would like to express profound gratitude and appreciation to the Education for Laser-based Manufacturing (ELbM) consortium (No. 2019-1973/5 – Project No 614655), funded by the European Union for the award of a scholarship to the first author. The JKUAT and BIUST management is well appreciated for their valuable support in availing essential academic online resources and facilities.

Disclosure statement

No potential conflict of interest was reported by the author (s).

Funding

This work was supported by European Commission: [Grant Number No. 2019-1973/5].

References

[1] Edreis E, Petrov A. Types of heat exchangers in industry, their advantages and disadvantages, and the study of their parameters. IOP Conf Ser Mater Sci Eng. 2020;963(1). doi:10.1088/1757-899X/963/1/012027
[2] Shah R, Sekulic D. Fundamentals of heat exchanger design. Hoboken (NJ): John Wiley & Sons; 2003.
[3] Kumar Mallick R, Ghosh M, Bahrami A, et al. Stress relaxation cracking failure in heat exchanger connection pipes in a petrochemical plant. Eng Fail Anal. 2023 February;147:107156, doi:10.1016/j.engfailanal.2023.107156
[4] Qiankun Z, Yafei S, Sixian R, et al. Corrosion failure analysis on heat exchanger pipes. J Fail Anal Prev. 2017;17(2):349–353. doi:10.1007/s11668-017-0248-9
[5] Mondi PR, Satish Kumar D, Kaza M, et al. Investigation on heat exchanger pipe failure. J Fail Anal Prev. 2019;19(6):1720–1725. doi:10.1007/s11668-019-00774-z
[6] Faes W, Lecompte S, Ahmed ZY, et al. Corrosion and corrosion prevention in heat exchangers. Corros Rev. 2019;37(2):131–155. doi:10.1515/corrrev-2018-0054
[7] Luo H, Dong CF, Li XG, et al. The electrochemical behaviour of 2205 duplex stainless steel in alkaline solutions with different PH in the presence of chloride. Electrochim Acta. 2012;64:211–220. doi:10.1016/j.electacta.2012.01.025
[8] Scott DA. Copper compounds in metals and colorants: oxides and hydroxides. Stud Conserv. 1997;42(2):93–100. doi:10.1179/sic.1997.42.2.93
[9] Lee W, Park SJ. Porous anodic aluminum oxide: anodization and templated synthesis of functional nanostructures. Chem Rev. 2014;114(15):7487–7556. doi:10.1021/cr500002z
[10] Sadeghi E, Markocsan N, Joshi S. Advances in corrosion-resistant thermal spray coatings for renewable energy power plants: part II—effect of environment and outlook. J Therm Spray Technol. 2019: 1789–1850.
[11] Cpm SA, Varghese B, Baby A. A review on functionally graded materials. Int J Eng Sci. 2014: 90–101.
[12] Mahamood RM, Akinlabi ET, Shukla M, et al. Functionally graded material: an overview. Lect Notes Eng Comput Sci. 2012 January;3:1593–1597.
[13] Owoputi AO, Inambao FL, Ebhota WS. A review of functionally graded materials : fabrication processes and applications. Int J Appl Eng Res. 2018;13(23):16141–16151.
[14] Olakanmi EO, Sepako M, Morake J, et al. Effect of energy density on the consolidation mechanism and microstructural evolution of laser cladded functionally-graded composite Ti-Al system. Solid Free Fabr. 2018. Proc. 29th Annu. Int. Solid Free. Fabr. Symp. – An Addit. Manuf. Conf. SFF 2018; 2020. p. 422–1438.
[15] Olakanmi EO, Sepako M, Morake J, et al. Microstructural characteristics, crack frequency and diffusion kinetics of functionally graded Ti-Al composite coatings: effects of laser energy density (LED). Jom. 2019;71(3):900–911. doi:10.1007/s11837-018-3272-7
[16] Bohidar SK, Sharma R, Mishra PR. Functionally graded materials: a critical review. Int J Res. 2014;1(7):289–301.
[17] Mahamood RM, Akinlabi ET. Laser metal deposition of functionally graded Ti6Al4V/TiC. Mater Des. 2015;84:402–410. doi:10.1016/j.matdes.2015.06.135
[18] Ravichandran KS. Thermal residual stresses in a functionally graded material system. Mater Sci Eng A. 1995;201(1–2):269–276. doi:10.1016/0921-5093(95)09773-2
[19] Zhang X, Li L, Liou F. Additive manufacturing of stainless steel – copper functionally graded materials via inconel 718 interlayer. J Mater Res Technol. 2021;15:2045–2058. doi:10.1016/j.jmrt.2021.09.027
[20] Liu Z, Liu C, Gao Y, et al. High temperature corrosion behaviors of 20 g steel, hastelloy C22 alloy and C22 laser coating under reducing atmosphere with H2S. Coatings. 2020;10(7). doi:10.3390/coatings10070617
[21] Bakhtiari R, Zangeneh S. Evaluation of hydrogen damage in a fire tube using microstructure/mechanical properties studies. Eng Fail Anal. 2018;90:231–244. doi:10.1016/j.engfailanal.2018.03.030
[22] Patel S. SHELL & tube heat exchanger thermal design with optimization of mass flow rate and baffle address for correspondence. Int J Adv Eng Res Stud. 2012;2(1):130–135.
[23] Jin HZ, Gu Y, Ou GF. Corrosion risk analysis of tube-and-shell heat exchangers and design of outlet temperature control system. Pet Sci. 2021;18(4):1219–1229. doi:10.1016/j.petsci.2021.07.002
[24] Dudziak T. Steam oxidation of Fe-based materials steam oxidation of Fe-based materials. 2018, No. November.
[25] Dayal RK, Parvathavarthini N. Hydrogen embrittlement in power plant steels. Sadhana – Acad Proc Eng Sci. 2003;28(3–4):431–451. doi:10.1007/BF02706442

[26] Djukic MB, Sijacki Zeravcic V, Bakic GM, et al. Hydrogen damage of steels: a case study and hydrogen embrittlement model. Eng Fail Anal. 2015;58:485–498. doi:10.1016/j.engfailanal.2015.05.017
[27] Wang X, Yang Z, Wang Z, et al. The influence of copper on the stress corrosion cracking of 304 stainless steel. Appl Surf Sci. 2019;478:492–498. doi:10.1016/j.apsusc.2019.01.291
[28] Saltzman D, Bichnevicius M, Lynch S, et al. Design and evaluation of an additively manufactured aircraft heat exchanger. Appl Therm Eng. 2018 February;138:254–263. doi:10.1016/j.applthermaleng.2018.04.032
[29] Bichkar P, Dandgaval O, Dalvi P, et al. Study of shell and tube heat exchanger with the effect of types of baffles. Proc Manuf. 2018;20:195–200. doi:10.1016/j.promfg.2018.02.028
[30] Franco A, Vaccaro M. Recent trends in the development of heat exchangers for geothermal systems. J Phys Conf Ser. 2017;923(1). doi:10.1088/1742-6596/923/1/012044
[31] Imran M. Effect of corrosion on heat transfer through boiler tube and estimating overheating. Int J Adv Mech Eng. 2014;4(6):629–638.
[32] Ishii M, Kaneko, M, Oda T. Titanium and its alloys as key materials for corrosion protection engineering; 2003.
[33] Wu D, Yuan Z, Liu S, et al. Recent development of corrosion factors and coating applications in biomass firing plants. Coatings. 2020;10(10):1–26. doi:10.3390/coatings10101001
[34] Oksa M, Auerkari P, Salonen J, et al. Nickel-based HVOF coatings promoting high temperature corrosion resistance of biomass-fired power plant boilers. Fuel Proc Technol. 2014;125:236–245. doi:10.1016/j.fuproc.2014.04.006
[35] Uusitalo MA, Vuoristo PMJ, Mäntylä TA. High temperature corrosion of coatings and boiler steels below chlorine-containing salt deposits. Corros Sci. 2004;46(6):1311–1331. doi:10.1016/j.corsci.2003.09.026
[36] Usman A, Khan AN. Failure analysis of heat exchanger tubes. Eng Fail Anal. 2008;15(1–2):118–128. doi:10.1016/j.engfailanal.2006.11.051
[37] Panahi H, Eslami A, Golozar MA, et al. An investigation on corrosion failure of a shell-and-tube heat exchanger in a natural gas treating plant. Eng Fail Anal. 2020;118(September):104918, doi:10.1016/j.engfailanal.2020.104918
[38] Allahkaram SR, Zakersafaee P, Haghgoo SAM. Failure analysis of heat exchanger tubes of four Gas coolers. Eng Fail Anal. 2011;18(3):1108–1114. doi:10.1016/j.engfailanal.2010.11.015
[39] Albanakis C, Yakinthos K, Kritikos K, et al. The effect of heat transfer on the pressure drop through a heat exchanger for aero engine applications. Appl Therm Eng. 2009;29(4):634–644. doi:10.1016/j.applthermaleng.2008.03.034
[40] Miller RL. Corrosion and materials selection for geothermal systems. Proc Intersoc Energy Convers Eng Conf. 1980;1(April):460–464.
[41] Davíðsdóttir S, Gunnarsson BG, Kristjánsson KB, et al. Study of corrosion resistance properties of heat exchanger metals in two different geothermal environments. Geoscience. 2021;11(12). doi:10.3390/geosciences11120498
[42] Lazić V, Arsić D, Nikolić RR, et al. Selection and analysis of material for boiler pipes in a steam plant. Procedia Eng. 2016;149(June):216–223. doi:10.1016/j.proeng.2016.06.659
[43] Saito N, Komai N, Sumiyoshi Y, et al. Development of materials for use in A-USC boilers. Mitsubishi Heavy Ind Tech Rev. 2015;52(4):27–36.
[44] Schwartz MP. Four types of heat exchanger failures. Plant Eng (Barrington, Illinois). 1981;35(21):145–150.
[45] Mousavian RT, Hajjari E, Ghasemi D, et al. Failure analysis of a shell and tube oil cooler. Eng Fail Anal. 2011;18(1):202–211. doi:10.1016/j.engfailanal.2010.08.022
[46] Corleto CR, Argade GR. Failure analysis of dissimilar weld in heat exchanger. Case Stud Eng Fail Anal. 2017;9(December 2016):27–34. doi:10.1016/j.csefa.2017.05.003
[47] Vasauskas V, Baskutis S. Failures and fouling analysis in heat exchangers. Mechanika. 2006;61(5):24–31.
[48] Permatasari R, Yusuf AM. Material selection for shell and tube heat exchanger using computational fluid dynamics method. AIP Conf Proc. 2018. 1977 (June). doi:10.1063/1.5043017
[49] Collins IL, Weibel JA, Pan L, et al. Evaluation of additively manufactured microchannel heat sinks. IEEE Trans Compon, Pack Manuf Technol. 2019;9(3):446–457. doi:10.1109/TCPMT.2018.2866972
[50] Kapranos P, Priestner R. Overview of metallic materials for heat exchangers for ocean thermal energy conversion systems. J Mater Sci. 1987;22(4):1141–1149. doi:10.1007/BF01233102
[51] Lister DH. SA NE M SC PL O E – C EO AP LS TE S M SC PL O E – C EO. *I*.
[52] Hruska J, Mlnarik J, Cizner J. High-temperature corrosion of nickel-based coatings for biomass boilers in chlorine-containing atmosphere. Coatings. 2022;12(2) doi:10.3390/coatings12020116
[53] Lima AS, Nascimento AM, Abreu HFG, et al. Sensitization evaluation of the austenitic stainless steel AISI 304L, 316L, 321 and 347. J Mater Sci. 2005;40 (1):139–144. doi:10.1007/s10853-005-5699-9
[54] Yoo HJ, Baek S, Kim JH, et al. Effect of laser surface cleaning of corroded 304L stainless steel on microstructure and mechanical properties. J Mater Res Technol. 2022;16:373–385. doi:10.1016/j.jmrt.2021.11.147
[55] Rezakhani D. Corrosion behaviours of several thermal spray coatings used on boiler tubes at elevated temperatures. Anti-Corros Meth Mater. 2007;54(4):237–243. doi:10.1108/00035590710762384
[56] Voisin T, Shi R, Zhu Y, et al. Pitting corrosion in 316L stainless steel fabricated by laser powder bed fusion additive manufacturing: a review and perspective. Jom. 2022;74(4):1668–1689. doi:10.1007/s11837-022-05206-2
[57] Saboori A, Aversa A, Marchese G, et al. Microstructure and mechanical properties of AISI 316L produced by directed energy deposition-based additive manufacturing: a review. Appl Sci. 2020;10(9) doi:10.3390/app10093310
[58] Pokhmurskii V, Student M, Gvozdeckii V, et al. Arc-sprayed iron-based coatings for erosion-corrosion protection of boiler tubes at elevated temperatures. J Therm Spray Technol. 2013. doi:10.1007/s11666-013-9921-z
[59] Reddy L, Sattari M, Davis CJ, et al. Influence of KCl and HCl on a laser clad FeCrAl alloy: in-situ SEM and controlled environment high temperature

corrosion. Corros Sci. 2019;158(July):108076, doi:10.1016/j.corsci.2019.07.003
[60] Hussain T, Simms NJ, Nicholls JR. Modelling fireside corrosion of thermal sprayed coatings in Co-firing of coal/biomass. Mater Corros. 2014;65(2):197–205. doi:10.1002/maco.201307063
[61] Losada R, Holberg S, Freire L, et al. High performance antifouling/anticorrosion coatings for protecting carbon steel and low alloying stainless steel heat exchangers in low enthalpy geothermal fluids.
[62] Hussain T, Dudziak T, Simms NJ, et al. Fireside corrosion behavior of HVOF and plasma-sprayed coatings in advanced coal/biomass co-fired power plants. J Therm Spray Technol. 2013 June: 797–807. doi:10.1007/s11666-013-9887-x
[63] Chanda UK, Padhee SP, Pandey AK, et al. Electrodeposited Ni–Mo–Cr–P coatings for AISI 1020 steel bipolar plates. Int J Hydrogen Energy. 2020;45(41):21892–21904. doi:10.1016/j.ijhydene.2020.06.014
[64] Qunshuang M, Yajiang L, Juan W. Effects of Ti addition on microstructure homogenization and wear resistance of wide-band laser clad Ni60/WC composite coatings. Int J Refract Met Hard Mater. 2017;64:225–233. doi:10.1016/j.ijrmhm.2016.11.002
[65] Cuevas-Arteaga C, Verhelst D, Alfantazi A. Performance of alloy 625 under combustion Gas environments: a review. ECS Trans. 2010;28(24):61–76. doi:10.1149/1.3496422
[66] Mahmood MH, Suryanto; Al Hazza MHF, Haidera FI. Developing of corrosion resistance nano copper oxide coating on copper using anodization in oxalate solution. Int J Eng Trans B Appl. 2018;31(3):450–455. doi:10.5829/ije.2018.31.03c.07
[67] Schleich W. Typical failures of CuNi 90/10 seawater tubing systems and how to avoid them.
[68] Goodenough J. The effects of paint-based protective films on the actual temporal water-side performance characteristics of steam surface condenser tubes; 2017.
[69] Jin L, Jiang K, Ren H, et al. A review of laser cladding on copper and copper alloys. Int J Electrochem Sci. 2022;17. doi:10.20964/2022.09.14
[70] Zhang P, Li M, Yu Z. Microstructures evolution and micromechanics features of Ni-Cr-Si coatings deposited on copper by laser cladding. Materials (Basel). 2018;11(6). doi:10.3390/ma11060875
[71] Yan H, Zhang P, Yu Z, et al. Microstructure and tribological properties of laser-clad Ni-Cr/TiB 2 composite coatings on copper with the addition of CaF 2. Surf Coat Technol. 2012;206(19–20):4046–4053. doi:10.1016/j.surfcoat.2012.03.086
[72] Balu P, Rea E, Deng J. Laser cladding of nickel-based alloy coatings on copper substrates. Ind Laser Appl Symp (ILAS 2015). 2015;*9657* (25):965703, doi:10.1117/12.2175966
[73] Lv J, Zhang C, Chen Z, et al. Fabrication and characterization of Ni60a alloy coating on copper pipe by plasma cladding with induction heating. Coatings. 2021;11(9). doi:10.3390/coatings11091080
[74] Ng KW, Man HC, Cheng FT, et al. Laser cladding of copper with molybdenum for wear resistance enhancement in electrical contacts. Appl Surf Sci. 2007;253(14):6236–6241. doi:10.1016/j.apsusc.2007.01.086
[75] Ahmad Z. Princles of corrosion engineering and corrosion control; 2006.
[76] Kracke A. Superalloys, the most successful alloy system of modern times-past. Pres Fut. 2016: 13–50. doi:10.7449/2010/superalloys_2010_13_50
[77] Wang R, Ouyang C, Li Q, et al. Study of the microstructure and corrosion properties of a Ni-based alloy coating deposited onto the surface of ductile cast iron using high-speed laser cladding. Materials (Basel). 2022;15(5):1643, doi:10.3390/ma15051643
[78] Wang Y, Liang Z, Zhang J, et al. Microstructure and antiwear property of laser cladding Ni–Co duplex coating on copper. Materials (Basel). 2016;9(8):634), doi:10.3390/ma9080634
[79] Yinghua L, Xuelong P, Jiacai K, et al. Improving the microstructure and mechanical properties of laser cladded Ni-based alloy coatings by changing their composition: a review. Rev Adv Mater Sci. 2020;59(1):340–351. doi:10.1515/rams-2020-0027
[80] Dhaiveegan P, Elangovan N, Nishimura T, et al. Corrosion behavior of 316L and 304 stainless steels exposed to industrial-marine-urban environment: field study. RSC Adv. 2016;6(53):47314–47324. doi:10.1039/c6ra04015b
[81] Tao K, Zhou X, Cui H, et al. Preparation and properties of a nanostructured NiCrC alloy coating for boiler tubes protection. Mater Trans. 2008;49(9):2159–2162. doi:10.2320/matertrans.MRP2008154
[82] Pedrazzini S, Child DJ, Aarholt T, et al. On the effect of environmental exposure on dwell fatigue performance of a fine-grained nickel-based superalloy. Metall Mater Trans A Phys Metall Mater Sci. 2018;49(9):3908–3922. doi:10.1007/s11661-018-4752-7
[83] Zhao T, Wang WY, Zhao Y, et al. Revealing sulfur- and phosphorus-induced embrittlement and local structural phase transformation of superlattice intrinsic stacking faults in L12-Ni3Al. J Mater Sci. 2022;57(26):12483–12496. doi:10.1007/s10853-022-07362-x
[84] Klapper HS, Klöwer J, Gosheva O. Hydrogen embrittlement: the game changing factor in the applicability of nickel alloys in oilfield technology. Philos Trans R Soc A Math Phys Eng Sci. 2017;375(2098). doi:10.1098/rsta.2016.0415
[85] Woodford D. Gas phase embrittlement and time dependent cracking of nickel based superalloys. Corrosion. 2005 April 3; 2005:NACE-05418.
[86] Rebak RB. Stress corrosion cracking (SCC) of nickel-based alloys. Stress Corros Crack Theory Pract. 2011:273–306. doi:10.1533/9780857093769.3.273
[87] Mostafaei A, Peighambari SM, Nasirpouri F. Failure analysis of monel packing in atmospheric distillation tower under the service in the presence of corrosive gases. Eng Fail Anal. 2013;28:241–251. doi:10.1016/j.engfailanal.2012.10.028
[88] Lu X, Ma Y, Wang D. On the hydrogen embrittlement behavior of nickel-based alloys: alloys 718 and 725. Mater Sci Eng A. 2020 March;792. doi:10.1016/j.msea.2020.139785
[89] Reeks W, Davies H, Marchisio S. A review: interlayer joining of nickel base alloys. J Adv Join Process. 2020 August;2:100030, doi:10.1016/j.jajp.2020.100030
[90] Makarov AV, Korobov YS, Soboleva NN, et al. Wear-resistant nickel-based laser clad coatings for high-temperature applications. Lett Mater. 2019;9(4):470–474. doi:10.22226/2410-3535-2019-4-470-474

[91] Sharma V, Kumar S, Kumar M, et al. High temperature oxidation performance of Ni-Cr-Ti and Ni-5Al coatings. Mater Today Proc. 2019;26(xxxx):3397–3406. doi:10.1016/j.matpr.2019.11.048
[92] Dudziak T, Olbrycht A, Polkowska A, et al. High temperature coatings from post processing Fe-based chips and Ni-based alloys as a solution for critical raw materials. IOP Conf Ser Mater Sci Eng. 2018;329(1). doi:10.1088/1757-899X/329/1/012010
[93] Prasad CD, Jerri A, Ramesh MR. Characterization and sliding wear behavior of iron-based metallic coating deposited by HVOF process on low-carbon steel substrate. J Bio- Tribo-Corrosion. 2020;6(3). doi:10.1007/s40735-020-00366-7
[94] Liu F, Liu C, Chen S, et al. Laser cladding Ni-Co duplex coating on copper substrate. Opt Lasers Eng. 2010;48(7–8):792–799. doi:10.1016/j.optlaseng.2010.02.009
[95] Solecka M, Kopia A, Radziszewska A, et al. Microstructure, microsegregation and nanohardness of CMT clad layers of Ni-base alloy on 16Mo3 steel. J Alloys Compd. 2018;751:86–95. doi:10.1016/j.jallcom.2018.04.102
[96] Li Y, Dong S, Yan S, et al. Surface remanufacturing of ductile cast iron by laser cladding Ni-Cu alloy coatings. Surf Coatings Technol. 2018 April;347:20–28. doi:10.1016/j.surfcoat.2018.04.065
[97] Harati E, Ghaini FM, Torkamany MJ, et al. Яковлев Д. А. 2, Борисов А. И. 2. Белый С А 2011;1(No. 2006):5–12.
[98] Singh H, Bala N, Kaur N, et al. Effect of additions of TiC and Re on high temperature corrosion performance of cold sprayed Ni-20Cr coatings. Surf Coat Technol. 2015;280:50–63. doi:10.1016/j.surfcoat.2015.08.002
[99] Mahamood R, Akinlabi E. Functionally graded materials; 2017. doi:10.1007/978-3-319-53756-6
[100] Hassanzadeh R, Bilgili M. Assessment of thermal performance of functionally graded materials in longitudinal fins. J Eng Phys Thermophys. 2018;91(1):79–88. doi:10.1007/s10891-018-1721-3
[101] Hamatani H, Shimoda N, Kitaguchi S. Effect of the composition profile and density of LPPS sprayed functionally graded coating on the thermal shock resistance. Sci Technol Adv Mater. 2003;4(2):197–203. doi:10.1016/S1468-6996(03)00023-8
[102] Sames WJ, List FA, Pannala S, et al. The metallurgy and processing science of metal additive manufacturing. Int Mater Rev. 2016;61(5):315–360. doi:10.1080/09506608.2015.1116649
[103] Nam S, Cho H, Kim C, et al. Effect of process parameters on deposition properties of functionally graded STS 316/Fe manufactured by laser direct metal deposition. Metals (Basel). 2018;8(8). doi:10.3390/met8080607
[104] Adomako NK, Noh S, Oh CS, et al. Laser deposition additive manufacturing of 17-4PH stainless steel on Ti-6Al-4 V using V interlayer. Mater Res Lett. 2019;7(7):259–266. doi:10.1080/21663831.2019.1596989
[105] Zelentsov VB, Lapina PA, Mitrin BI. Wear of functionally graded coatings under frictional heating conditions. Nanomaterials. 2022;12(1). doi:10.3390/nano12010142
[106] Sathish M, Radhika N, Saleh B. A critical review on functionally graded coatings: methods. Prop Challen Comp Part B Eng. 2021 April;225:109278, doi:10.1016/j.compositesb.2021.109278
[107] Polat A, Sarikaya O, Celik E, et al. Effects of porosity on thermal loadings of functionally graded Y2O3-ZrO2/NiCoCrAlY coatings. Mater Des. 2002;23(7):641–644. doi:10.1016/S0261-3069(02)00064-X
[108] EL-Wazery M, EL-Desouky A. A review on functionally graded ceramic-metal materials. J Mater Environ Sci. 2015;6(5):1369–1376.
[109] Boswell JH, Clark D, Li W, et al. Cracking during thermal post-processing of laser powder bed fabricated CM247LC Ni-superalloy. Mater Des. 2019;174; doi:10.1016/j.matdes.2019.107793
[110] Molobi E, Sacks N, Theron M. Crack mitigation in laser engineered net shaping of WC-10wt%FeCr cemented carbides. Addit Manuf Lett. 2022;2:100028, doi:10.1016/j.addlet.2022.100028
[111] Pellizzari M, Massignani D, Amirabdollahian S, et al. Thermal fatigue behavior of AISI H13 hot work tool steel produced by direct laser metal deposition. Steel Res Int. 2022 September. doi:10.1002/srin.202200449
[112] Megahed M, Mindt HW, N'Dri N, et al. Metal additive-manufacturing process and residual stress modeling. Integrat Mater Manufact Innov. 2016;5; doi:10.1186/s40192-016-0047-2
[113] Frazier WE. Metal additive manufacturing: a review. J Mater Eng Perform. 2014;23(6):1917–1928. doi:10.1007/s11665-014-0958-z
[114] Teixeira Ó, Silva FJG, Ferreira LP, et al. A review of heat treatments on improving the quality and residual stresses of the Ti–6Al–4 V parts produced by additive manufacturing. Metals (Basel). 2020;10(8):1–24. doi:10.3390/met10081006
[115] Sobczak JJ, Drenchev LB. Metal based functionally graded materials. Met Based Funct Graded Mater. 2009. No. May 2014. doi:10.2174/97816080503831090101
[116] Vassen R, Kassner H, Stuke A, et al. Functionally graded thermal barrier coatings with improved reflectivity and high-temperature capability. Mater Sci Forum. 2010;631–632:73–78. doi:10.4028/www.scientific.net/MSF.631-632.73
[117] Burlayenko VN, Altenbach H, Sadowski T, et al. Modelling functionally graded materials in heat transfer and thermal stress analysis by means of graded finite elements. Appl Math Model. 2017;45:422–438. doi:10.1016/j.apm.2017.01.005
[118] del Val J, Arias-González F, Barro O, et al. Functionally graded 3D structures produced by laser cladding. Procedia Manuf. 2017;13:169–176. doi:10.1016/j.promfg.2017.09.029
[119] Rodriguez J, Hoefer K, Haelsig A, et al. Functionally graded SS 316 l to Ni-based structures produced by 3D plasma metal deposition. Metals (Basel). 2019;9(6):1–19. doi:10.3390/met9060620
[120] Liang X, Wu D, Li Q, et al. Laser rapid manufacturing of stainless steel 316L/Inconel718 functionally graded materials: microstructure evolution and mechanical properties. Int J Opt. 2010;2010:1–6. doi:10.1155/2010/802385
[121] Luo K, Li S, Xu G, et al. Hot corrosion behaviors of directed energy deposited inconel 718/haynes 25 functionally graded material at 700 and 900°C. Corros Sci. 2022;197:110040, doi:10.1016/j.corsci.2021.110040
[122] Ben-Artzy A, Reichardt A, Borgonia JP, et al. Compositionally graded SS316 to C300 maraging

steel using additive manufacturing. Mater Des. 2021;201:109500, doi:10.1016/j.matdes.2021.109500
[123] Sun Z, Ji X, Zhang W, et al. Microstructure evolution and high temperature resistance of Ti6Al4V/Inconel625 gradient coating fabricated by laser melting deposition. Mater Des. 2020;191:108644. doi:10.1016/j.matdes.2020.108644
[124] Meng B, Wan M, Zhao R, et al. Micromanufacturing technologies of compact heat exchangers for hypersonic precooled airbreathing propulsion: a review. Chin J Aeronaut. 2021;34(2):79–103. doi:10.1016/j.cja.2020.03.028
[125] Adesina OS, Oki M, Farotade GA, et al. Effect of nickel-based laser coatings on phase composition and corrosion behaviour of titanium alloy for offshore application. Mater Today Proc. 2021;38 (xxxx):830–834. doi:10.1016/j.matpr.2020.04.671
[126] Pardal G, Ganguly S, Williams S, et al. Dissimilar metal joining of stainless steel and titanium using copper as transition metal. Int J Advan Manufact Techn. 2016. doi:10.1007/s00170-015-8110-2
[127] Mokgalaka MN, Pityana SL, Popoola PAI, et al. Niti intermetallic surface coatings by laser metal deposition for improving wear properties of Ti-6Al-4 V substrates. Adv Mater Sci Eng. 2014. doi:10.1155/2014/363917
[128] Ahmed MH, El IM, Bassiouny G, et al. Functionally graded materials classifications and development trends from industrial point of view. SN Appl Sci. 2019 November;1:1–23. doi:10.1007/s42452-019-1413-4
[129] Chmielewski M, Pietrzak K. Metal-Ceramic functionally graded materials - manufacturing, characterization. Appl Bull Polish Acad Sci Tech Sci. 2016;64 (1):151–160. doi:10.1515/bpasts-2016-0017
[130] Hassanzadeh R, Pekel H. Assessment of thermal performance of the functionally graded materials in annular fins. J Eng Thermophys. 2016;25(3):377–388. doi:10.1134/S1810232816030073
[131] Reichardt A, Shapiro AA, Otis R, et al. Advances in additive manufacturing of metal-based functionally graded materials. Int Mater Rev. 2021;66(1):1–29. doi:10.1080/09506608.2019.1709354
[132] Robinson AJ, Colenbrander J, Deaville T, et al. A wicked heat pipe fabricated using metal additive manufacturing. Int J Thermofluids. 2021;12:100117, doi:10.1016/j.ijft.2021.100117
[133] Gong G, Ye J, Chi Y, et al. Research status of laser additive manufacturing for metal: a review. J Mater Res Technol. 2021;15:855–884. doi:10.1016/j.jmrt.2021.08.050
[134] Wang C, Li J, Wang T, et al. Microstructure and properties of pure titanium coating on Ti-6Al-4 V alloy by laser cladding. Surf Coat Technol. 2021 January;416:127137, doi:10.1016/j.surfcoat.2021.127137
[135] Roy T, Paradowska A, Abrahams R, et al. Effect of cladding direction on residual stress distribution in laser cladded rails. World Acad Sci Eng Technol Int J Civ Environ Eng. 2017;11(9):1359–1363.
[136] Updike DP, Kalnins A, Caldwell SM. Residual stresses in transition zones of heat exchanger tubes. J Press Vessel Technol Trans ASME. 1992;114 (2):149–156. doi:10.1115/1.2929022
[137] Elijah K. A. materials processing principles of laser; 2009.
[138] Li Z, Yu G, He X, et al. Surface tension-driven flow and Its correlation with mass transfer during L-DED of co-based powders. Metals (Basel). 2022;12 (5). doi:10.3390/met12050842
[139] Le TN, Lo YL. Effects of sulfur concentration and marangoni convection on melt-pool formation in transition mode of selective laser melting process. Mater Des. 2019;179:107866, doi:10.1016/j.matdes.2019.107866
[140] Unless R, Act P, Rose W, et al. This is a repository copy of laser melting functionally graded composition of Waspaloy ((R)) and zirconia powders. White rose research online URL for this paper : version : accepted version article : Mumtaz, K. A. and Hopkinson, N. Laser. 2007.
[141] Goodarzi DM, Pekkarinen J, Salminen A. Analysis of laser cladding process parameter influence on the clad bead geometry. Weld World. 2017;61(5):883–891. doi:10.1007/s40194-017-0495-0
[142] Addepalli S, Eiroa D, Lieotrakool S, et al. Degradation study of heat exchangers. Procedia CIRP. 2015;38:137–142. doi:10.1016/j.procir.2015.07.057
[143] Singh J, Thakur L, Angra S. Effect of argon flow rate and standoff distance on the microstructure and wear behaviour of WC-CoCr TIG cladding. J Phys Conf Ser. 2019;1240(1). doi:10.1088/1742-6596/1240/1/012162
[144] Ocelík V, Nenadl O, Palavra A, et al. On the geometry of coating layers formed by overlap. Surf Coat Technol. 2014;242:54–61. doi:10.1016/j.surfcoat.2014.01.018
[145] Wei C, Zhang Z, Cheng D, et al. An overview of laser-based multiple metallic material additive manufacturing : from macro-To. Int J Ext Manufact. 2021.
[146] Watring DS, Benzing JT, Hrabe N, et al. Effects of laser-energy density and build orientation on the structure–property relationships in as-built inconel 718 manufactured by laser powder bed fusion. Addit Manuf. 2020;36. doi:10.1016/j.addma.2020.101425
[147] Siddiqui AA, Dubey AK. Recent trends in laser cladding and surface alloying. Opt Laser Technol. 2021;134:106619. doi:10.1016/j.optlastec.2020.106619
[148] Jing Z, Cao Q, Jun H. Corrosion, wear and biocompatibility of hydroxyapatite bio-functionally graded coating on titanium alloy surface prepared by laser cladding. Ceram Int. 2021;47(17):24641–24651. doi:10.1016/j.ceramint.2021.05.186
[149] Cheng Yh, Cui R, Wang Hz, et al. Effect of processing parameters of laser on microstructure and properties of cladding 42CrMo steel. Int J Adv Manuf Technol. 2018;96(5–8):1715–1724. doi:10.1007/s00170-017-0920-y
[150] Mahamood RM, Akinlabi ET, Shukla M, et al. Laser metal deposition of Ti6Al4V: a study on the effect of laser power on microstructure and microhardness. Lect Notes Eng Comput Sci. 2013;2203:994–999.
[151] Cheng M, Luo G, Xiao X, et al. Effect of molten pool spatial arrangement on texture evolution in pulsed laser additive manufacturing of inconel 718. Materials (Basel) 2022;15(9):1–13. doi:10.3390/ma15093286
[152] Ocylok S, Weisheit A, Kelbassa I. Functionally graded multi-layers by laser cladding for increased

wear and corrosion protection. Phys Procedia. 2010;5:359–367. doi:10.1016/j.phpro.2010.08.157
[153] Song B, Hussain T, Voisey KT. Laser cladding of Ni50Cr: a parametric and dilution study. Phys Procedia. 2016;83:706–715. doi:10.1016/j.phpro.2016.08.072
[154] Lian G, Zhang H, Zhang Y, et al. Optimizing processing parameters for multi-track laser cladding utilizing multi-response grey relational analysis. Coatings. 2019;9(6). doi:10.3390/coatings9060358
[155] Ostolaza M, Arrizubieta JI, Lamikiz A, et al. Applied sciences functionally graded AISI 316L and AISI H13 manufactured by L-DED for die and mould applications; 2021.
[156] Carroll BE, Otis RA, Borgonia JP, et al. Functionally graded material of 304L stainless steel and inconel 625 fabricated by directed energy deposition: characterization and thermodynamic modeling. Acta Mater. 2016;108:46–54. doi:10.1016/j.actamat.2016.02.019
[157] Balaji C, Kumar SVA, Kumar SA, et al. Evaluation of mechanical properties of Ss 316 L weldments using tungsten inert gas welding. Int J Eng Sci Technol. 2012;4(5):2053–2057.
[158] Jagdheesh R, Kamachi Mudali U, Nath AK. Laser processed Cr-SiC coatings on AISI type 316L stainless steel. Surf Eng. 2007;23(2):93–98. doi:10.1179/174329407X169421
[159] Jagdheesh R, Sastikumar D, Mudali UK, et al. Laser processed metal-ceramic coatings on AISI type 316L stainless steel. Surf Eng. 2004;20(5):360–366. doi:10.1179/026708404225014997
[160] Jagdheesh R, Kamachi Mudali U, Sastikumar D, et al. Laser cladding of Si on austenitic stainless steel. Surf Eng. 2005;21(2):113–118. doi:10.1179/174329405X40885
[161] Chen B, Su Y, Xie Z, et al. Development and characterization of 316L/Inconel625 functionally graded material fabricated by laser direct metal deposition. Opt Laser Technol. 2020;123; doi:10.1016/j.optlastec.2019.105916
[162] Stein F, Leineweber A. Laves phases: a review of their functional and structural applications and an improved fundamental understanding of stability and properties. J Mater Sci. 2021;56(9):5321–5427. doi:10.1007/s10853-020-05509-2
[163] Mahamood RM, Akinlabi ET. Effect of powder flow rate on surface finish in laser additive manufacturing process. IOP Conf Ser Mater Sci Eng. 2018;391(1). doi:10.1088/1757-899X/391/1/012005
[164] Tiwari GK, Dubey AK, Siddiqui AA. A hybrid approach for modelling and optimization of laser cladding process. Int J Adv Prod Ind Eng. 2020;5(1):17–24. doi:10.35121/ijapie202001142
[165] Marrey M, Malekipour E, El-Mounayri H, et al. A framework for optimizing process parameters in powder bed fusion (PBF) process using artificial neural network (ANN). Procedia Manuf. 2019;34:505–515. doi:10.1016/j.promfg.2019.06.214
[166] Nyadongo ST, Pityana SL, Olakanmi EO. Isothermal oxidation performance of laser cladding assisted with preheat (LCAP) tribaloy t-800 composite coatings deposited on En8. Coatings. 2021;11(7). doi:10.3390/coatings11070843
[167] Sadhu A, Choudhary A, Sarkar S, et al. A study on the influence of substrate pre-heating on mitigation of cracks in direct metal laser deposition of NiCrSiBC-60%WC ceramic coating on inconel 718. Surf Coat Technol. 2020 January;389:125646. doi:10.1016/j.surfcoat.2020.125646
[168] Jendrzejewski R, Navas C, Conde A, et al. Properties of laser-cladded stellite coatings prepared on preheated chromium steel. Mater Des. 2008;29(1):187–192. doi:10.1016/j.matdes.2006.10.020
[169] Meng W, Zhang W, Zhang W, et al. Fabrication of steel-inconel functionally graded materials by laser melting deposition integrating with laser synchronous preheating. Opt Laser Technol. 2020 June;131:106451, doi:10.1016/j.optlastec.2020.106451
[170] Zhang, Y., Tu, Y., Xi, M., et al. Characterization on laser clad nickel based alloy coating on pure copper. Surf Coat Technol. 2008;202(24):5924–5928. doi:10.1016/j.surfcoat.2008.06.163
[171] Banait SM, Paul CP, Jinoop AN, et al. Experimental investigation on laser directed energy deposition of functionally graded layers of Ni-Cr-B-Si and SS316L. Opt Laser Technol. 2020;121:105787, doi:10.1016/j.optlastec.2019.105787
[172] Shang C, Wang C, Li C, et al. Eliminating the crack of laser 3D printed functionally graded material from TA15 to Inconel718 by base preheating. Opt Laser Technol. 2020 January;126:106100, doi:10.1016/j.optlastec.2020.106100
[173] Corbin DJ, Nassar AR, Reutzel EW, et al. Effect of substrate thickness and preheating on the distortion of laser deposited Ti-6Al-4V. J Manuf Sci Eng Trans ASME. 2018;140(6) doi:10.1115/1.4038890
[174] Liu Y, Xu T, Li G. Research on wear and corrosion resistance of Ni60-WC coating fabricated by laser on the preheated copper alloy. Coatings. 2022;12(10). doi:10.3390/coatings12101537
[175] Li G, Zhang J, Shi T, et al. Experimental investigation on laser metal deposition of Ti-6Al-4V alloy with coaxial local shielding gas nozzle. J Mater Eng Perform. 2020;29(12):7821–7829. doi:10.1007/s11665-020-05283-x
[176] Tanigawa D, Abe N, Tsukamoto M, et al. Effect of laser path overlap on surface roughness and hardness of layer in laser cladding. Sci Technol Weld Join. 2015;20(7):601–606. doi:10.1179/1362171815Y.0000000044
[177] Birger EM, Moskvitin GV, Polyakov AN, et al. Industrial laser cladding: current state and future. Weld Int. 2011;25(3):234–243. doi:10.1080/09507116.2010.540880
[178] Zhao Y, Chen Y, Zhang T, et al. Laser fabricated nickel-based coating with different overlap modes. Mater Manuf Process. 2021;36(14):1618–1630. doi:10.1080/10426914.2021.1926490
[179] Li Y, Ma J. Study on overlapping in the laser cladding process. Surf Coat Technol. 1997;90(1–2):1–5. doi:10.1016/S0257-8972(96)03022-8
[180] Tuominen J, Näkki J, Pajukoski H, et al. Microstructural and abrasion wear characteristics of laser-clad tool steel coatings. Surf Eng. 2016;32(12):923–933. doi:10.1080/02670844.2016.1180496
[181] Stanciu EM, Pascu A, Țierean MH, et al. Dual coating laser cladding of NiCrBSi and inconel 718. Mater Manuf Process. 2016;31(12):1556–1564. doi:10.1080/10426914.2015.1103866